TECHNISCHE UNIVERSITÄT MÜNCHEN

Department Chemie

Lehrstuhl für Biotechnologie

Structural requirements for IgM oligomerization

Džana Pašalić

Vollständiger Abdruck der von der Fakultät für Chemie der Technischen Universität München zur Erlangung des akademischen Grades eines **Doktors der Naturwissenschaften (Dr. rer. nat.)** genehmigten Dissertation.

Vorsitzender:		Univ. - Prof. Dr. Matthias Feige
Prüfer der Dissertation:	1.	Univ. - Prof. Dr. Johannes Buchner
	2.	Univ. - Prof. Dr. Michael Sattler

Die Dissertation wurde am 05.02.2015 bei der Technischen Universität München eingereicht und durch die Fakultät für Chemie am 01.04.2015 angenommen.

To my family

Index

1 Summary

The C-terminal IgM domains Cμ3, Cμ4 and the tail piece (tp) were shown to determine the formation of immunoglobulin M (IgM) polymers, i.e. decamers and dodecamers (Poon *et al*., 1995; Sorensen *et al*., 1999; Yoo *et al*., 1999; Braathen *et al*., 2002). The 18 amino acid long tp was identified to be the essential element for polymerization (Davis *et al*., 1989; Davis and Shulman, 1989). *In vitro* the Cμ4 domain formed dodecameric structures only in fusion with the tp (Müller *et al*., 2013).

The characterization of the oligomerization process *in vitro* performed in this work allowed to ascertain that the Cμ4-tp fragment possesses the ability to spontaneously undergo self-association upon C575 oxidation, indicating that the oligomerization property of Cμ4 fused to the tp is encoded in the amino acid sequence. Furthermore, it was possible to establish that oligomerization occurs in two steps, via covalent dimers forming first, which non-covalently assemble into dodecamers, i.e. hexamers of dimers.

By serially replacing every single tp amino acid with alanine 18 Cμ4-tp and analogous 18 IgM-tp mutants were generated and their oligomerization ability was assessed *in vitro* and in HEK293 cells, respectively. SEC-MALS and the aUC analysis of the former mutants and WB analysis of the latter allowed determining that the tp regulates the oligomerization properties not only of the Cμ4-tp domain but also of the whole IgM antibody**.** To date, no other sequence on the μ chain was shown to exert such a strong control on oligomerization. Six of its total 18 amino acids control in the cell whether dimers or decamers and dodecamers are secreted and three amino acids whether aggregation occurs. The N563Q mutant indicated on the other hand that glycosylation might contribute to IgM decamer formation. C575 was already shown to lead to a prevalent dimer secretion when mutated to alanine or serine (Davis *et al.,* 1989; Sitia *et al,*. 1990). Within this work an additional region located in the N-terminal half of the tail piece, the hydrophobic core, was identified, whose amino acids had an even a more potent effect on oligomerization, in that the replacement of any of them led to the exclusive secretion of dimers.

CD spectroscopy of synthesized tp point mutants showed that substitution of single hydrophobic amino acids disrupts the tp secondary structure. This allows to hypothesize that only the presence of the intact hydrophobic core ensures the correct three-dimensional conformation of the tp. This in turn enables the establishment of non-covalent intra-subunit and covalent inter-subunit interactions, both essential for the formation of IgM oligomers.

IgM decamers incorporate the joining (J) chain whereas it has never been shown to be present in the dodecameric IgM (Davis *et al*., 1988; Randall *et al*., 1990; Meng *et al*., 1990; Brewer and Corley, 1997). J chain of isolated human IgM showed a specific arrangement of intra- and inter-chain disulfide bonds (Frutiger *et al.,* 1992). The MALDI-TOF analysis of tryptic digests of the recombinant monomeric human and murine J chain, performed in this work, however allowed establishing the occurrence of more than one disulfide bond arrangement. Moreover, *in vitro* J chain did not show any tendency to bind either the Cμ4-tp domain or the chaperones BiP or βHsp90.

2 Zusammenfassung

Die Bildung von Immunoglobulin M (IgM) Oligomeren (i.e. Dekameren und Dodekameren) wird durch die C-terminalen Domänen Cμ4, Cμ3 und das "Schwanzstück" (tail piece, tp) dirigiert (Poon *et al*., 1995; Sorensen *et al*., 1999; Yoo *et al*., 1999; Braathen *et al*., 2002). Das 18 Aminosäuren lange tp ist für die Oligomerisierung essentiell (Davis *et al*., 1989; Davis and Shulman, 1989). *In vitro* bildet die Cμ4 Domäne nur in Fusion mit dem tp Dodekamere (Müller *et al*., 2013).

In dieser Arbeit wurde die *in vitro* Oligomerisierung des Cμ4-tp Fragmentes charakterisiert. Dies hat gezeigt, dass Cμ4-tp bei der Oxidation von C575 spontan assembliert und die Oligomerisierung dieser Fusion daher in der Aminosäure-Sequenz kodiert ist. Die Oligomerisierung verläuft zweistufig, wobei sich zuerst kovalente Dimere bilden, die sich schließlich zu nicht-kovalenten Dodekameren, i.e. Hexameren aus Dimeren, zusammenlagern.

Durch serielle Substitution aller tp-Aminosäuren durch Alanin wurden 18 Cμ4-tp- und 18 entsprechende IgM-Mutanten generiert und ihre Oligomerisierungseigenschaften wurden *in vitro* und in HEK293-Zellen untersucht. Durch SEC-MALS-Analyse und analytische Ultrazentrifugation ersterer und Western-Blot-Analyse letzterer konnte gezeigt werden, dass das tp nicht nur die Oligomerisierung der isolierten Cμ4 Domäne reguliert, sondern auch die des gesamten IgM Antikörpers. Bisher war von keiner anderen Sequenz in der μ Kette ein solch starker Einfluss auf die Oligomerisierung bekannt. Sechs der insgesamt 18 Aminosäuren determinieren in der Zelle, ob Dimere oder Dekamere und Dodekamere sezerniert werden, und drei Aminosäuren, ob es zur Aggregation kommt. Die N563Q Mutante zeigte, dass auch die Glykosylierung an dieser Position Einfluss auf die IgM Dekamer-Bildung hat. Von C575 war bereits aus früheren Studien bekannt, dass es vorwiegend zur Sekretion von Dimeren führt, wenn es zu Alanin oder Serin mutiert ist (Davis *et al.,* 1989; Sitia *et al*., 1990). In dieser Arbeit konnte jedoch gezeigt werden, dass es zusätzlich in der N-terminalen Hälfte des tp eine Region gibt, den hydrophoben Kern, deren

Reste einen noch stärkeren Einfluss auf die Oligomerisierung haben, weil hier jegliche Substitution zur ausschließlichen Sekretion von Dimeren führt.

Die CD-spektroskopische Untersuchung von synthetisierten tp Punkt-Mutanten zeigte, dass Substitutionen von einzelnen hydrophoben Aminosäuren die Sekundärstruktur des tp zerstören. Dies erlaubt die Spekulation, dass ausschliesslich das Vorliegen des intakten hydrophoben Kerns die korrekte dreidimensionale Konformation des tp sicherstellt. Diese ermöglicht die Bildung von nicht kovalenten intra- und kovalenten inter-Untereinheitsbindungen, die für die Bildung von Oligomeren essentiell sind.

Decamere IgM Moleküle enthalten die J-Kette (joining, J), wohingegen dies nie für dodecamere IgM Moleküle gefunden wurde (Davis *et al*., 1988; Randall *et al*., 1990; Meng *et al*., 1990; Brewer and Corley, 1997). Von der J-Kette aus humanem IgM war bisher bekannt, dass es eine spezifische Anordnung von intra- und intermolekularen Disulfidbrücken gibt (Frutiger *et al.,* 1992). Mittels MALDI-TOF-Analyse tryptischer Verdaue von rekombinanten monomeren humanen und murinen J-Ketten konnte in dieser Arbeit jedoch gezeigt werden, dass es mehr als eine Disulfidbrücken-Kombinationsmöglichkeit gibt. *In vitro* zeigte die J-Kette ausserdem keinerlei Bindungstendenz für Cμ4-tp und das BiP- und das βHsp90-Chaperone.

3 Introduction

The first antibody being produced in primary immune responses and the prevalent isotype being secreted in T cell-independent immune responses is the IgM (Brewer and Corley, 1997). Together with IgA, it belongs to the group of polymeric Ig (pIg) (Klimovich, 2011). Like all immunoglobulins, IgM subunit consists of μ heavy (H) and light (L) chains assembled into H_2L_2 structures. Prior to antigen infection, IgM is expressed and anchored on the surface of B cells, where it acts as a membrane receptor. Upon activation due to antigen binding, IgM subunits oligomerize into ring-like covalent polymers, which are secreted as decamers or pentamers of covalent dimers ($(H_2L_2)_5$) and as dodecamers or hexamers of covalent dimers ($(H_2L_2)_6$) (Davis and Shulman, 1989; Brewer *et al.*, 1994). These two oligomers differ not only in the number of μ_2L_2 subunits, but in the ability to incorporate an additional polypeptide, the J chain. Dodecameric IgM do not contain the J chain (Davis *et al*., 1988; Randall *et al*., 1990; Meng *et al*., 1990), whereas decameric IgM frequently include this small protein (Brewer and Corley, 1997).

J chain modulates assembly of IgM determining their effector functions, in that IgM dodecamers are up to 100 times more efficient in fixing complement than IgM decamers. Furthermore, J chain is necessary for binding of IgM and IgA to the polymeric immunoglobulin receptor (pIgR) present on epithelial cells, allowing their transcytosis into extravascular fluids (Wiersma *et al.*, 1997).

Assembly into polymers helps not only increasing the avidity of Ig for antigen but also improving their effector functions, namely complement activation and binding to Fc receptors (Smith and Morrison, 1994; Smith *et al.*, 1995). Understanding the structural requirements for oligomerization and how it is regulated is thus of great interest, since it may provide basis to develop new engineered antibodies or their derivatives with enhanced activity and pharmacokinetic properties.

3.1 IgM – functional aspects

3.1.1 Natural versus immune IgM

IgM belongs to the immunoglobulin class which first appeared in the curse of evolutionary development of vertebrates starting from cartilaginous fish (Flajnik *et al*., 2003). During embryonic development and upon antigen infections they are the first to arise (Henry and Jerne, 1968; Hardy and Hayakawa, 1994). They can be present in the organism as antigen receptors on the cell surface of B lymphocytes (Reth, 1992), and as circulating oligomers in blood as well as on mucous membranes and excretory glands (Woof and Mestecky, 2005). IgM are produced by two different types of B lymphocytes, B1 and B2 lymphocytes.

B1 lymphocytes are the first cells to produce IgM during embryonic development (Henry and Jerne, 1968; Hayakawa and Hardy, 2000). They descend from embryonic liver cells (Montecino-Rodriguez *et al*., 2006) and are confined in abdominal and pleural cavities (Kantor *et a*l., 1993; Martin and Kearney, 2001). There are two subpopulations of B1 lymphocytes, the B1a, which possesses the CD5 marker, and the B1b, which is devoid of it (Haas *et al*., 2005; Alugupalli, *et al*., 2004). The former are not able to undergo V gene rearrangement, isotype switching, and somatic hypermutation and IgM produced by them are encoded by germline genes (Feeney, 1990). These IgM are referred to as natural antibodies (NAb) as they emerge without any outer antigen stimuli (Casali and Schettino, 1996).

B2 lymphocytes arise during postnatal period. They originate from hematopoietic stem cells of bone marrow (Baba *et al*., 2004) which migrate to spleen where they differentiate occupying the marginal zone and lymphoid follicles (Pillai *et al*., 2005). Unlike the B1a, B2 lymphocytes start producing IgM when stimulated by the contact with the antigen and the T helper. They undergo isotype switching and affinity maturation and turn into plasma cells or memory cells (McHeyzer-Williams and McHeyzer-Williams, 2005). IgM antibodies produced by B2 lymphocytes are called thus immune or immunization induced (Klimovich, 2011) and they are usually decameric and rarely dodecameric (Schroeder and Cavacini, 2010).

B1b cells represent a cell type which combines characteristic of B1a and B2 lymphocytes. Like B1a cells, they produce germline IgM transcripts. However, like B2 lymphocytes, under antigenic stimuli or influence of cytokines they can activate the mechanisms of somatic hypermutation switching to IgA synthesis (Klimovich, 2011).

However, after secretion of IgM polymers has been induced by antigen, its synthesis persists from 3 to 5 days and its levels do not exceed ca. 1,5 g/l. Then it is switched to production of antibodies of other classes (Klimovich, 2011).

Immune IgM differ from natural IgM in the structure of antigen binding centers, their affinity and specificity repertoire (Baumgarth *et al*., 2000).

Due to their immaturity, IgM dimers have a low antigen affinity, which is compensated by high avidity of decameric and dodecameric IgM. IgM oligomers exert their effector functions either by opsonizing antigens or fixing complement (Schroeder and Cavacini, 2010).

3.1.2 IgM decamers vs dodecamers

IgM decamers differ from IgM dodecamers in several aspects. First, decameric, but not dodecameric, IgM can incorporate the J chain (Schroeder and Cavacini, 2010). Second, IgM dodecamers are up to 100-fold more efficient in activating complement than IgM decamers probably due to differences in the conformation of the complement binding site, which in dodecamers may facilitate the binding (Brewer *et al*., 1994, Wiersma *et al*., 1998; Hughey *et al*., 1998). Finally, only decameric IgM can be secreted into extravascular fluids due to transcytosis in epithelial cells performed by pIg receptor upon binding to the J chain (Wiersma *et al.*, 1997).

Data about secretion of IgM decamers and dodecamers as well as about their ability to activate complement derive prevalently from studies performed with cell lines producing IgM. From an intact organism however, data about IgM dodecamers were mainly obtained from sera of patients suffering rare diseases such as cold agglutinins syndrome or Waldenstrom's macroglobulinemia (Klimovich, 2011). The biological role of dodecameric IgM thus still remains not fully clarified. Petrusic *et al*. (2011) demonstrated that, unlike IgM decamers, which can exist as natural antibodies and antibodies induced by antigen, dodecameric IgM are exclusively immune, suggesting that their occurrence as NAb might be deleterious.

3.1.3 Regulation of IgM dodecamer secretion

The J chain abundance in plasma cells affects the size of secreted lgM polymers. In presence of high levels of J chain the plasma cells secrete prevalently lgM decamers. On the contrary, high levels of IgM dodecamers are secreted when low levels of J chain are synthesized.

However, the decamer to dodecamer ratio differs depending on the antigen and its ability to induce the expression of the J chain (Brewer *et al*., 1994).

Brewer *et al*. (1994) suggested a possible involvement of IgM dodecamers only in particular cases of immune response, namely when high levels of complement activation are requested for elimination of antigens such as bacteria. Therefore, dodecameric IgM, acting as T cell-independent immunogens, could activate B cells but not the production of lymphokines in high amounts, which induce the expression of J chain, leading thus to prevalent secretion of dodecamers. On the contrary, for neutralization of pathogens such as viruses antigen opsonization is sufficient. These immune responses would lead to prevalent secretion of decameric IgM, as they often require T cell participation, which activate the transcription of J chain.

The same authors proposed an explanation for a natural tendency of the immune system to react to antigens by producing IgM decamers. Highly lytic dodecameric IgM possess the ability to recognize autoantigens as well as cell-surface molecules. Their occurrence in the natural antibody repertoire, where B cells lack specificity and bind to foreign as well as to autoantigens due to the expression of germline V-genes, might thus lead to autoimmunity.

3.1.4 IgM effector functions

IgM antibodies have low affinity. By assembling into polymers, they increase the number of antigen binding sites from 2 to 10 in decamers or to 12 in dodecamers, and thus their binding ability (avidity). However, due to sterical hindrances the occupancy of all binding sites can be achieved only with antigens which MW does not exceed 1.5 kDa (Edberg *et al*., 1972). The high valence of IgM oligomers enables them to provoke agglutination and aggregation of antigens, which represents one important defense mechanism exerted by IgM (Edberg *et al*., 1972; Bendtzen *et al*., 1998; Notkins, 2004). Moreover, IgM can further increase their avidity due to the contacts of their glycans which can react with lectins of bacteria and viruses (Czajkowsky and Shao, 2009; Arnold *et al*., 2007). Compared to that of IgG, the agglutination ability of IgM is 100 – 10.000 times higher (Klimovich, 2011).

However, the most important and studied effector function of IgM is complement activation through the classical pathway (Nielsen *et al*., 2000). When IgM binds to C1q molecule forming an immune complex, the complement cascade is activated (Feinstein *et al*., 1986).

The IgM structure modeled by Czajkowsky and Shao (2009) support the hypothesis of Feinstein *et al*. (1986) according to which the exposure of C1q binding sites on IgM by conformational rearrangement is needed for complement activation.

Dimeric IgM are not able to activate complement (Klimovich, 2011). Decameric IgM are 1000 times more efficient in activating complement than IgG molecules (Cooper *et al.,* 1983) and the ability to activate complement of IgM dodecamers is 10 – 100 fold higher compared to that of IgM decamers (Hughey *et al*., 1998).

3.2 IgM - Folding, assembly and quality control

Once activated plasma cells must ensure that only correctly folded and assembled IgM "monomers", namely H_2L_2 units, polymerize into mature secretory IgM, since "monomeric" IgM can bind the antigen but fail to fix complement. Thus, the quality control (QC) mechanisms within the endoplasmatic reticulum (ER) must, on the one hand, promote polymerization and secretion and, on the other hand, prevent that unassembled "monomers" travel further along the secretory pathway avoiding their incorporation into oligomers (Figure 3.1) (Anelli and van Anken, 2013).

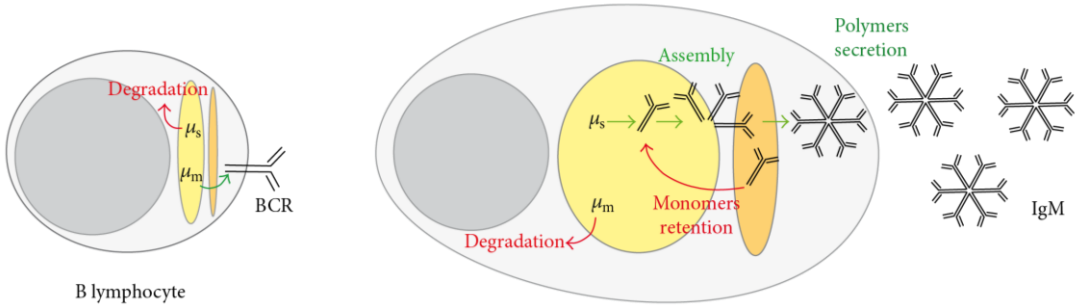

	B lymphocyte	Plasma cell
Rules that change	Produce μ_m (for membrane BCR)	Degrade μ_m
	Never assemble polymeric IgM	Assemble polymeric IgM
	Never secrete antibodies	Secrete antibodies at full gear
Common rules	Never secrete unassembled antibodies, degrade them instead	

Figure 3.1 Processing of membrane and secretory IgM in B lymphocytes and plasma cells. B lymphocytes degrade the μs HC but assemble and integrate the μm HC into the BCR. On the contrary, plasma cells degrade μm but efficiently assemble and secrete IgM oligomers containing the μs HC. Retention of incomplete IgM subunits in the secretory pathway gives another chance to them to be inserted into a polymer or to be finally degraded (Figure taken from Anelli and van Anken, 2013).

Membrane and secretory proteins including immunoglobulins are synthesized and folded in the ER. During folding glycans are added and disulfide bonds are formed (Cortini and Sitia, 2010; Anelli *et al*., 2007). ER and ER-Golgi intermediate compartment (ERGIC) chaperones and oxidoreductases assist nascent proteins in these processes by recognizing and binding exposed immature regions on folding and assembly intermediates until they reach their correct conformation (Braakman and Bulleid, 2011; Anelli and van Anken, 2013). Thus BiP interact with hydrophobic regions (Anelli *et al*., 2003); calreticulin and calnexin recognize immature N-glycans (Hochstenbach *et al*., 1992), while ERp44 is a key player in thiol-mediated retention forming reversible disulfide bonds with exposed free cysteines (Cortini and Sitia, 2010; Anelli and van Anken, 2013).

The synthesis of secretory IgM occurs stepwise, with μ-L assembly preceding polymerization (Hendershot and Sitia, 2005; Anelli *et al*., 2007). These two steps are independently regulated. BiP assists the rapid assembly of LC-HC by binding the unfolded CH1 domain and facilitating thus the retention of the HC until LC manages to displace BiP (Feige *et al*., 2009; Lee *et al*., 1999). The μ_2L_2 units oligomerize then slowly via disulfide bonds involving Cys575 (Davis *et al*., 1989; Sitia *et al*., 1990) present in the C-terminal μ_s tail piece ($\mu_s$tp). Cys575 has a three-fold function, mediating assembly, retention and degradation of unpolymerized subunits (Fra *et al*., 1993).

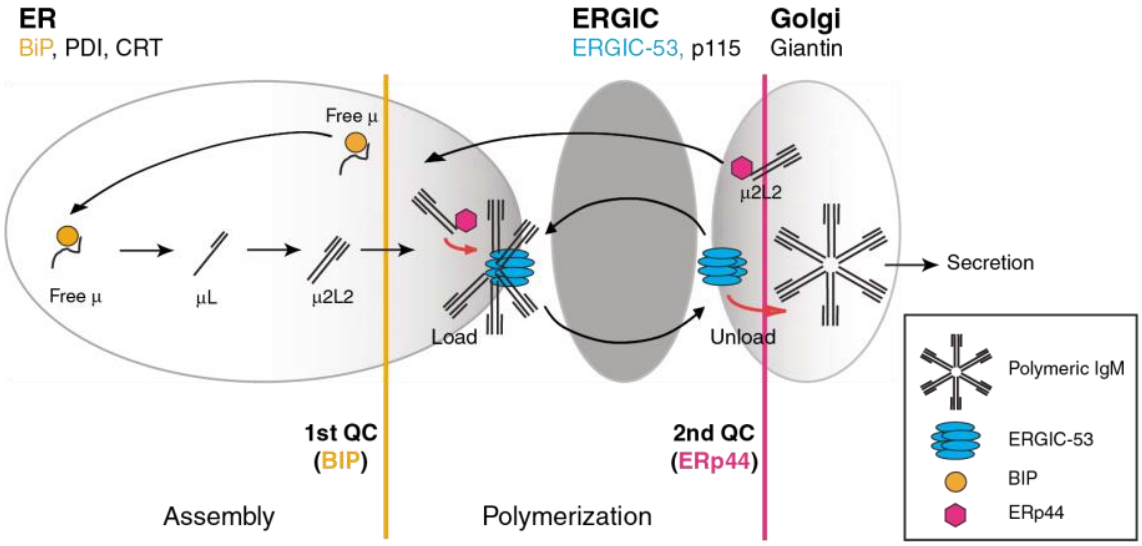

Figure 3.2 IgM polymerization and quality control. IgM polymer assembly occurs in the early secretory pathway. The first check point involving BiP ensures that only μ chain assembled with L chain proceeds along the secretory pathway. The hexameric lectin ERGIC-53 captures μ_2L_2 assisting the polymerization and transferring the polymers to the Golgi. In the Golgi IgM polymers are released from ERGIC-53 and can be secreted. Unassembled IgM are retrotranslocated to the ER by the ERp44 which forms a S-S bond through its Cys29 and the IgM C575 (Figure taken from Anelli *et al*., 2007).

Successfully folded and assembled proteins proceed rapidly along the secretory pathway. Lectins such as ERGIC-53 act as transmembrane cargo receptors which concentrate certain glycoproteins at ER exit sites facilitating their export (Figure 3.2). They insert selected glycoproteins in forward-directed vesicles and release them in the Golgi in a Ca^{2+}- and pH-dependent manner (Appenzeller *et al*., 1999; Hauri *et al*., 2000; Cortini and Sitia, 2010). Both ERp44 and ERGIC-53 bind μ chains assembled to L chains. Anelli *et al*. (2007) suggested that ERp44 and ERGIC-53, which is hexameric, might provide a polymerization platform for IgM, accepting μ_2L_2 subunits that have already been approved by BiP. Moreover, ERp44, which is present at high levels in the Golgi, binds unpolymerized IgM subunits and transports them back to the ER.

3.3 IgM structure

3.3.1 Membrane-bound IgM versus secretory IgM

The membrane and secreted IgM represent two forms of the same molecular device which ensures that secreted antibodies recognize exactly the same immunogen originally presented to the B cell receptor (BCR). Membrane-bound IgM consists of two μ heavy chains (HC) covalently linked by a disulfide bond and of two light chains (LC) also covalently linked to HC via Cys136 of the Cμ1 (Figure 3.3). HC and LC are formed of domains which possess the β sandwich or Ig-fold stabilized by an intra-domain disulfide bond. The variable region of the HC, located on its N-terminus, is composed of one variable domain (VH) whereas the constant region carries four domains (Cμ1–Cμ4 from N to C terminus). The LC have also one variable domain (VL), which is juxtaposed to the VH, and a single constant domain (CL) facing the Cμ1 (Anelli and van Anken, 2013).

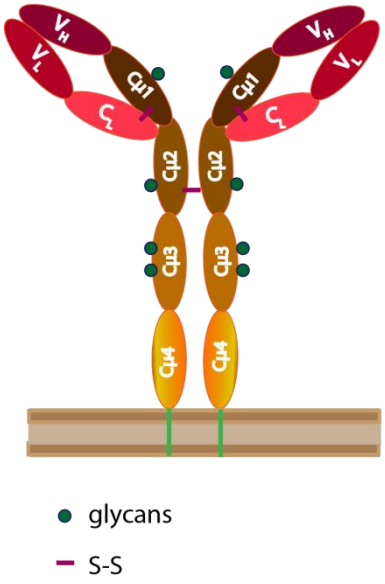

Figure 3.3 Schematic representation of membrane-bound IgM.

The specificity of the BCR for an antigen is determined by the VH and VL together. The anchoring of the BCR to the membrane of B lymphocytes is ensured by a transmembrane domain located at the very C-terminal part of the μ HC, downstream of Cμ4 (Klimovich, 2011; Anelli and van Anken, 2013). It consists of 42 amino acids (a.a.), 3 of which are cytoplasmic, 25 are included in the transmembrane hydrophobic region and 14 are exposed to the extracellular part (Rogers *et al*., 1980; Vassalli *et al*., 1980). Ligand binding and signal transmission of the BCR are spatially separated (Kurosaki, 1999). The IgM $\mu_{m2}L_2$ "monomer"

represents the ligand binding part of the receptor whereas two glycoproteins, Igα (CD79α) and Igβ (CD79β) form the component responsible for signal transduction via tyrosine motifs contained in the cytoplasmic domains of Igα and Igβ (Reth and Wienands, 1997; Brezski and Monroe, 2008).

Once the antigen has bound to BCR, B lymphocytes undergo maturation and become plasma cells which secrete decameric [$(\mu_2L_2)_5$] and dodecameric [$(\mu_2L_2)_6$ IgM (Figure 3.4). Secretory IgM oligomers consist of almost identical H_2L_2 units with the only difference that secretory μ_s HC differ from membrane bound μ_m HC in their C-terminus. Due to alternative splicing the last exons have been replaced and instead of the transmembrane domain, the C-terminus of μ_s HC displays a more hydrophilic tail piece (tp) which consists of 18 a.a., does not have a defined secondary structure, and does not belong to the Cμ4 domain (Anelli e van Anken, 2013). The μ tp is a highly conserved element of secretory IgM with one cysteine, the Cys575, crucial both for preventing secretion of unassembled dimers and for the assembly of mature secretory IgM (Klimovich 2011; Anelli and van Anken, 2013).
Unlike dodecameric IgM, decameric IgM have a single 15 kDa protein, the J chain (Randall *et al*., 1990). J chain is covalently linked via disulfide bond to the C-terminal cysteine (Cys575) of two μ HC in IgM decamers (Fazel *et al*., 1997).
Secretory IgM are covalently assembled oligomers. Inter-chain disulfide bonds are mediated by three cysteines, whose role in assembling dimers and polymeric IgM is only partially understood (Wiersma and Shulman, 1995). Thus, Cys337 in the Cμ2 domain is involved in intra-subunit bonding, whereas Cys414, in the Cμ3 domain, and Cys575, the penultimate amino acid in the Cμ4-tp domain mediate inter-subunit bonding (Fazel *et al*., 1997). Cys575 seems to be crucial to oligomerization, since its replacement with serine or alanine leads to secretion of high amounts of dimers (Sorensen *et al*., 1996). Furthermore, Cys575 is also involved in intracellular quality control as it acts as a retention and degradation signal for unassembled IgM dimers (thiol-mediated retention) (Fra *et al*., 1993; Wiersma and Shulman, 1995; Anelli *et al*., 2007).

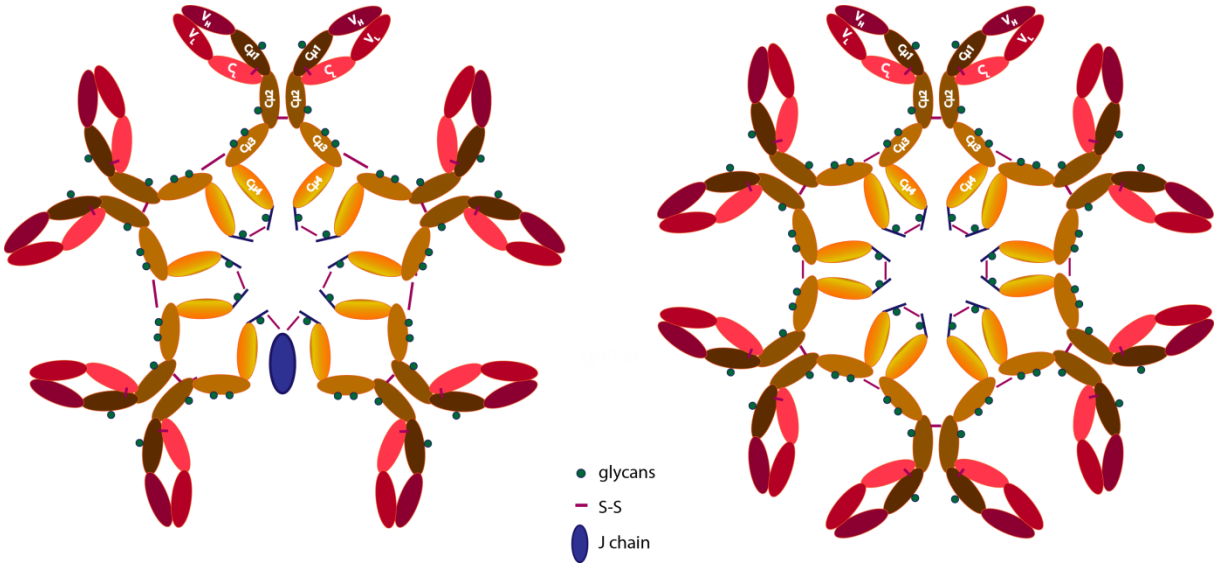

Figure 3.4 Schematic representation of decameric and dodecameric secretory IgM.

Altogether decameric IgM consists of 21 polypeptides bearing in total 51 N-glycans, contain 98 disulfide bonds and possess a MW exceeding 1 megadalton (Anelli and van Anken, 2013). Secretory IgM carry an additional structure, the secretory component (SC) which is linked to IgM via non-covalent interactions (Plaut and Tomasi, 1970). It is assumed that the conformation of IgM decamer prevents the formation of covalent bonds with the SC (Zikan and Bennett, 1973).

IgM do not have a region enriched by proline and cysteine, similar to IgG hinge region. However, at the border of the Cμ1 and Cμ2 domains there are proline residues. During mild treatment of IgM with denaturing agents, Cμ2 region shows some conformational flexibility characteristic for the hinge region. Cμ3 and Cμ4 domains represent real domains of IgM Fc region, whereas the Cμ2 domain is a structure typical only for IgM, which was lost or transformed into hinge region during the evolutionary formation of other Ig classes (Fazel *et al*., 1997; Klimovich, 2011).

3.3.2 Glycosylation

The carbohydrate content of IgM varies from 7 to 12% of the total mass of the molecule (Klimovich, 2011). Each μ chain contains five N-linked glycosylation sites in human secreted IgM (Figure 3.4). Asn171, Asn332, and Asn395 are occupied by complex glycans, which terminate predominantly in galactose or sialic acid, or in a few cases in acetylglucosamine (GlcNAc). Asn402 and Asn563 are occupied by oligomannose glycans (Arnold *et al*., 2005; Klimovich, 2011). LC (κ or λ) are devoid of conserved N-linked glycosylation sites. The J chain

carry a single N-linked glycosylation site at Asn48 with a composition similar to that of complex glycans found in IgM, suggesting that the J chain is fully exposed for glycan processing (Arnold *et al*., 2005).

Glycosylation is important for IgM oligomerization, and essential for IgM secretion and B cell surface presentation (Arnold *et al*., 2005). In particular, glycosylation at Asn563 seems to be important for incorporation of J chain and for the formation of oligomers of correct size. In the absence of the μ tp glycans, decamers cannot be assembled and oligomers consisting of six or more subunits are secreted (de Lalla *et al*., 1998; Klimovich, 2011).

Oligosaccharyl-transferase is the enzyme that attaches a branched oligosaccharide consisting of three glucoses, nine mannoses and two N-acetylglucosamines ($Glu_3Man_9GlcNAc_2$) to the Asn once it has recognized an appropriate sequence, namely Asn-Aaa-Ser/Thr (where Aaa is any amino acid except proline) on the nascent polypeptide (de Lalla *et al*., 1998; Fagioli and Sitia, 2001; Arnold *et al*., 2005). Nilsson and von Heijne (1993) suggested that Asn563 may be a poor substrate for the enzyme due to its proximity to the Cμ4 domain. However, the μ_s tp of most secreted IgM bear high-mannose oligosaccharides moieties (Cals *et al.*, 1996, de Lalla *et al*., 1998, Arnold *et al*., 2005). Wormald *et al.,* (1991) suggested that the presence of oligomannose sugars might confer rigidity to the peptide backbone in the surrounding region.

In general, secreted proteins contain N-linked complex glycans (Kornfeld and Kornfeld, 1985). Glycans of complex type originate from the $Glu_3Man_9GlcNAc_2$ precursors due to activity of glycosidases and glycosyl-transferases spatially distributed in order to allow the sequential processing along the exocytic pathway (Kornfeld and Kornfeld, 1985; Nilsson *et al*., 1993). However, certain glycans of some glycoproteins are not processed and remain in the high-mannose state, which is characteristic for ER resident proteins. IgM are one example of proteins carrying non-processed as well as processed carbohydrates (Cals *et al*., 1996). In effect, glycans of polymeric and dimeric IgM are processed differently. This is mainly due to different accessibility of their glycans, mostly Asn563 glycan. When IgM are secreted in the dimeric form, Asn563 glycan undergoes Golgi mediated processing. When polymers are assembled however, it becomes inaccessible to Golgi enzymes, remaining thus in high-mannose state. Therefore, the occurrence of non-processed glycans at Asn563 implies that IgM oligomerization occurs before encountering Golgi enzymes, such as mannosidase II, likely in a pre-Golgi compartment (Cals *et al*., 1996).

3.3.3 Spatial model

The first model of the IgM oligomer structure derives from negative-stain electron microscopy (EM) images obtained from Feinstein and Munn (1969). They have shown that in the absence of the antigen, the IgM decamer possess a star-shaped, planar conformation with the Fab domains being located at the extremity of each radial arm. When bound to the antigen, the decamer was found to adopt a table-like conformation, with the Fc domains defining the plane which lies on the Fab domains bent away from the plane. In 1991 Perkins *et al*. came to similar conclusion of the IgM antigen-free form from small angle x-ray scattering (SAXS) data. Their molecular models were based on the only antibody crystallographic structures available at the time of the studies, namely on the IgG structure. Thus, the chains in their model formed a plane as well (Czajkowsky and Shaoa, 2009).

Fourteen years later Arnold *et al*. (2005) proposed a spatial model of IgM oligomers on the basis of their glycosylation characteristics. In their model IgM has a disk shape with two qualitatively different surfaces, one containing Cμ4 domains and the J chain, and the other containing Fab domains and complex glycans groups.

Homology analysis of IgM and IgE constant domains and data of crystal structure of IgE Fc region, complemented by observations of atomic force microscopy, allowed Czajkowsky and Shaoa (2009) to produce a more detailed spatial model for IgM oligomers which has one significant difference from the above mentioned one. Assuming that all cysteine residues form disulfide bonds between subunits, the authors concluded that the decameric IgM is mushroom-shaped (Figure 3.5). In their model the plane is formed by radially directed Fab regions whereas the protruding part is formed by Cμ4 domains rotated by 90° to the plane. Müller *et al*. (2013) proposed a similar model of dodecameric IgM Fc based on data of crystal and nuclear magnetic resonance (NMR) structures of single IgM Fc domains and SAXS analysis of Cμ4-tp hexamers of dimers. Thereby, in according with the model of Arnold *et al.* (2005), antigen binding sites and glycan groups would be located on the surface opposite to the protrusion (Klimovich, 2011).

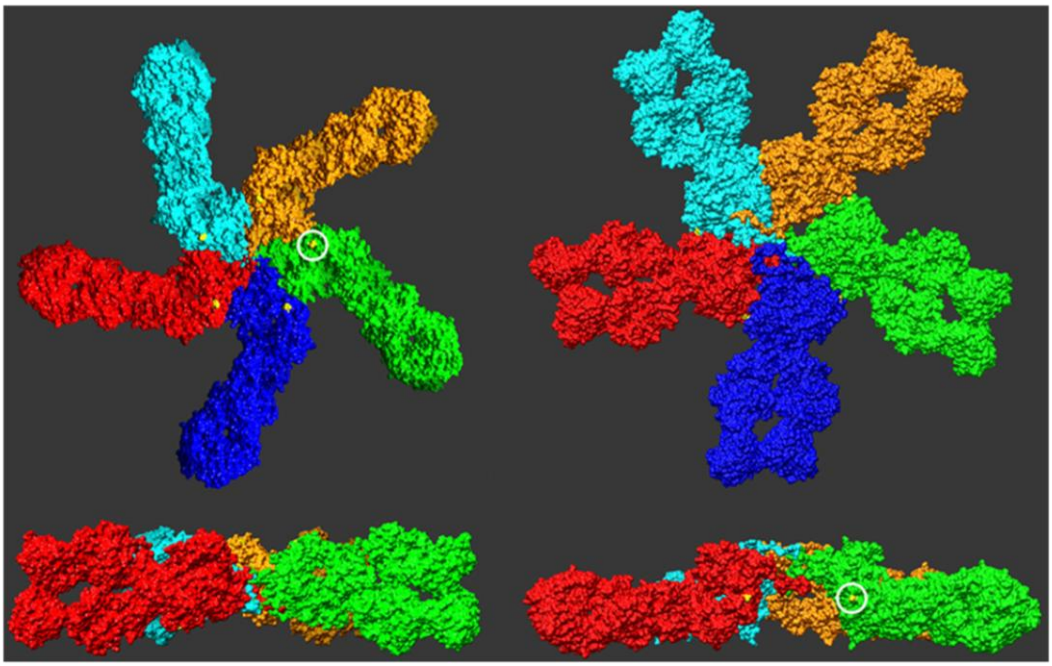

Figure 3.5 Mushroom-shaped model of IgM decamers. In the planar model on the left, the Cys291 residues (circled) are not in a position which enables interaction with a neighboring subunit. By rotating each by 90° about its long axis, the inter-subunit interactions are enabled. However, as shown on the right, the oligomer is not planar anymore, but exhibits a central protrusion, formed by the Cμ4 domains (Figure taken from Czajkowsky and Shaoa, 2009).

3.3.4 Structural requirements for polymerization

3.3.4.1 Non-covalent interactions between μ chains in the IgM polymer

Beale and Buttress (1969) have shown that selective reduction of the Cys337 disulfide bond of mouse polymeric IgM gives non-covalent polymers, whereas reduction of all three inter-chain disulfide bonds gives monomers in physiological buffers, indicating that non-covalent interactions linking μ chains either do not exist or are weak. Furthermore, double mutant IgM-S(414,575) investigated by Wiersma *et al.* (1995) assembled only dimers, giving additional support to this assumption. Hester *et al*. (1975) and Bubb and Conradie (1978) tested more directly interactions between the Cμ3 or Cμ4 domains enzymatically cleaved from isolated and recombinant IgM, respectively. Neither dimerization of Cμ3 as well as of Cμ4 nor any Cμ3-Cμ4 non-covalent interactions could be observed. Müller *et al*., (2013) analyzed oligomerization properties of single recombinant Cμ2-S337, Cμ3-S414, Cμ4 and Cμ4-tp-S575 mutants *in vitro* confirming the occurrence of strong non-covalent interactions between Cμ2 domains (K_d ca. 2 μM) and the absence of them between Cμ3 domains.

However, they observed weak non-covalent Cμ4 and Cμ4-tp-S575 dimers with a K_d of 84 μM and 224 μM, respectively.

All these data indicate that non-covalent interactions involved in the assembly of IgM oligomers are relatively weak. Nevertheless, those occurring between Cμ2 domains in the case of mutants IgM-S337 and IgM-S(337,414) are sufficient to maintain polymers of μ_2L_2 units. Wiersma and Shulman (1995) suggested that polymerization might cause some conformational changes which can enhance non-covalent interactions.

3.3.4.2 Covalent interactions

Based on electron microscopy and synchrotron x-ray scattering data as well on results of studies with cysteine IgM mutants, the actual state of knowledge suggest that covalent interactions in IgM polymers take place between like domains, namely Cμ2-Cμ2, Cμ3-Cμ3, and Cμ4-tp--Cμ4-tp, giving rise to S-S bonds among C337-C337, C414-C414 and C575-C575. Studies with domain-deleted IgM mutants performed by Davis and Shulman (1989) suggested that covalent Cμ2-Cμ2 interactions are important for formation of IgM dimers. Data from structural and mutagenesis studies suggest that covalent Cμ3-Cμ3 as well as Cμ4-tp--Cμ4-tp interactions mediate formation of IgM polymers (Wiersma and Shulman, 1995).

Single-point cysteine mutants investigated by Davis *et al.* (1989) have shown that neither C337 nor C414 nor C575 is absolutely required for polymerization. Both IgM-Ser414 and IgM-Ser575 formed some covalently assembled polymers (decamers and dodecamers, respectively) and IgM-Ser337 gave non-covalent polymers. Comparing the three single-point mutants, the absence of the C575-C575 covalent bond led to the most drastic effect, in that very little polymer was seen, and formation of dimer was also impaired, since the ratio of dimer to monomer was lower than in IgM-wt (Wiersma and Shulman, 1995).

In 1995 Wiersma *et al.* investigated the polymerization ability of double and the triple IgM cysteine mutants. Elimination of all inter-chain bonds by either chemical reduction and alkylation or by mutagenesis resulted in production of solely monomers (μL). Each of the six double mutants produced mixtures of polymers, dimers, and monomers. The authors concluded that: 1) Cys575 was both necessary and sufficient for efficient assembly of IgM polymers and sufficient but not necessary for efficient assembly of dimers; 2) Cys414 was neither necessary nor sufficient for efficient formation of either dimers or polymers;

3) Cyst337 was sufficient but not necessary for efficient assembly of dimers, and was neither sufficient nor necessary for formation of polymers.

Subsequently Wiersma *et al.* (1998) suggested that in dodecameric IgM each μ chain might be linked to three rather than to only two μ chains, as it is conventionally depicted.

However, the exact role of these cysteines in IgM assembly and oligomerization still needs to be deeply elucidated.

3.3.4.3 Fcμ domains

The occurrence of an additional domain on the C-terminus, the 18-residue tail segment in the μ and α heavy chains, suggests that it might be relevant for assembly of polymers. Davis *et al*. (1989) observed that deletion of the tp by introducing stop codons at the end of the Cμ4 domain prevented polymer production, indicating that this segment is essential for assembly of IgM polymer.

To delineate the motifs in the α and μ chains that regulate class-specific polymerization several research groups have constructed chimeras containing IgM/IgA, IgA/IgM or IgM/IgG elements (Johansen *et al*., 2000). Chimeric human IgM containing the α tp (IgM-αtp) was found to polymerize like IgM, however with increased dodecamer formation (Sorensen *et al*., 1996). The reciprocal IgA-μtp mutant led to formation of some polymers bigger than wild type pIgA (Braathen *et al*., 2002). IgG containing either μ or α tp induced formation of polymers including decamers and dodecamers (Smith and Morrison, 1994; Smith *et al*., 1995; Sorensen *et al*., 1996; Yoo *et al*., 1999). All these results suggested that although the secretory tp is sufficient to lead to polymerization process, alone it is not able to direct the number of subunits incorporated into the polymers (Braathen *et al*., 2002).

Sorensen *et al*. (1999), Yoo *et al*. (1999) and Braathen *et al*. (2002) performed additional studies with domain-swap mutants aiming to the same above mentioned end. Their studies have demonstrated that the Cμ1 domain does not influence the number of subunits incorporated during polymerization. This conclusion is supported by observations of Kohler *et al*. (1982) which indicated that IgM lacking the Cμ1 domain is also secreted as polymers and of Bornemann *et al*. (1995) who showed that immunoglobulin LC, normally bound to the Cμ1 domain, are not required for efficient polymerization of IgM. Cμ2 region was found to be non-essential for IgM decamer assembly (Poon *et al*., 1995; Sorensen *et al*., 2000). Cμ3 and Cμ4 domains were identified as most important for IgM-like polymerization (Sorensen *et*

al., 1999; Yoo *et al*., 1999; Braathen *et al*., 2002). Müller *et al*., (2013) found that recombinant Cμ4-tp domain is sufficient to form hexamers of covalent Cμ4-tp dimers *in vitro*.

By studying residues on the Cμ3 domain which could affect the complement-dependent cytolytic activity, Arya *et al*. (1994) identified some residues which impair IgM polymerization. Mutations such as D356A, K361A and D417G significantly impaired polymer formation probably by affecting the folding of the domain, whereas H430A/N/Q mutations led to assembly only of dimers.

3.3.4.4 Glycosylation

The glycans present on both α and μ tp as well as on J chain play a role in polymerization. When μ tp is devoid of carbohydrates, IgM decamers cannot be assembled and dodecamers and aggregates are secreted (de Lalla *et al*., 1998; Klimovich, 2011).

Elimination of the carbohydrate from either J chain or α tp leads to increased formation of polymers bigger than wild type pIgA (Yoo *et al*., 1999). The μ tp oligosaccharide has been shown to be required for incorporation of J chain (Wiersma *et al*., 1997). This glycan has been reported to be in the high-mannose state (Arnold *et al*., 2005), whereas that of the α tp of IgA1 is a complex oligosaccharide (Yoo *et al*., 1999). The differences in composition between IgA and IgM tp carbohydrates suggest that the two tps differ in their accessibility to glycosyl-transferases, responsible for glycan processing. The glycosylation of chimeric IgA-μ tp is heterogeneous and contains glycans in oligomannose state, sensitive to Endo H digestion, whereas all of the glycans on wild type IgA are complex, and thus Endo H-resistant. The observation that the tp glycan of chimeric IgA-μtp is similar to that of the IgM tp glycan suggests that changing the tp alters the overall three-dimensional conformation of the polymeric IgA-μtp, which results in limited accessibility of its tp glycan for processing by the glycosyl-transferases (Yoo *et al*., 1999).

Hickman and Kornfeld (1978) and Tartakoff and Vassalli (1979) investigated the effect of glycosylation inhibitors, such as tunicamycin, on polymerization. Their data showed that although IgM secretion is severely inhibited by tunicamycin, the IgM polymers can still form, indicating that glycosylation of the μ heavy chain is not essential for formation of IgM polymers.

3.4 J chain

3.4.1 Functional aspects

The J chain is a small polypeptide which is incorporated exclusively into polymeric IgA or decameric IgM. It is expressed by mucosal and glandular plasma cells (Johansen *et al*., 2000; Schroeder and Cavacini, 2010).

Up to date, two functions have been attributed to J chain. First, it regulates the assembly of IgM and IgA by modulating their structure and thereby their effector functions (Wiersma *et al*., 1997; Sorensen *et al*., 2000). In the presence of J chain, relatively more decamers and less dodecamers are assembled and tetrameric IgA are formed (Wiersma *et al*., 1998). Second, by binding the pIgR it allows pIgA as well as decameric IgM to be secreted into extravascular fluids (Figure 3.6) (Wiersma *et al.*, 1997; Johansen *et al*., 2000). The pIgR mediates transcytosis of pIg from the basolateral to the apical face of exocrine epithelial cells, releasing them into mucosal fluids (Johansen *et al*., 2000).

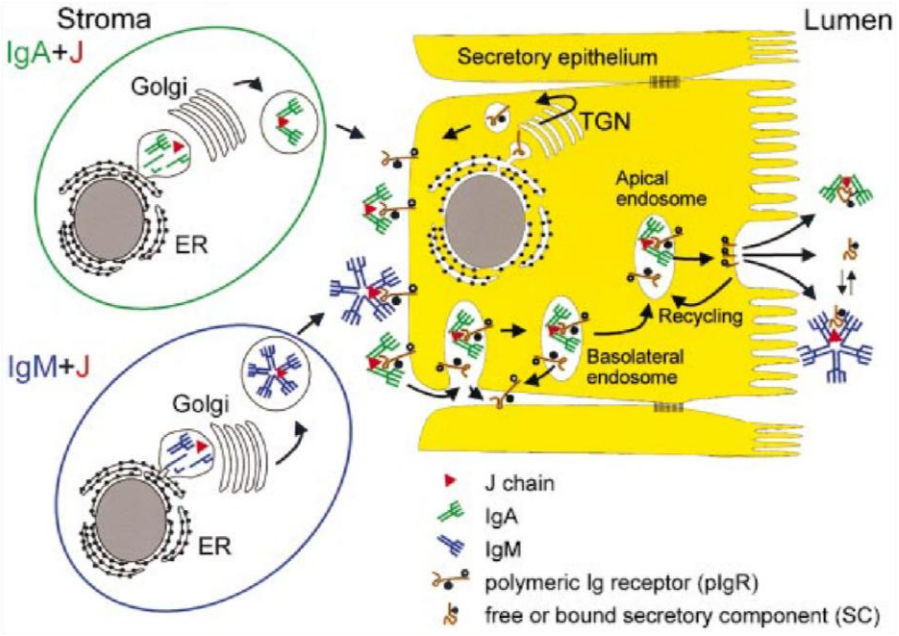

Figure 3.6 Model for assembly of pIg. IgA and IgM plasma cells produce tetrameric IgA and decameric IgM by incorporating J chain during assembly occurring in the ER. Only correctly assembled oligomers leave the ER to be processed in the Golgi prior to secretion into the extracellular space. pIgR/transmembrane SC is expressed in the secretory epithelial cells, where it is incorporated into the basolateral plasma membrane via trans-Golgi network (TGN). The binding of pIg to pIgR mediated by J chain is followed by endocytosis. Basolateral endosomes are transcytosized to apical endosomes. Here most pIgR is cleaved and pIgA, pIgM and free SC are released to the lumen. SC is covalently linked to pIgA and non-covalently to pIgM (Figure taken from Johansen *et al*., 2000).

Although J chain is not required either for IgM assembly or for its secretion, it does affect assembly, since its presence significantly increases the amount of secreted decameric IgM (Davis and Shulman, 1989; Brewer and Corley, 1997). Randall *et al*. (1992) showed that J chain is incorporated late in the polymerization process and Brewer and Corley (1997) suggested that its insertion might be thermodynamically favored over incorporation of the sixth IgM subunit. J chain has never been shown to be present in IgM dodecamers (Davis *et al*., 1988; Randall *et al*., 1990). The fact that only the non-cytolytic IgA and the less cytolytic decameric IgM are transcytosized suggests that the organism might have some physiologic advantage of it, such as avoiding inflammatory reactions in tissues strongly exposed to antigens. Here simple aggregation of foreign immunogens might thus suffice for efficient and effective neutralization (Wiersma *et al*., 1998). Unlike that of IgM, the assembly of IgA strongly depends on J chain, although small amounts of tetrameric IgA have been shown to form in J chain knockout mice (Sorensen *et al*., 2000).

Furthermore, the rate of IgM assembly or secretion does not seem to be influenced by J chain presence in that decamers and dodecamers appear to possess similar kinetics with this regard (Randall *et al*., 1992; Brewer *et al*., 1994; Brewer and Corley, 1997).

3.4.2 J chain structure

The J chain is a highly conserved 15 kDa polypeptide (Schroeder and Cavacini, 2010). The mouse and human J chain consists of 137 amino acids. One their interesting feature is an unusually high content of negatively charged residues (Glu and Asp), a low content of phenylalanine, glycine, and serine and the absence of tryptophan (Klimovich, 2008). J chain contains 8 cysteine residues. Six of them form three intra-chain disulfide bonds (Cys12–Cys100, Cys71–Cys91, Cys108–Cys133), and two (Cys14 and Cys68) form S-S bonds to the tp penultimate cysteine, the Cys575 in decameric IgM (Frutiger *et al.,* 1992) or the Cys495 in tetrameric IgA (Bastian *et al*., 1992).

J chain has no homologues since it failed to be attributed to any family of known proteins. Sequence analysis of J chain genes in mammals, amphibians, reptiles, and cartilaginous fishes has shown a homology degree varying from 33% to 70%. The mouse and the human J chain share 77% of similarity. The J chain gene is present in all vertebrate classes except for cyclostomes and bony fishes (Klimovich, 2008). Takahashi *et al.* (1996) published data about the presence of the J chain gene homologues in invertebrates, tunicates, and cyclostomes.

However, Hohman *et al*. (2003) indicated the necessity of revising the notion regarding the presence of J chain in invertebrates.

The J chain of vertebrates contains several highly conserved sites. These are the eight cysteines which are found in practically identical positions, the residues surrounding the cysteines and the site of N glycosylation, Asn48 in mouse and Asn49 in human, suggesting that they might be functionally important (Klimovich, 2008).

Due to the presence of eight cysteines, the secondary structure of J chain might be complex. Attempts to study its three-dimensional conformation with traditional methods, such as roentgen-structure analysis and NMR, have failed. However, three hypothetical models on J chain structure have been developed based on amino acid sequence analysis, absorption spectra and data on disulfide bonds arrangement (Klimovich, 2008). The first model was proposed by Cann *et al*. (1982) on the basis of differences in amino acid sequences in N and C terminal parts. The authors proposed a two-domain model, with the N-terminal region having β sheet conformation and the C-terminal α helical segments (Figure 3.7A).

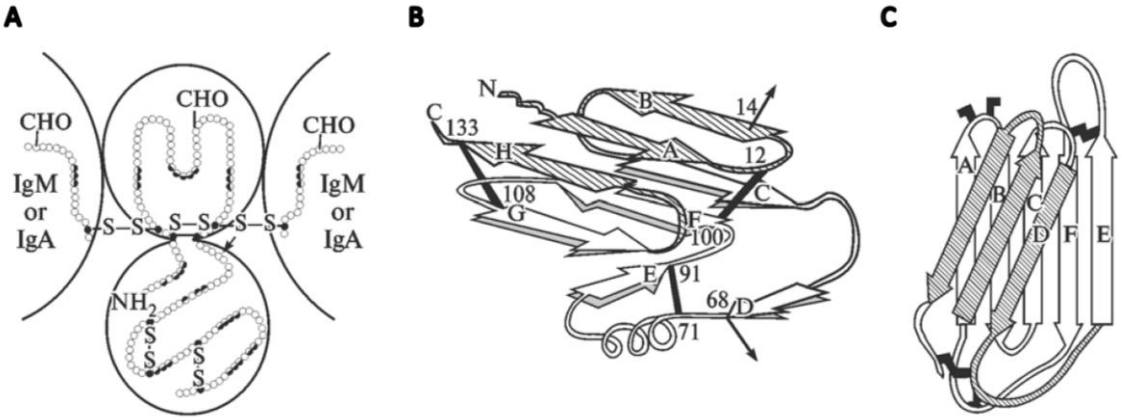

Figure 3.7 Three hypothetical models of the three-dimensional structure of J chain. (A) Two-domain model proposed by Cann *et al*. (1982). Hydrophobic amino acids are highlighted by semi-hatched circles and cysteine residues by fully hatched circles. (B) Two-domain model modified by Frutiger *et al*. (1992). β strands are indicated by large arrows (A-H) and intra-chain disulfide bonds by bold lines; disulfide bonds taking place between heavy α or μ chains and cysteines 14 and 68 are shown by arrows. A, B, G, H, and F strands form the first, whereas C, D strands and E α spiral site between two latter form the second domain. (C) Single-domain model suggested by Zikan *et al*. (1985). β strands are represented by light wide arrows and possible location sites of disulfide bonds by black zigzags (Figure taken from Klimovich *et al*., 2008).

Frutiger *et al*. (1992) subsequently modified this model as result of resolution of the precise disulfide bond pairing in J chain. In their two-domain model the C-terminal region displays a mixture of α helices and β strands (Figure 3.7B). The second model, a single-domain model, was developed by Zikan *et al*. (1985) on the basis of measurement of circular dichroism (CD)

and computer analysis of the ratio of hydrophobic to hydrophilic parts. According to this model, J chain adopts a β barrel structure consisting of eight folded antiparallel β strands organized to form two sheets, namely an Ig-like domain (Figure 3.7C) (Johansen *et al*., 2000; Klimovich, 2008).

However, the real three-dimensional structure of J chain still has to be determined. The major difficulties are due to the tendency of the J chain to form covalent aggregates via its free thiol groups. Replacement of N-terminal cysteine residues with serine might allow obtaining soluble protein (Redwan *et al*., 2006; Klimovich, 2008).

3.4.3 Structural requirements for J chain incorporation

J chain insertion into pIgs depends not only on the amount of J chain available but also on structural characteristics in the C-terminal domains of the μ and α chain (Yoo *et al*., 1999).

Non-covalent interactions in IgM between μ heavy chains and J chain are relatively weak, since J chain dissociates from them upon disruption of disulfide bonds by reduction and alkylation under non-denaturing conditions (Wiersma *et al.,* 1997). However, in tetrameric IgA it can be present in non-covalently bound form (Johansen *et al.*, 2001).

In the last two decades several studies have been performed by different groups with the aim to identify motifs in the heavy chains required for J chain incorporation. To this purpose the ability of hybrid molecules IgM/IgA, IgA/IgM or IgM/IgG as well as of single-point cysteine mutants for J chain insertion has been investigated.

Thus, IgM-αtp formed prevalently dodecamers lacking J chain, whereas IgA-μtp several polymers containing J chain (Yoo *et al*., 1999). IgG/IgM chimeric molecules confirmed the relevance of Cμ4 and Cμ3 domains in addition to Cys414 for J chain incorporation into IgM polymers, while Cμ1 and Cμ2 did not seem to be specifically required (Sorensen *et al*., 2000; Johansen *et al*., 2000).

Moreover, J chain was absent in polymeric IgM-S575, which is mainly dodecameric (Davis *et al.*, 1988; Davis and Shulman, 1989). Only decameric and octameric IgM-S414 contained J chain, whereas no J chain was found in smaller polymers or dodecamers (Yoo *et al*., 1999; Sorensen *et al*., 2000). J chain is present also in IgM-S337 (Davis *et al*., 1988; Davis and Shulman, 1989).

These results suggested that J chain can be inserted only into several IgM polymers, which is in agreement with the assumption of Brewer and Corley (1997), who hypothesized that J

chain binds the IgM polymer at a late stage during polymerization and that binding with J chain is established only then when a specific polymeric conformation has been achieved (Sorensen *et al.,* 2000).

All these data demonstrate the critical role of the tp, the Cμ4 domain, and the Cμ3 domain for J chain inclusion into IgM. Moreover, whereas J chain insertion is limited to several IgM polymers, IgA polymers seem to incorporate J chain equally efficient (Sorensen *et al.,* 2000).

Furthermore, Wiersma *et al*. (1997) and de Lalla *et al*. (1998) found that glycosylation at Asn563 of μ tp affect J chain incorporation. Glycan absence in this position by replacement of either Asn563 by tyrosine or Ser565 by alanine led to decreased J chain incorporation and increased production of IgM dodecamers and aggregates (Sorensen *et al*., 2000).

4 Objectives

This work had three main objectives: first, to characterize the process of Cμ4-tp oligomerization which leads to the formation of dodecameric units; second, to better define the structural requirements necessary for formation of IgM polymers and, finally, to characterize the J chain, a small protein incorporated in IgM decamers but not dodecamers.

The characterization of the Cμ4-tp oligomerization process was achieved by performing kinetic studies and analyzing the effect of the parameters which influence association processes such as temperature and reactant concentration. Moreover, the role of covalent and non-covalent interactions, which together lead to the formation of Cμ4-tp dodecamers was investigated. To this end, on the one hand point mutants have been generated where the C575 was replaced with alanine, which is isovolumetric and hydrophobic, and with serine, isosteric and polar (Xia *et al*., 2014). On the other hand free C575 of the wt Cμ4-tp was irreversibly blocked in kinetics experiments.

One structural motif that has been demonstrated to be essential for IgM polymerization (Davis *et al*., 1989; Davis and Shulman, 1989) and for formation of Cμ4-tp dodecamers (Müller *et al*., 2013) is the tail piece, an 18-amino acid extension of the μ chain located on its C-terminus. To better elucidate the role of this segment and define the participation of its amino acids in the oligomerization process, point mutants were generated by serially replacing every single tp amino acid with alanine in the Cμ4-tp as well in the IgM context. The ability to form oligomers of the former was investigated *in vitro*, whereas that of the latter in transfected HEK293 cells. Furthermore, additional mutants were generated in order to study the relevance of the tp S-S bond position, the role of T576 and whether and to which extent the tp is able to drive class- and the isotype-specific oligomerization. Finally, the oligomeric state and secondary structure of the synthesized tp and its mutants were investigated.

The murine and human J chain was characterized by analysing the secondary structure and disulfide bond arrangement of the isolated monomeric form. Moreover, its ability to interact with the Cμ4-tp and two chaperones such as BiP and βHsp90 *in vitro* was evaluated.

5 Results

5.1 Characterization of the Cμ4-tp refolding process

The Cμ4-tp domain was obtained from *E. coli* as inclusion bodies (IBs). It was therefore necessary first to denature, oxidize and then to isolate the monomer before starting studying its oligomerization properties *in vitro* (Figure 5.1).

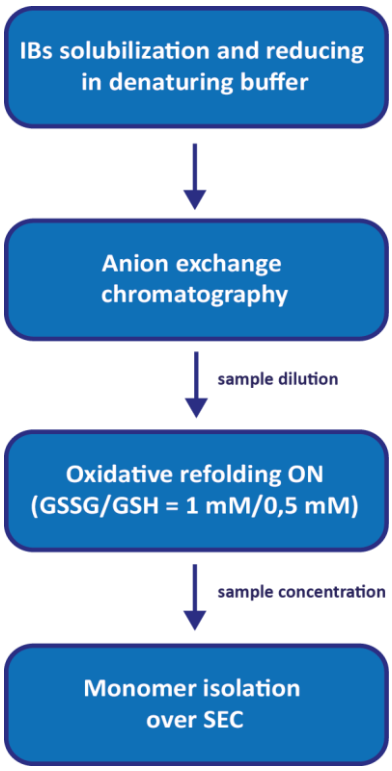

Figure 5.1 Schematic overview of the standard overnight (ON) refolding and purification process of the Cμ4-tp domain.

Like all Ig domains, the IgM Cμ4-tp domain also needs to be stabilized by an intra-domain disulfide bond (S-S bond) in order to stably maintain the so called Ig-fold, which is made of two β sheets, each consisting of 7-9 antiparallel β strands around a central hydrophobic core. The single intra-domain Cμ4-tp S-S bond between the Cys474 and the Cys536 (Müller *et al*., 2013) bridges the two sheets. To allow the oxidation of these cysteines a mixture of oxidized and reduced glutathione (GSSG/GSH = 1 mM/0,5 mM) was added to the refolding

buffer, with the oxidized form in excess. The Cμ4-tp domain possesses one additional cysteine (Cys575) located in the penultimate position of the tail piece which can form an inter-domain S-S bond with the Cys575 of an adjacent tp. To better investigate how fast the intra-domain S-S bond forms during the refolding step, the oxidation kinetics was investigated by addition of AMS (4-acetamido-4′-maleimidylstilbene-2,2′-disulfonic acid) at definite time points. The samples were subsequently analyzed by SDS-PAGE (Figure 5.2). AMS irreversibly binds the free thiols of reduced proteins hindering thus the formation of S-S bonds between the blocked cysteines (Vestweber and Schatz, 1988; Balciunas, 1993).

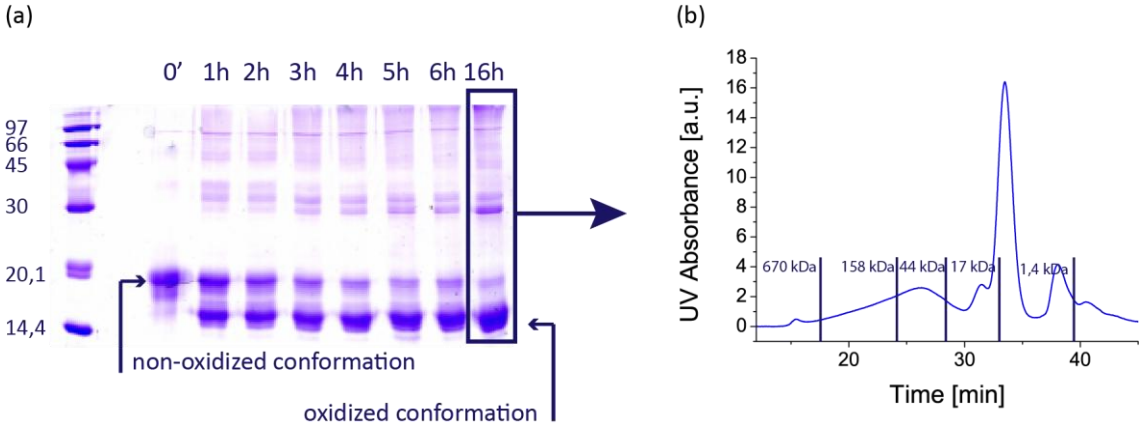

Figure 5.2 Kinetics of disulfide bond formation during refolding of Cμ4-tp. a) The Q FF flow through was subjected to refolding via dialysis and AMS was added in large excess (10 mM final concentration) to the samples at the indicated time points which were then analysed by non-reducing 15% SDS-PAGE. b) SEC-HPLC profile (Superdex 200 10/300 GL) of the Cμ4-tp domain after an ON refolding step.

The SDS-PAGE analysis showed that the Cμ4-tp monomer (ca. 14,7 kDa) was the prevalent species present during as well as after the refolding step (Figure 5.2a). Moreover, a progressive shift of the monomer band from ca. 19 kDa to ca. 15 kDa could be observed. This is due to the formation of the intra-domain S-S bond which renders the monomer structure more compact, allowing thus a faster electrophoretic migration. Furthermore, the oxidation of cysteines forming the intra-domain S-S bond began immediately and occurred mostly within the first 4-5 hours**.** The formation of S-S bonds beween two Cμ4-tp domains due to Cys575 oxidation, and therefore the formation of covalent dimers, was much slower and after an ON refolding their amount was very low, as indicated by the small band around 30 kDa. The size exclusion chromatography (SEC) profile under native conditions (in PBS) of the

refolded sample further confirmed that the main species present after the refolding step was the Cμ4-tp monomer represented by the main peak eluting at ca. 33 min (Figure 5.2b).

To investigate its oligomerization properties, the Cμ4-tp monomer was isolated by processing the 15-fold concentrated refolded sample over a preparative size exclusion column. Its purity was checked by analytical SEC (Figure 5.3a). The far-UV CD spectrum of the isolated monomer confirmed the β sheet conformation and therefore the correct folding state as indicated by the single ellipticity minimum at ca. 219 nm (Figure 5.3b).

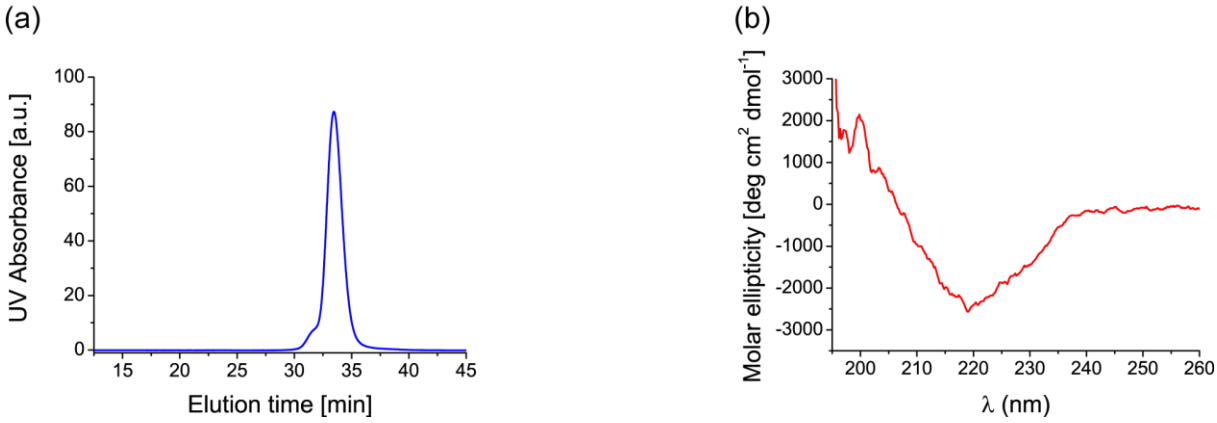

Figure 5.3 Characterization of the isolated Cμ4-tp monomer in PBS at 20°C: a) SEC-HPLC profile on the Superdex 200 10/300 GL; b) Far-UV CD spectrum acquired at a protein concentration of 20 μM (ca. 0,3 mg/ml).

5.2 Characterization of the Cμ4-tp oligomerization process

5.2.1 Analysis of the oligomerization kinetics

The Cμ4-tp domain was shown to possess oligomerization properties and associate into dodecamers or hexamers of covalent dimers i.e. $[(C\mu4\text{-}tp)_2]_6$ (Müller *et al*., 2013). In an experiment aimed to investigate the oligomeric state of the Cμ4-tp domain, surprisingly a dodecamer was detected analyzing the monomer sample on SEC-HPLC several days after its isolation and storage at 4°C. Therefore, to assess whether the Cμ4-tp domain is spontaneously able to undergo a self-association process once it has been refolded and isolated, a kinetic study was performed starting immediately upon monomer isolation. To better resolve the dodecamer formation, the monomer samples were stored at 4°C over 30 days and analyzed at definite time points on SEC-HPLC. The HPLC chromatograms indicated the presence of four species already one day after isolation (day 1), corresponding to the dodecamer (eluting at ca. 22 min.), to the octamer (eluting at ca. 26.5 min.), to the dimer (eluting at ca. 31 min.) and to the monomer (eluting at ca. 33 min.) (Figure 5.4a). The Cμ4-tp dodecamer began to form immediately and the oligomerization went on over the entire time rage under investigation, although with a much decreased rate from day 9 onwards, indicating that the oligomerization rate depends on the concentration of the reactants. This was confirmed also by the form of the monomer curve which is not a straight line, typical for zero-order kinetics, independent of reactant concentration (Figure 5.4b). While the Cμ4-tp dodecamer amount increased and that of the monomer decreased over the time, the amount of the octamer and the dimer significantly increased only from day 0 to 1 reaching levels (peak area ca. 2% and 25%, respectively) that remained almost unaltered the following days, with a slight tendency to decrease.

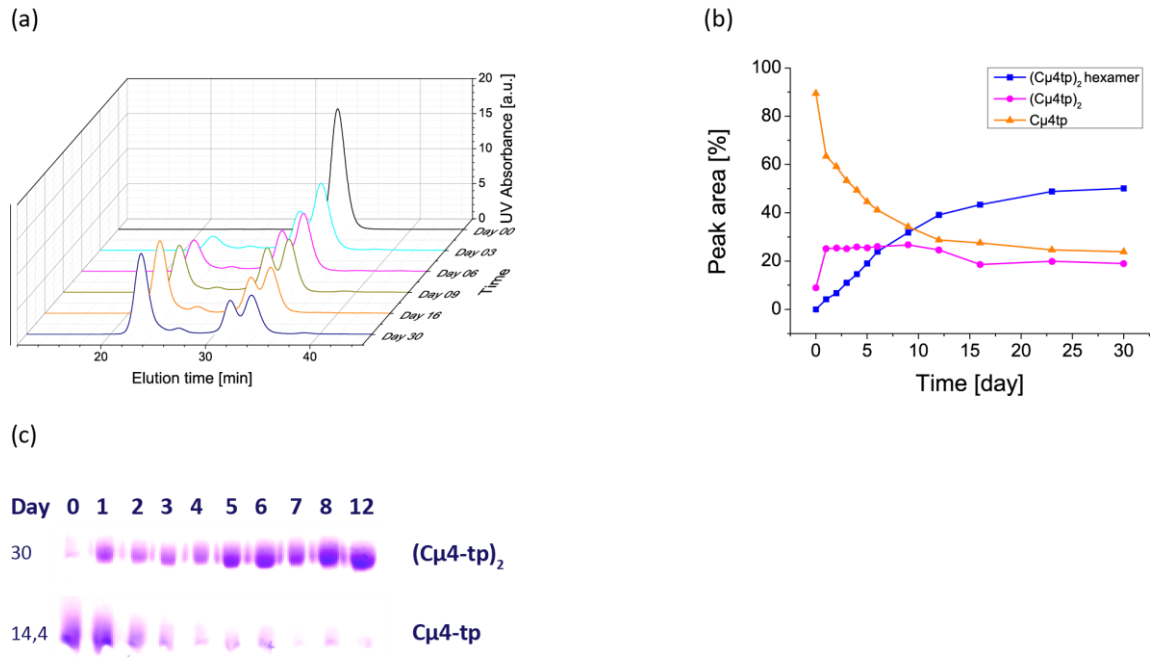

Figure 5.4 Kinetics of the formation of the Cμ4-tp dodecamer. Cμ4-tp was refolded and purified as outlined above. SEC fractions containing the Cμ4-tp monomer were pooled and the concentration was adjusted to 1 mg/ml (69 µM). Aliquots were stored at 4°C and analyzed at the indicated time points. a) SEC-HPLC profiles on Superdex 200 10/300 GL in PBS at 20°C. For each time point 100 µg of sample were injected. b) Monomer, dimer and dodecamer formation over time. c) SDS-PAGE analysis under non-reducing conditions of AMS-blocked samples. At each time point, 100 µl of sample were removed from the aliquot and an excess of AMS (10 mM final) was added.

On the other hand, the SDS-PAGE analysis of the same kinetic samples treated with AMS clearly showed an increase in intensity of the band corresponding to the covalent dimer (Figure 5.4c). Thus, together the SEC-HPLC and the SDS-PAGE data indicated that the Cμ4-tp dodecamer is a result of non-covalently assembled covalent dimers suggesting that the overall reaction of the Cμ4-tp dodecamer formation must proceed with two elementary steps, the first one consisting in the formation of the covalent dimers, which then non-covalently associate into hexamers of dimers.

5.2.1.1 Analysis of the temperature effect on the oligomerization kinetics

An increase in temperature accelerates a reaction not only because at higher temperatures reactants collide more frequently but mainly because a higher portion of molecules possess sufficient energy to react, i.e. their energy (E) is greater than the activation energy (E_a). To examine whether the dodecamer formation can be accelerated by increasing the temperature and by additionally enhancing the chances of reactants to collide, a kinetic study was performed under two conditions. In both cases the monomer samples were

stored at 25°C but in the first case with no additional motion and in the second case they were stirred.

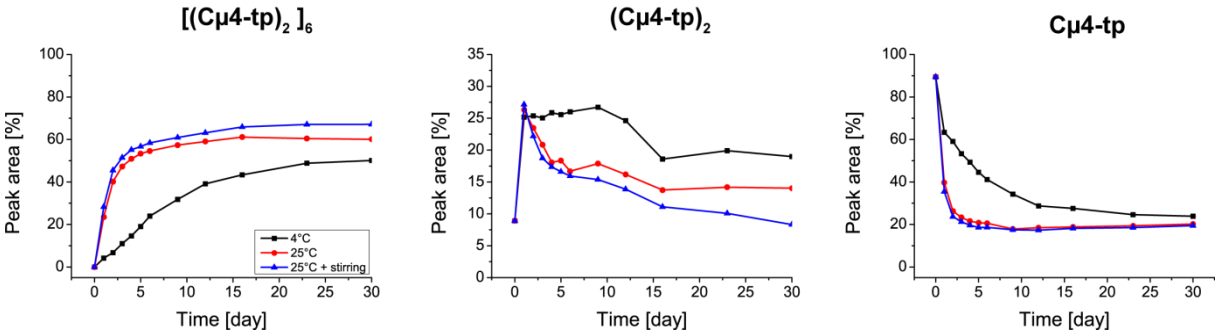

Figure 5.5 Effect of the temperature and stirring on the rate of dodecamer formation. Cμ4-tp was refolded and purified as described above. SEC fractions containing the Cμ4-tp monomer were pooled and the concentration was adjusted to 1 mg/ml (69 μM). Aliquots were stored at 25°C with no additional motion (red line) and under stirring (blue line). SEC-HPLC runs were performed injecting 100 μg of protein for each run at the indicated time points.

As expected, dodecamer formation occurred significantly faster at 25°C compared to that at 4°C, reaching the plateau on day 15, whereas the plateau at 4°C seemed not to be reached within the time of investigation (Figure 5.5). Additionally, stirring samples did not further increase the oligomerization rate, confirming that the temperature effect on the reaction rate is due mainly to the higher thermal energy of the molecules.

5.2.1.2 Analysis of the concentration effect on the oligomerization kinetics

Next how Cμ4-tp dodecamer formation rate varies with increasing concentration of the Cμ4-tp monomer (Figure 5.6) was investigated. The experiment was performed at concentrations ranging from 1 mg/ml to 30 mg/ml. SEC-HPLC data indicated that the oligomerization process could be accelerated simply by concentrating the monomer. The higher the initial monomer concentration was, the faster the dodecamer formed and also its amount increased.

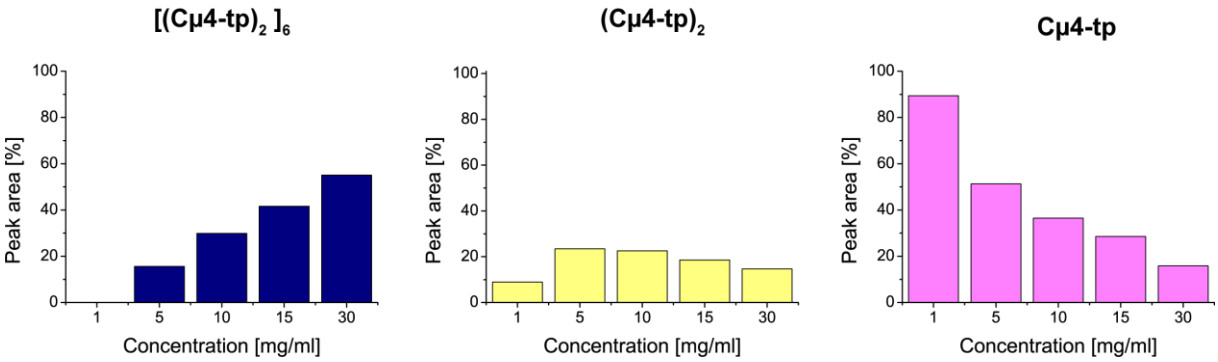

Figure 5.6 Effect of the increase of the initial monomer concentration on the rate of dodecamer formation. The Cμ4-tp domain was refolded and isolated under standard conditions. After isolation the protein concentration was adjusted to 1, 5, 10, 15 and 30 mg/ml. SEC-HPLC runs were performed injecting 100 µg of protein for each run.

However, even at a concentration of 30 mg/ml it was not possible to obtain the pure dodecamer. Müller *et al*. (2013) showed that the Cμ4-tp dimer and dodecamer are in an equilibrium which is concentration dependent. A possible reason for the fact that the monomer has not been consumed might be that the concentration of 30 mg/ml was not high enough or that the monomer left was completely in the non-oxidized form. Indeed, when the remaining monomer left was isolated, concentrated to 15 mg/ml and then processed over a preparative SE column for the second time, it showed a negligible amount of dimers as well as of dodecamers, indicating that oligomerization was blocked due to the fact that no further dimer formation was possible (data not shown).

Furthermore, to test whether the monomer would have been completely consumed over time, freshly isolated Cμ4-tp monomer was concentrated to 10 mg/ml, 20 mg/ml and 30 mg/ml and analysed over 5 days at room temperature (Figure 5.7). The monomer amount decreased upon concentration, but over time it surprisingly increased, whereas those of dimers and dodecamers decreased. This effect was much more pronounced, the higher the initial monomer concentration was. The most probable explanation for this is the increase of the GSH concentration in the sample as that of the dodecamer increases, which then leads to the inverse reaction. During the oxidative refolding the GSSG reacts with the Cys575-thiolate of some Cμ4-tp monomers producing Cμ4-tp-S-SG, which is the precursor of the covalent dimer, and one molecule of free GSH. During oligomerization the remaining free Cμ4-tp-thiolate reacts with the dimer precursor producing the covalent Cμ4-tp dimer and a second molecule of free GSH. Thus, for every molecule of covalent dimer being formed, two molecules of GSH are produced. The higher the rate of oligomerization and amount of

dodecamer formed, the higher the rate of release and amount of GSH produced. Thus, at a highest analyzed concentration, namely 30 mg/ml the amount of GSH produced was the highest, shifting thus faster the reaction towards monomer formation.

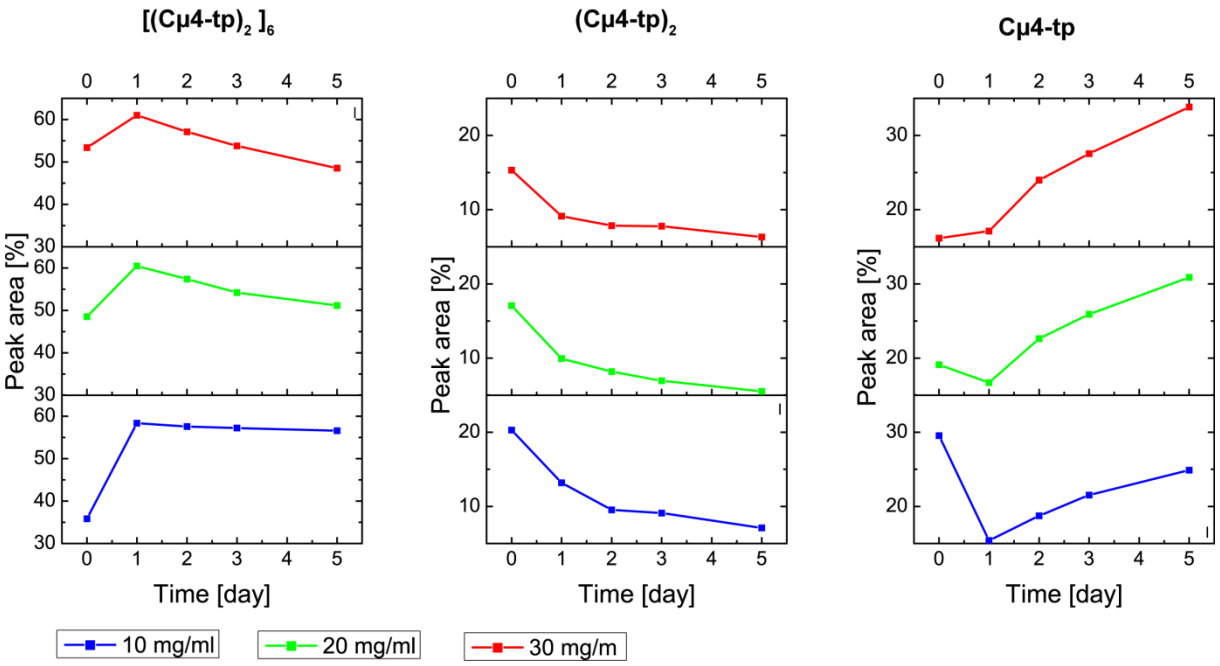

Figure 5.7 Effect of the increase of the initial monomer concentration on dodecamer formation over time. The Cμ4-tp domain was refolded and isolated under standard conditions. After isolation the protein concentration was increased to 10, 20 and 30 mg/ml. Samples were aliquoted and stored at room temperature. SEC-HPLC runs were performed injecting 100 µg of protein for each run.

5.2.1.3 Analysis of the influence of the redox system on the oligomerization kinetics

Previous results indicated that S-S bonds might be decisive for the oligomerization process. To acquire a deeper understanding of the role of the formation of the inter-domain S-S bond on the Cμ4-tp oligomerization process, the extent of its formation was varied. One way to manipulate the formation of S-S bonds is to act on cysteine oxidation by varying the concentration of the redox system during the refolding step as well as during the oligomerization step. To this point, two parallel experiments were performed. In the first experiment in addition to the standard ratio of the redox system (GSSG/GSH = 1 mM/0,5 mM) used to refold the Cμ4-tp domain, three additional redox conditions were investigated during the refolding step (Figure 5.8a). After refolding, the sample was processed following the standard protocol for monomer isolation as described above. In the second experiment, the sample was refolded under the standard ratio of the redox system and then processed

according to the standard protocol. After monomer isolation, the monomer was additionally dialysed overnight (ON) against PBS containing the same four redox system conditions (Figure 5.8b). In both experiments the monomer sample was aliquoted and stored at 4°C. Each aliquot was analysed with SEC-HPLC at definite time points.

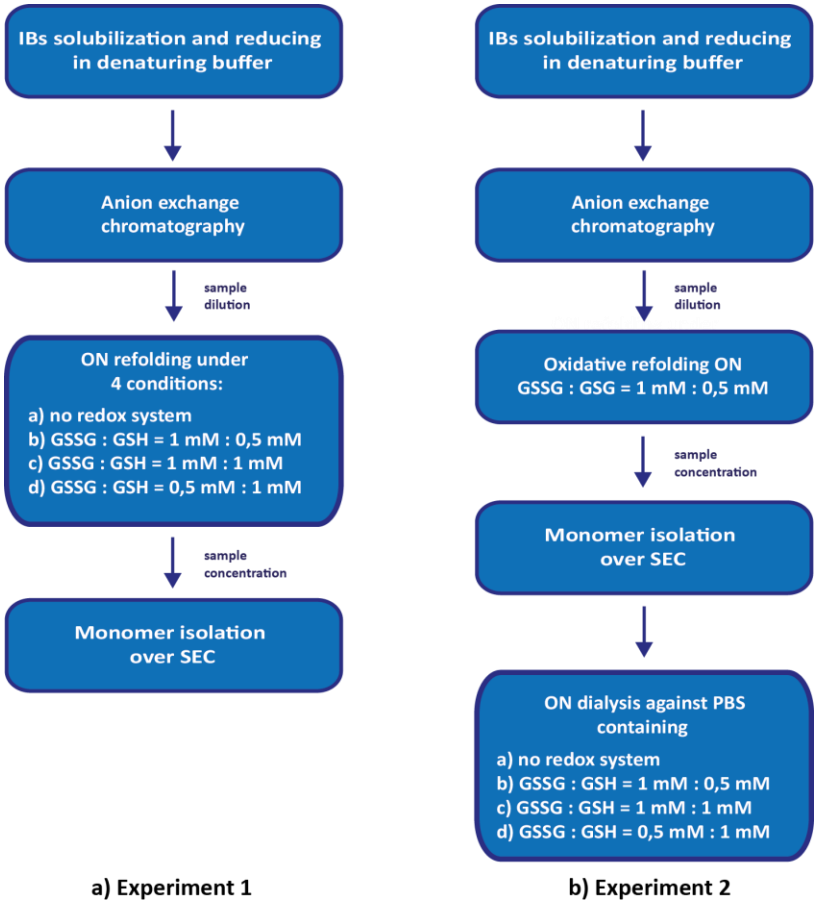

Figure 5.8 Schematic overview of two experiments performed in order to investigate the role of S-S bonds in the oligomerization process. Experiment 1: the Cμ4-tp domain was refolded under four different redox conditions and then processed according to the standard protocol. Experiment 2: the Cμ4-tp domain was refolded under the standard GSSG/GSH ratio. After monomer isolation an additional dialysis step was performed in order to introduce the redox system during oligomerization step.

The experiments showed that the oligomerization process proceeded faster when the Cμ4-tp domain was refolded in a more oxidizing environment (Figure 5.9, red bar). Under this condition, more GSSG can undergo the thiol-disulfide exchange reaction upon nucleophilic attack by the Cμ4-tp thiolate of Cys575 resulting in the formation of Cμ4-tp-S-SG, the precursor of the covalent dimer. The latter is formed when another Cμ4-tp thiolate attacks this disulphide bond producing a covalent Cμ4-tp-S-S-tp-Cμ4 dimer. When refolding occurred under more reducing conditions (excess of GSH) dodecamers could still be formed

although to a much smaller extent (Figure 5.9, pink bar). Of note, in the absence of the redox system Cμ4-tp oligomerization could, although much slower, still occur due to cysteine oxidation most likely due to air oxidation. For this condition, the monomer decrease over time resembled more a straight line than a curve, indicating that the reaction might be concentration-independent in the absence of any catalyst such as glutathione at an oxidizing ratio.

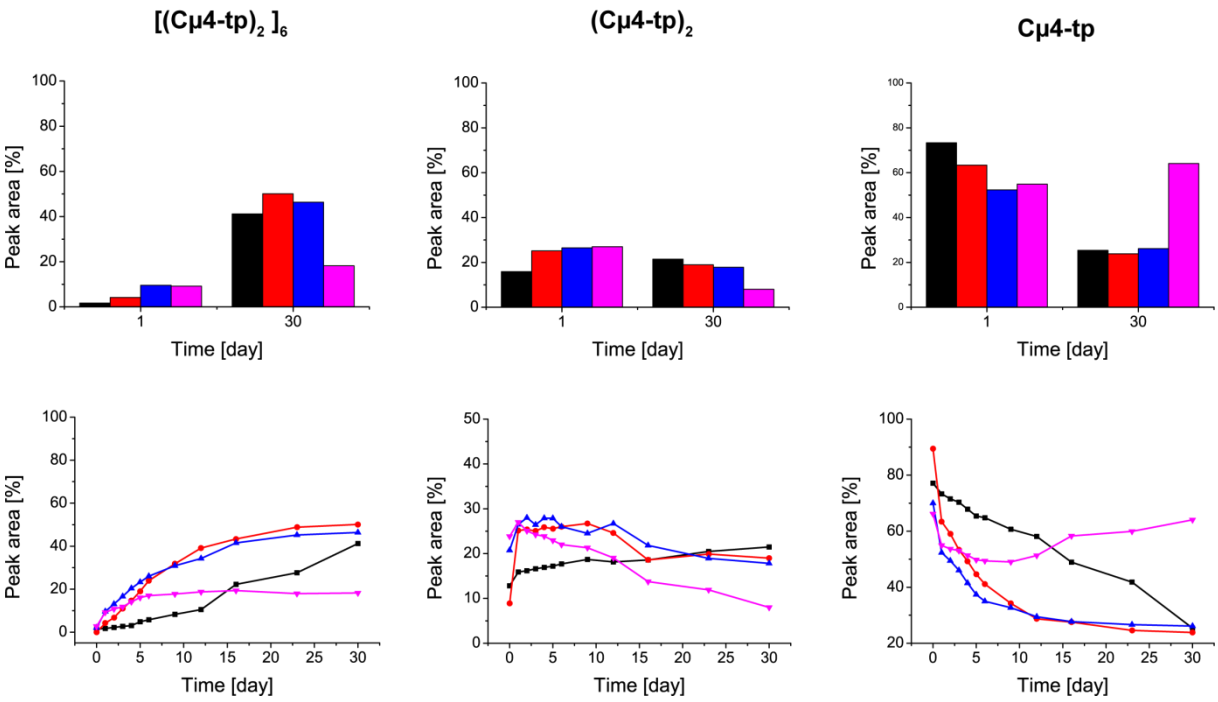

Figure 5.9 Effect of the redox system (GSSG/GSH) concentration during refolding on dodecamer formation. Cμ4-tp domain was refolded under four different redox conditions and the monomer was isolated according to the standard protocol. After isolation the protein concentration was adjusted to 1 mg/ml. Aliquots were stored at 4°C and analyzed at the indicated time points by SEC-HPLC on Superdex 200 10/300 GL in PBS at 20°C. For each time point 100 µg of sample were injected. Black bars: no GSSG/GSH; red bars: GSSG/GSH = 1 mM/0,5 mM; blue bars: GSSG/GSH = 1 mM/1 mM; pink bars: GSSG/GSH = 0,5 mM/1 mM.

On the other hand, when the Cμ4-tp monomer was refolded under standard conditions, isolated and then dialyzed against PBS containing the three different ratios of the redox system, dodecamer formation was, irrespective of the ratio used, arrested from the very beginning and over the whole time of analysis (Figure 5.10). This is very likely due to the too oxidative environment at any of the investigated ratio so that almost all Cμ4-tp monomer was converted to its oxidized dimer precursor (Cμ4-tp-S-SG). Since no free Cμ4-tp thiolate which could have exerted the nucleophilic attack remained, the formation of further covalent dimers and therefore of dodecamers was completely arrested.

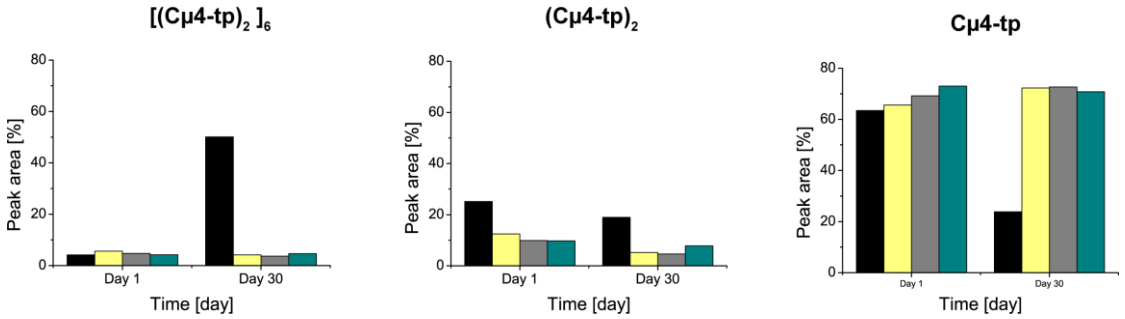

Figure 5.10 Effect of GSSG/GSH concentration during oligomerization on dodecamer formation. The Cμ4-tp domain was refolded under the standard GSSG/GSH ratio and the monomer was isolated as outlined above. After isolation the protein concentration was adjusted to 1 mg/ml and the sample was dialyzed ON against PBS containing three different ratios of the redox system. Aliquots were stored at 4°C and analyzed at the indicated time points by SEC-HPLC on Superdex 200 10/300 GL in PBS at 20°C. For each time point 100 µg of sample were injected. Black bars: no GSSG/GSH; yellow bars: GSSG/GSH = 1 mM/0,5 mM; grey bars: GSSG/GSH = 1 mM/1 mM; green bars: GSSG/GSH = 0,5 mM/1 mM.

5.2.1.4 Analysis of the effect of the C575 irreversible modification on the oligomerization process

The results obtained in previous experiments indicated that the rate of S-S bond formation might influence the oligomerization rate (Figure 5.9 and Figure 5.10). To test whether the formation of the covalent dimer is the rate limiting step for oligomerization, a kinetic study was performed where the formation of the inter-domain disulphide bonds was arrested at different time points by addition of an excess of AMS (Figure 5.11). Indeed, upon AMS addition neither the dodecamer nor the dimer increased over time, confirming that the formation of the inter-domain Cys575-Cys575 disulfide bond is the rate limiting step of the overall Cμ4-tp oligomerization process.

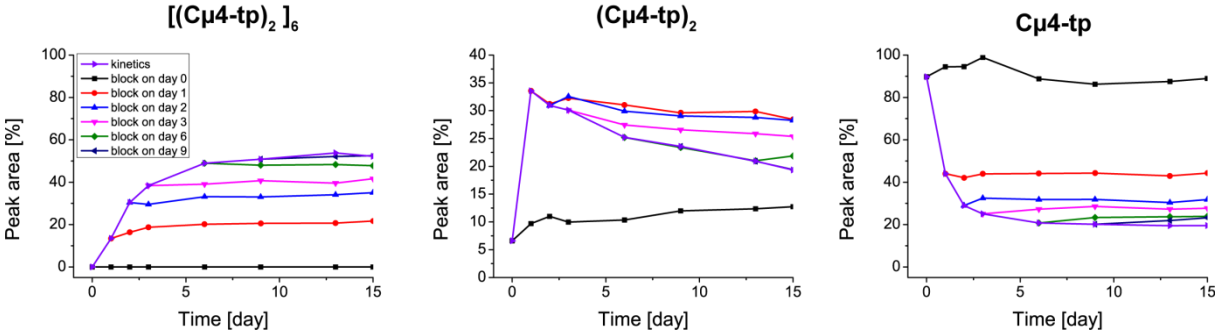

Figure 5.11 Effect of the blocking of disulfide bond formation by addition of AMS on dodecamer formation. The Cμ4-tp domain was refolded and isolated under standard conditions. After isolation of monomer the protein concentration was adjusted to 1 mg/ml. The sample was aliquoted and stored at room temperature. On day 0, 1, 2, 3, 6 and 9 AMS wad added (10 mM final concentration) and samples were run on Superdex 200 10/300 GL injecting 100 µg of protein for each run.

Furthermore, the fact that the dimer peak area did not increase over time indicated that no interaction between the remaining Cμ4-tp monomers had occurred. This suggested that non-covalent interactions may take place only after covalent dimers have been formed. To better investigate this hypothesis two single-point Cμ4-tp mutants were generated in which the Cys575 was replaced with serine (isosteric and polar) and with alanine (isovolumetric and hydrophobic, Xia *et al*., 2014). The monomer of both mutants was isolated and concentrated to 1 mg/ml and 15 mg/ml and analyzed with SEC-HPLC (Figure 5.12a). The latter concentration was considered sufficiently high to allow the formation of non-covalent species if any of them could have been formed. Thus, the lack of their formation at this concentration allowed to exclude the possibility for non-covalent interactions to occur. Both mutants showed a similar profile at both concentrations with the monomer peak area varying from 99% at 1 mg/ml to 96% at 15 mg/ml and that of the dimer from 1% to 4%, indicating the existence of very weak non-covalent interactions between monomers in the absence of S-S bonds.

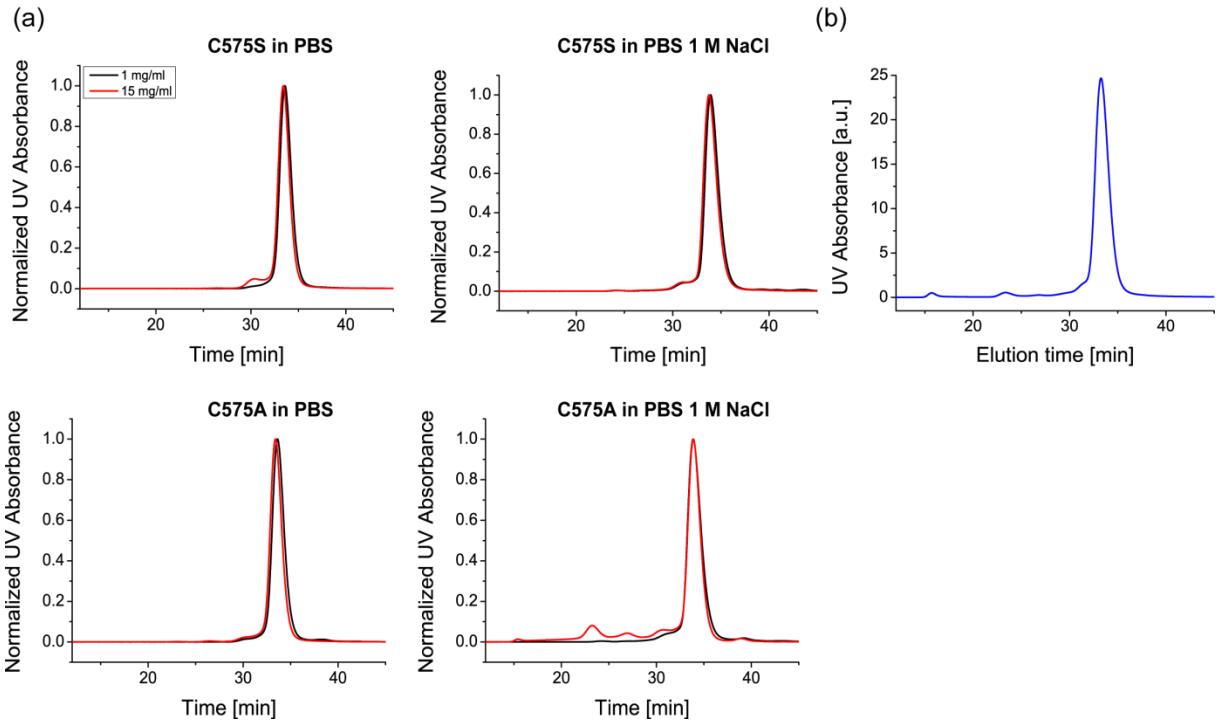

Figure 5.12 Analysis of non-covalent interactions between Cμ4-tp monomers in the absence of disulfide bonds. (a) Cμ4-tp C575S and C575A monomer was isolated and concentrated to 1 mg/ml and 15 mg/ml directly in PBS and after dialysis against PBS 1 M NaCl. (b) Cμ4-tp wt monomer was isolated and the C575 was blocked immediately by addition of excess of AMS (10 mM final concentration). Finally, the sample was concentrated to 15 mg/ml. The SEC-HPLC runs (a and b) were performed injecting 100 μg of sample on Superdex 200 10/300 GL column.

Since hydrophobic interactions can be favoured in the presence of salt, both mutant monomers were dialyzed against PBS containing 1 M NaCl. Here a slightly different behaviour between the two mutants could be observed, however only at a concentration of 15 mg/ml. The Cμ4-tp C575S mutant was present again almost only in a monomeric form whereas in the case of the C575A mutant very small peak corresponding to that of dimers, octamers as well as to dodecamers (peak area 6%) appeared. Compared to cysteine, serine is slightly polar whereas alanine is slightly hydrophobic. It might be that a hydrophobic interaction between A575 compensated the S-S bond enabling further non-covalent interactions to occur which helped dodecamers to form at a very low degree.

Moreover, to further confirm this hypothesis in a more native context, AMS was added to the wild type Cμ4-tp monomer immediately upon isolation, in order to irreversibly block C575. The sample was then concentrated to 15 mg/ml and analysed with SEC-HPLC. No significant peak was observed apart from the monomer giving support to the above-mentioned hypothesis (Figure 5.12b).

The data from the two concentrated cysteine mutants and the wild type monomer blocked with AMS clearly indicate the very low propensity of Cμ4-tp monomers to exert non-covalent interactions in the absence of the inter-domain disulfide bonds linking them.

5.3 Structural requirements for Cμ4-tp oligomerization *in vitro*

5.3.1 Characterization of Cμ4-tp dodecamers

To obtain the dodecamer for its characterization, the monomer sample was concentrated to allow assembly and processed on a preparative SE column and fractions containing the dodecamer were pooled. A molecular mass (MM) of 201 kDa and a sedimentation coefficient of 8,5 S, from which a MM of 185 kDa was calculated, was confirmed by SEC-MALS (multi-angle light scattering) and analytical ultracentrifugation (aUC), respectively (Figure 5.13a and b). The values corresponded to a 12-mer. The chromatograms indicated the presence of other two species, the dimer and the monomer**.** The SDS-PAGE analysis under non-reducing conditions indicated two bands, the lower at ca. 14,4 kDa corresponding to the monomer and the upper main band (ca. 28 kDa) which corresponds to covalent dimers (Figure 5.13c) indicating that the dodecamer is non-covalently assembled of covalent dimers. The presence of a β sheet structure similar to that of the monomer was revealed by far-UV CD spectroscopy (Figure 5.13d).

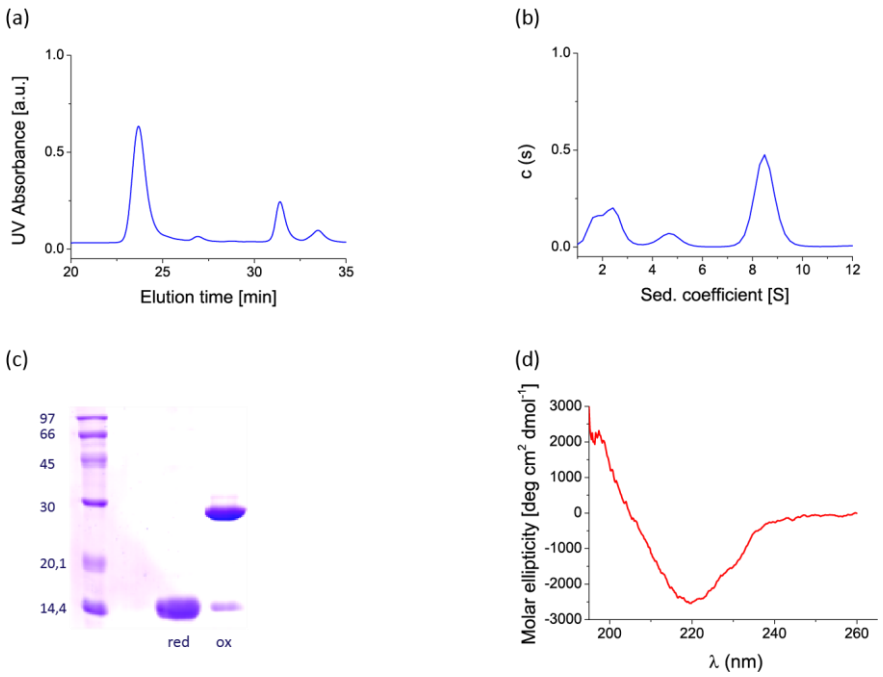

Figure 5.13 Characterization of the Cμ4-tp dodecamer. Cμ4-tp monomer was refolded and isolated according to the standard protocol. After isolation the monomer was concentrated and processed over a preparative SE column. Fractions containing the dodecamer were pooled and its concentration was adjusted to 1 mg/ml for SEC-MALS (a) and to 0,5 mg/ml for aUC (b) analysis, respectively. (c) SDS-PAGE under reducing and non-reducing conditions. (d) The far-UV CD spectrum acquired in PBS at 20°C.

To assess the (ir)reversibility of the oligomerization process, i.e. how dodecamers behave upon concentration or dilution was investigated. To this aim, SEC fractions containing the dodecamer were pooled and the resulting sample was concentrated or diluted in order to obtain concentration values ranging from 0,1 mg/ml to 26 mg/ml. Samples were then analyzed with SEC-HPLC (Figure 5.14).

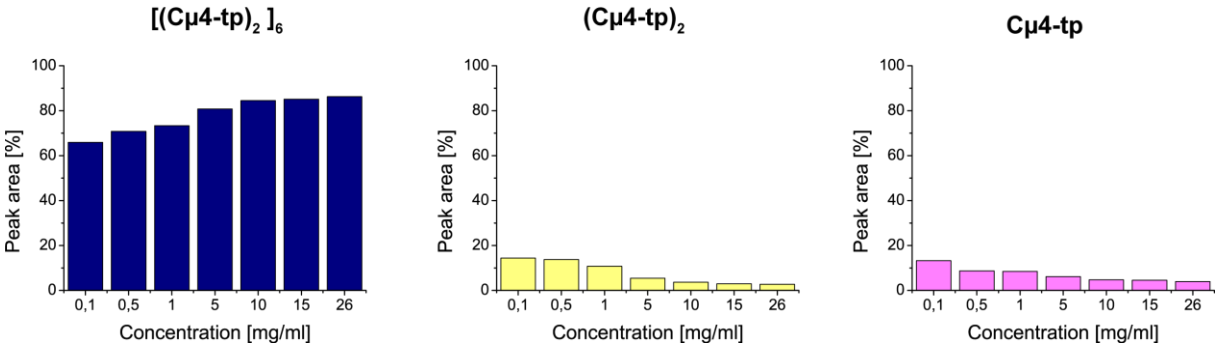

Figure 5.14 Effect of the protein concentration on the Cμ4-tp dodecamer. The Cμ4-tp dodecamer was isolated according to the standard protocol described above. After isolation the dodecamer concentration was adjusted to 0,1, 0,5, 1, 5, 10, 15 and 26 mg/ml. SEC-HPLC runs were performed injecting 50 μg of protein for each run.

Interestingly within the analyzed range there was no concentration at which the dodecamer was the only species nor one at which the monomer or the dimer was the prevalent one. However, as the sample concentration increased, the relative fraction of the two latter decreased from 15% to 5% each. On the other hand, the dodecamer portion was always above 60% even at the lowest analyzed concentration, meaning that the simple dilution could not strongly weaken the non-covalent interactions between covalent dimers and thus, could not significantly shift the equilibrium towards dimers.

Furthermore, to investigate whether non-covalent interactions can be maintained after disulfide bond disruption, once they have been established, a reducing agent such as DTT (dithiothreitol) was added to the dodecamer (conc. 69 μM) at a final concentration of 1 mM at which only the Cys575-Cys575 disulfide bond is reduced but not the intra-domain one (Figure 5.15). The dodecamer began disassembling immediately upon DTT addition and after an ON incubation with DTT both dodecamers and covalent dimers were completely disrupted. The prevalent species left was the Cμ4-tp monomer (peak area 91%) giving further evidence that non-covalent interactions are very weak.

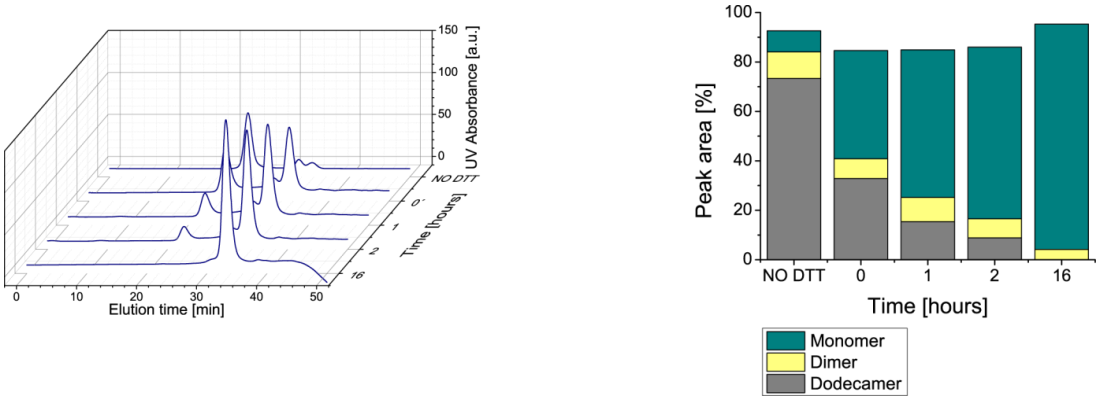

Figure 5.15 Effect of the disulfide bond disruption by addition of DTT on the dodecamer. The Cμ4-tp dodecamer was obtained by processing the concentrated monomer sample over the preparative SE column. Fractions containing the dodecamer were pooled and the protein concentration was adjusted to 1 mg/ml and finally DTT (1 mM final concentration) was added. After addition of DTT the sample was aliquoted, stored at room temperature and analyzed with SEC-HPLC at time 0', 1 h, 2 h and 16 h.

Moreover, the C575S mutant was employed to assess the stability of covalent and non-covalent forces within the dodecamer. To this purpose the Cμ4-tp dodecamer was diluted with an increasing amount of the C575S monomer (Figure 5.16). The volume ratio was always maintained (V(wt) : V(C575S) = 1:1) in order to keep the dilution factor of the dodecamer always the same.

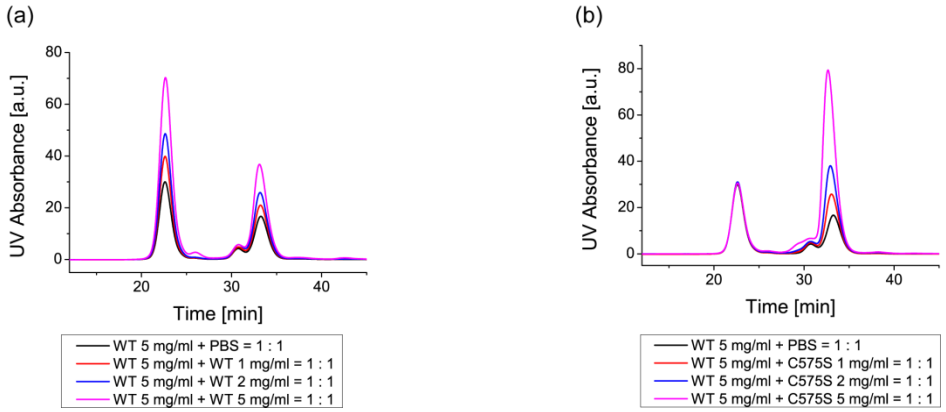

Figure 5.16 Effect of the dilution of the dodecamer with an increasing amount of the dodecamer (a) and C575S monomer (b). The Cμ4-tp dodecamer and C575S monomer were obtained as described above. After isolation the concentration was increased to 1, 2 and 5 mg/ml. The dodecamer having the concentration of 5 mg/ml was diluted 1:2 with an increasing amount of dodecamer (a) and of C575S monomer (b). The final samples were analyzed on analytical Superdex 200 10/300 GL by injecting 100 µg for each run.

As expected, the monomer peak increased as the amount of the added C575S mutant increased, whereas the dodecamer peak area remained unaltered. These data indicated that the dodecamer was not perturbed at all upon addition of the C575S monomer and

therefore, that the existing covalent disulfide bonds as well as non-covalent interactions between them are stable enough to keep the dodecamer intact.

How stable the Cμ4-tp dodecamer is was further determined by the analysis of the dodecamer which was concentrated up to 50 mg/ml and 100 mg/ml. The SEC-HPLC chromatograms did not indicate any tendency to aggregate or to form other species but dodecamers (data not shown).

All together data obtained by characterizing the oligomerization kinetics and Cμ4-tp dodecamers indicated that the Cμ4-tp monomer undergoes spontaneous oligomerization process upon C575 oxidation. The oligomerization is first driven by covalent interactions resulting in formation of covalent dimers. The latter, once formed, only then can associate via non-covalent interactions allowing the dodecamer to form. Within dimers, covalent and non-covalent interactions must thus occur on different, most likely two opposing, interfaces.

5.3.2 Analysis of the oligomerization ability of tp mutants

The IgM Cμ4 domain without the tp forms prevalently monomers (Bubb and Conradie, 1978; Müller *et al*., 2013) whereas the Cμ4-tp domain possesses oligomerization properties which allow the single domain to organize into bigger and defined structures consisting of twelve Cμ4-tp monomeric units or of six dimeric units. The Cμ4-tp differs from the Cμ4 domain in that it possesses an 18-amino acid extension located on its C-terminus, which seems to confer oligomerization properties to the Cμ4 domain. Therefore, for investigating the structural requirements for oligomerization the focus was given primarily on the tp region.

5.3.2.1 Analysis of Cμ4-tp-alanine mutants

To obtain a deeper understanding of the structural bases which leads to oligomerization, 18 single-point mutants were generated by replacing each tail piece amino acid with alanine and their oligomerization ability was tested. To compare them, all mutants were processed under the same conditions (Figure 5.17). To accelerate the oligomerization process, the monomer, once isolated, was concentrated to 15 mg/ml and then run over a preparative SE column. This concentration was considered high enough to allow weak interactions to occur. Thus, in cases where no oligomers formed due to the mutation effect, the occurrence of any significant interaction leading to oligomerization was excluded. Where oligomers could form, fractions containing the oligomer were pooled and the resulting sample was analyzed with SEC-MALS and with aUC as well. For mutants which could not form oligomers, monomer and

dimer fractions were pooled and analyzed.

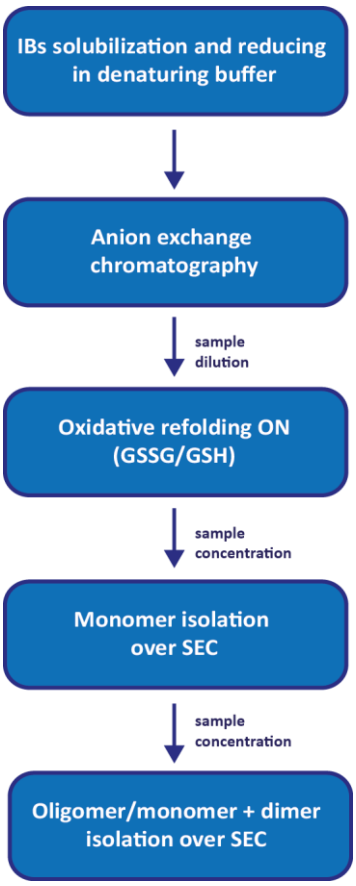

Figure 5.17 Schematic overview of the process applied for evaluating the oligomerization properties of Cμ4-tp mutants *in vitro*. Mutants were refolded and their monomers were isolated as previously described. To accelerate the oligomerization process, the monomer was concentrated to 15 mg/ml and then run over a preparative SE column. In cases where oligomerization occurred, fractions containing the oligomer were pooled and its concentration was adjusted to 0,5 mg/ml for aUC and to 1 mg/ml for the SEC-MALS analysis. If no oligomers formed, fractions containing monomer and dimers were pooled and analyzed at the same concentrations.

The Cμ4-tp-alanine mutants behaved differently and in total three phenomena were observed: oligomerization, aggregation or, no oligomerization at all (Figure 5.18).

Amino acid position	tp -amino acid being replaced with A (ala)	Mutation effect on Cμ4-tp *in vitro*	MM (SEC-MALS)	S value (aUC)
559	P (Pro)	oligomerization (12x)	211	8,49
560	T (Thr)	oligomerization (12x)	192	8,41
561	L (Leu)	oligomerization (12x)	195	8,41
564	S (Ser)	oligomerization (12x)	179	7,67
568	M (Met)	oligomerization (10x)	168	7,45
569	S (Ser)	oligomerization (12x)	191	8,14
571	T (Thr)	oligomerization (12x)	198	8,42
572	G (Gly)	oligomerization (12x)	197	8,19
573	G (Gly)	oligomerization (12x)	193	8,25
574	T (Thr)	oligomerization (12x)	200	8,52
576	A (Ala)	oligomerization (12x)	191	8,55
563	N (Asn)	aggregation	-	-
570	D (Asp)	aggregation	-	-
562	Y (Tyr)	dimerization (2x)	16,6; 28	1,65; 2,48
564	V (Val)	dimerization (2x)	17,1; 28,9	1,67; 2,49
566	L (Leu)	dimerization (2x)	16,9; 28,3	1,66; 2,46
567	I (Ile)	dimerization (2x)	16,5; 28,4	1,71; 2,56
575	C (Cys)	no oligomerization (1x)	14,2	1,66

Figure 5.18 Summary of the behavior of all Cμ4-tp alanine mutants *in vitro*. The generic representation of the Cμ4-tp domain depicts the tail piece sequence in the single-letter amino acid code. Coding indicates: proline 559, threonine 560, leucine 561, tyrosine 562, asparagine 563, valine 564, serine 565, leucine 566, isoleucine 567, methionine 568, serine 569, aspartate 570, threonine 571, glycine 572, glicyne 573, threonine 574, cysteine 575 and tyrosine 576. Molecular mass (MM) 1x, 2x or 12x indicates the formation of monomers, dimers and 12-mers.

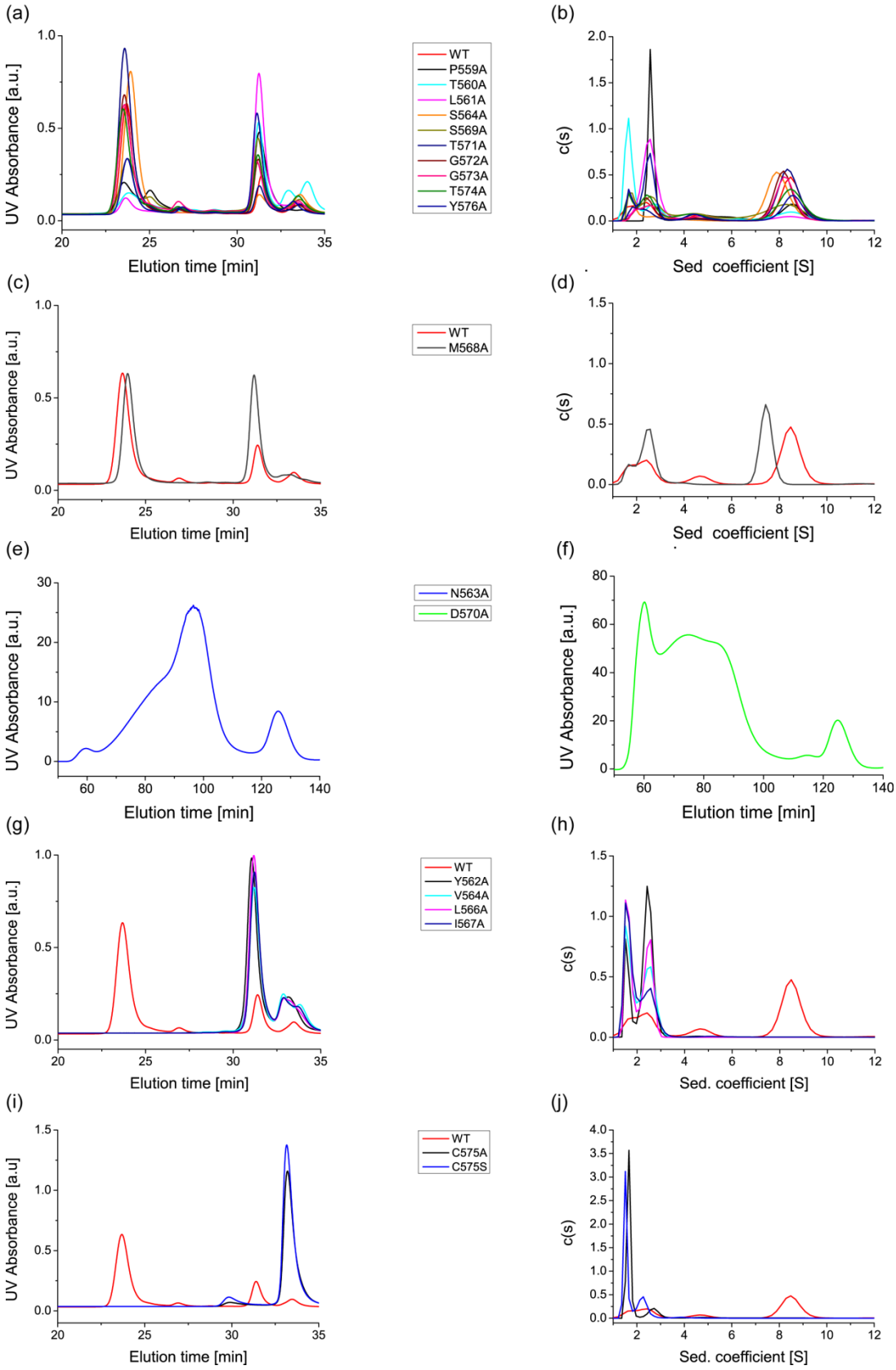

Figure 5.19 Oligomerization ability of the Cμ4-tp alanine mutants *in vitro*. (a), (c) and (g) - SEC-MALS profiles at 1 mg/ml in PBS. (b), (d) and (h) - aUC profiles at 0,5 mg/ml in PBS. (e) and (f) - preparative SEC profile of the monomer at 15 mg/ml in PBS.

Among mutants able to form oligomers, most of them (8 of 11) preserverd the ability to solely form dodecamers i.e hexamers of covalent dimers (Figure 5.19a and b). Two mutants, P559A and S569A formed also smaller oligomers, although their overall oligomerization ability was notably reduced. Thus, mutants in which polar, uncharged tp amino acids (such as threonine and serine) were replaced with alanine maintained the ability to form dodecamers indicating that polar interactions such as hydrogen bonds or Van der Waals forces are not significantly contributing to non-covalent interactions occuring between covalent dimers. Here the exception was T560 located on the N-terminal part of the tp, the replacement of which preserved, although significantly decreased, the oligomerization ability. Two other mutants whose ability to form dodecamers was considerably reduced, were those were a hydrophobic amino acid such as L561 and Y576 was replaced with alanine. M568A was the only mutant among those able to oligomerize to solely form decamers, suggesting a relevant role for another hydrophobic amino acid in oligomerization (Figure 5.19c and d). All oligomerizing mutants formed oligomers consisting of covalent dimers (SDS-PAGE data not shown).

Two mutants, N563A and D570A could not organize in well defined structures and aggregated (Figure 5.19e and f). To investigate whether both mutants aggregate also at lower concentrations, the monomer was concentrated to 0,5 mg/ml for aUC and 1 mg/ml for SEC-MALS analysis. N563A as well as D570A did not show aggregation propensity at lower concentration but rather the tendency to form decamers and eicosamers (20-mers), respectively (Figure 5.20).

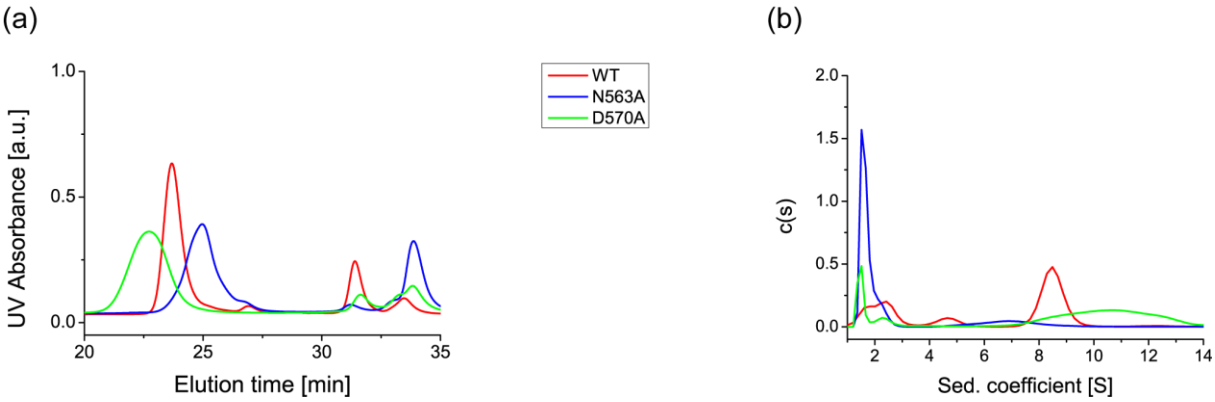

Figure 5.20 Oligomerization ability of the Cμ4-tp N563A and D570A monomer at lower concentrations *in vitro*. (a) SEC-MALS profiles at 1 mg/ml in PBS. (b) aUC profiles at 0,5 mg/ml in PBS.

All mutants except C575A (Figure 5.19i and j), which completely lost the oligomerization ability were Y562A, V564A, L566A and I567A (Figure 5.19g and h). Here a more hydrophobic amino acid such as leucine, valine and isoleucine was replaced with alanine, the least hydrophobic amino acid. These mutants however, preserved the capacity to form covalent dimers (SDS-PAGE data not shown). The four mutants together with L561A and Y576A indicated that hydrophobic interactions play a significant role in the assembly of dodecamers.

To assess whether the effect of the mutation could be overcome by high salt concentration and therefore oligomerization restored, the four non-oligomerizing mutants were dialyzed into PBS containing 1 M NaCl. Only I567A showed a detectable oligomerization tendency at higher concentrations only, whereas the Y562A, V564A and L566A mutants showed no oligomerization propensity at all, indicating that the mutation effect could not be compensated by buffer conditions which favor hydrophobic interactions (Figure 5.21).

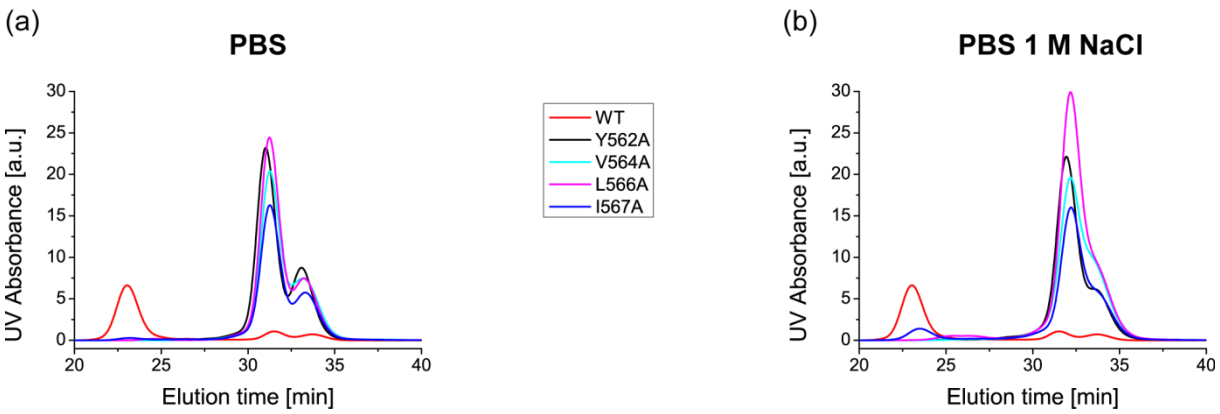

Figure 5.21 Oligomerization ability of the Cμ4-tp Y562A, V564A, L566A and I567A mutants after dialysis against PBS with 1 M NaCl. After isolation the pool containing monomers and dimers was concentrated to 15 mg/ml (a) and dialyzed against PBS containing 1 M NaCl and then concentrated (b). The samples were analyzed on SEC-HPLC injecting 100 µg of protein.

To analyze the β-aggregation propensity and aggregation hot spots of the tp alone as well as to predict the impact of the eighteen mutations on its aggregation propensity, the TANGO and AGGRESCAN algorithms were applied (Figure 5.22). Both predicted one region situated in the N-terminal-middle part of the tp and encompassing residues 559-569 (TANGO) and 559-570 (AGGRESCAN), respectively, which participate in the aggregation process. Surprisingly, this region corresponded to the region mapped by mutagenesis experiments to be sensitive to alanine mutations. Moreover, TANGO as well as AGGRESCAN predicted on

one the hand a strikingly higher aggregation propensity for the tp N563A mutant and, on the other hand, a significantly lower aggregation propensity for L561A, Y562A, V564A, L566A and I567A. For D570A a significantly higher aggregation propensity was predicted only by AGGRESCAN. Exept S565A for which a notably higher and M568A for which a lower aggregation propensity was predicted by TANGO and AGGRESCAN, respectively, the predictions concerning the remaining tp mutants were fully in agreement with the *in vitro* observations of the corresponding Cμ4-tp mutants, indicating that the tp govern the oligomerization of the entire Cμ4-tp domain.

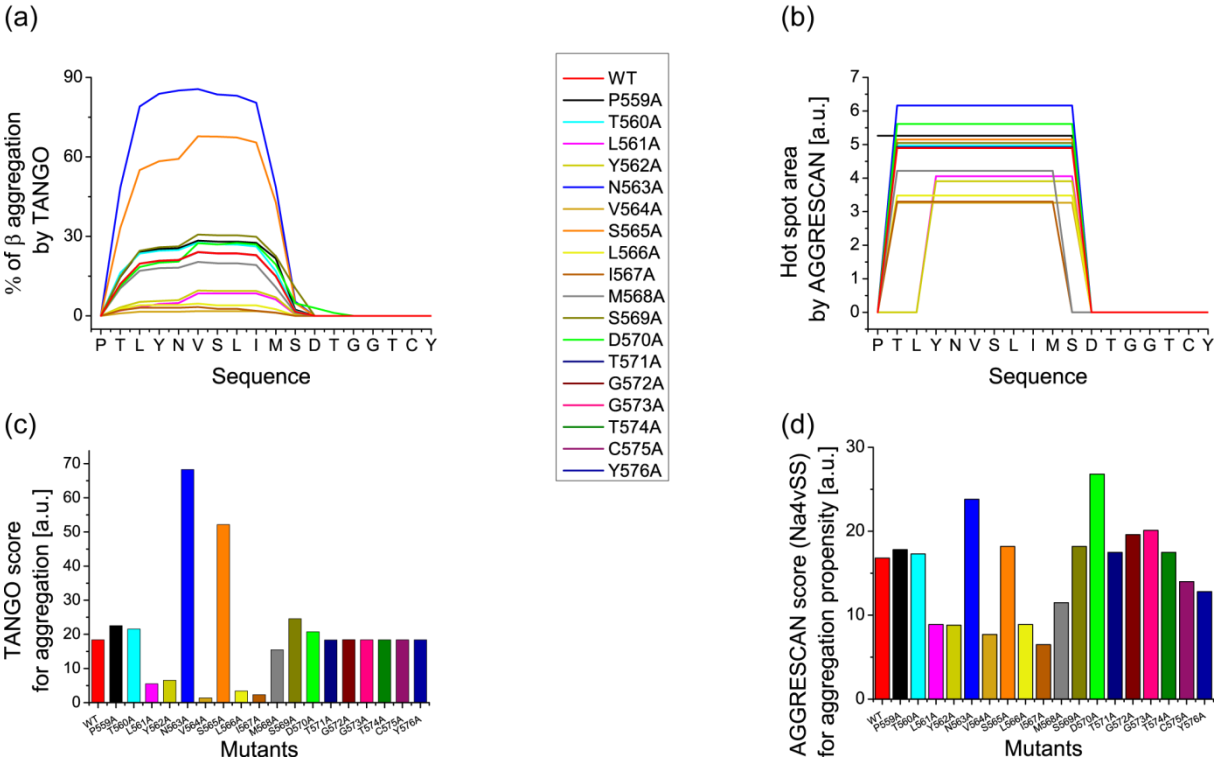

Figure 5.22 Schematic representation of the predicted aggregating region by TANGO (a) and by AGGRESCAN (b) of the wild type tp peptide and eighteen alanine tp mutants. Comparison of the mutation effect on aggregation propensity: TANGO (c) and AGGRESCAN (d).

5.3.2.2 Analysis of deletion and insertion mutants of Cμ4-tp

To assess the importance of N and C-terminal tp amino acids for oligomerization, five deletion mutants were generated. Four of them were sequentially shortened by serial deletion of one amino acid starting from the first N-terminal amino acid P559. The fifth mutant was lacking the last amino acid, T576. Moreover, additional four mutants were generated by deleting one or both glycines (position 572 and 573) or inserting one or two glycines between them with the aim to assess the shortening/elongation effect of the C-

terminal half of the tail piece. The oligomerization ability was seriously affected already by deleting the first N-terminal amino acid and completely abolished by further deletions (Figure 5.23a and b), indicating that shortening the tp N-terminal part by deleting P559, T560, L561 and Y562 has a more destructive impact on oligomerization than the replacement of the same amino acids with alanine. Similarly, the deletion of the C-terminal tyrosine drastically reduced the ability to form dodecamers, giving additional support to the hypothesis that the hydrophobic amino acids of the tp are essential for non-covalent interactions (Figure 5.23c and d). All five mutants preserved the ability to form covalent dimers (SDS-PAGE data not shown), although that of the ΔY576 mutant was significantly reduced, probably due to the absence of the phenolic oxygen which in the wild type increases the electronegativity of the cysteine thiol group, facilitating thus disulfide bond formation.

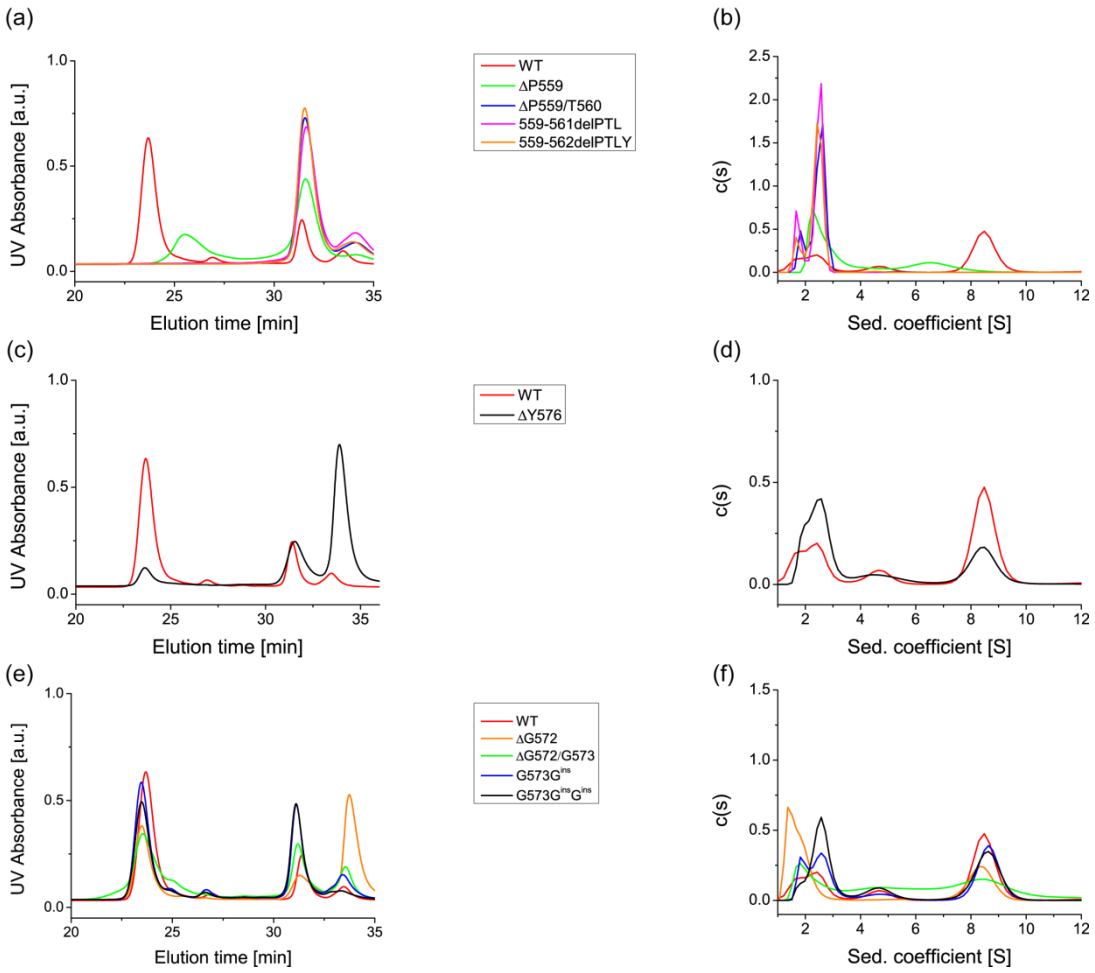

Figure 5.23 Oligomerization ability of the Cμ4-tp deletion and insertion mutants *in vitro*. (a), (c) and (e): SEC-MALS profiles at 1 mg/ml in PBS. (b), (d) and (f) - aUC profiles at 0,5 mg/ml in PBS.

Shortening the tp C-terminal middle region by deleting one of its two glycines also reduced, and the deletion of the second glycine impaired the oligomerization abilty. On the contrary, tp elongation by inserting one or two glycines still supported oligomerization (Figure 5.23e and f).

5.3.2.3 Analysis of Tyr576-tp mutants

Replacement of the hydrophobic C-terminal tyrosine with alanine reduced (Figure 5.19) and its deletion significantly affected (Figure 5.23) the oligomerization ability of the Cμ4-tp. To assess whether an increase in hydrophobicity at the very last position of the tp can favor the association of covalent dimers leading to an increase of dodecamers, three Cμ4-tp mutants were generated where T576 was replaced with glycine, a non-hydrophobic amino acid, and with two other amino acids, tryptophan, which is more hydrophobic than tyrosine and with phenylalanine, the most hydrophobic amino acid.

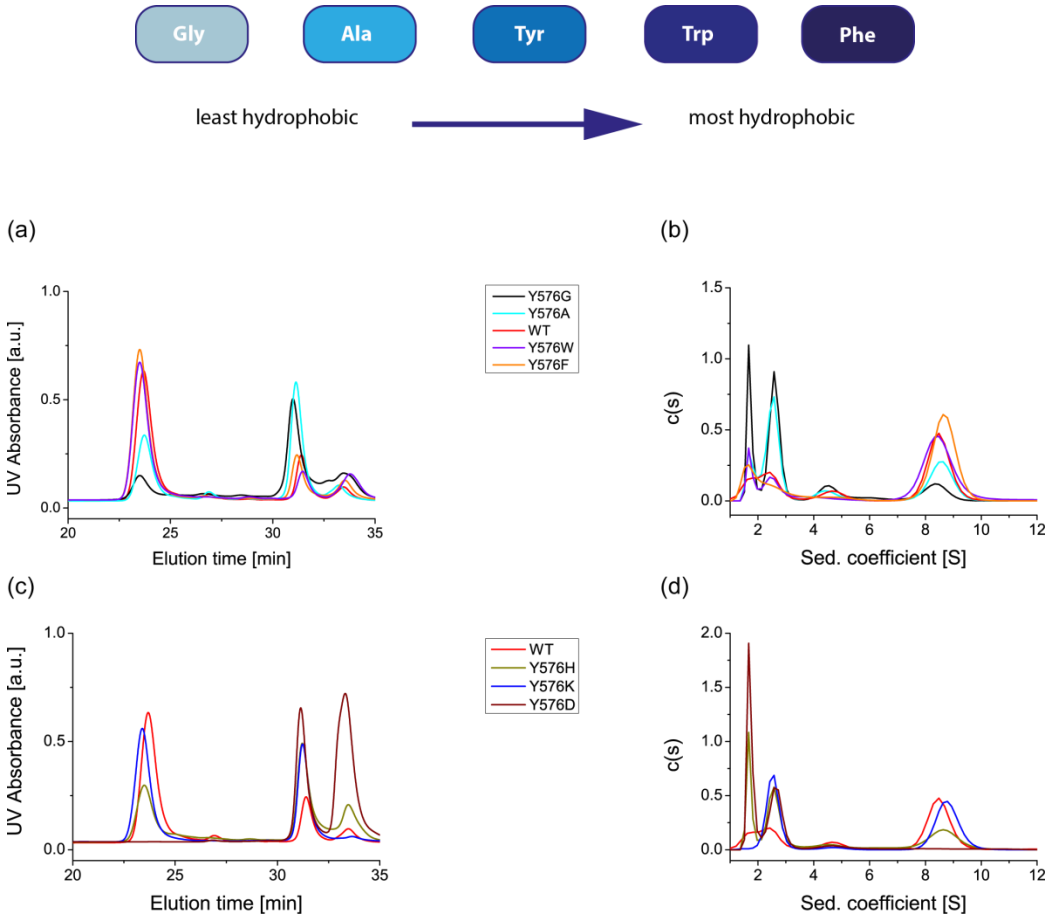

Figure 5.24 Oligomerization ability of the Cμ4-tp T576-mutants *in vitro*. (a) and (c) – SEC-MALS profiles at 1 mg/ml in PBS. (b) and (d) - aUC profiles at 0,5 mg/ml in PBS.

Indeed, the influence of the hydrophobicity at the very last tp position on the oligomerization was confirmed (Figure 5.24a and b). The mutant with the most hydrophobic amino acid at the 576 position formed more dodecamers than other mutants with less hydrophobic amino acid in the same position. Thus, the higher the hydrophobicity in position 576 is, the higher is the oligomerization propensity.

To assess the effect of the charge at the same position on oligomerization, T576 was replaced with two positively charged amino acids, lysine and histidine, which is hydrophobic as well, and with the negatively charged glutamate. Surprisingly, the ability to oligomerize was supported by the presence of the positive charge as well, since both T576K and T576H mutants could form dodecamers (Figure 5.24c and d). It is likely that the positive charge in this position facilitates the thiolate state of the neighboring cysteine, favoring thus the formation of covalent dimers. Interestingly, the combination of hydrophobicity and positive charge on the same amino acid (T576H) was less effective than the positive charge alone (T576K) in supporting oligomerization. Accordingly, the T576D mutant carrying the negative charge close to the tp cysteine had completely the opposite effect. No oligomerization occurred, most likely due to the repulsion of the negative charges in the neighboring positions 575 and 576.

5.3.2.4 Analysis of Cys575-tp mutants

The effect of the replacement of Cys575 with alanine and serine was already described above (Figure 5.12a). These mutants were not able to establish any kind of interaction and only monomers were present in the sample (Figure 5.19i and j).

To investigate the relevance of the cysteine position within the tp and therefore the position of disulfide bonds within the dodecamers, the cysteine was shifted towards the tp N-terminus. To this point, three double mutants were generated, where the C575 was replaced with serine and another amino acid such as P559, S565 and S569 was replaced with cysteine. The ability to form dodecamers as well as to oligomerize was seriously compromised (Figure 5.25a and b). All three double mutants aggregated when their monomers were concentrated to 15 mg/ml (data not shown). However, at a concentration of 1 mg/ml, the P559CC575S mutant did not indicate an oligomerization tendency and the remaining two double mutants could not form well defined structures. Thus, the change of the cysteine position towards the tp N-terminus severely compromised the oligomerization ability.

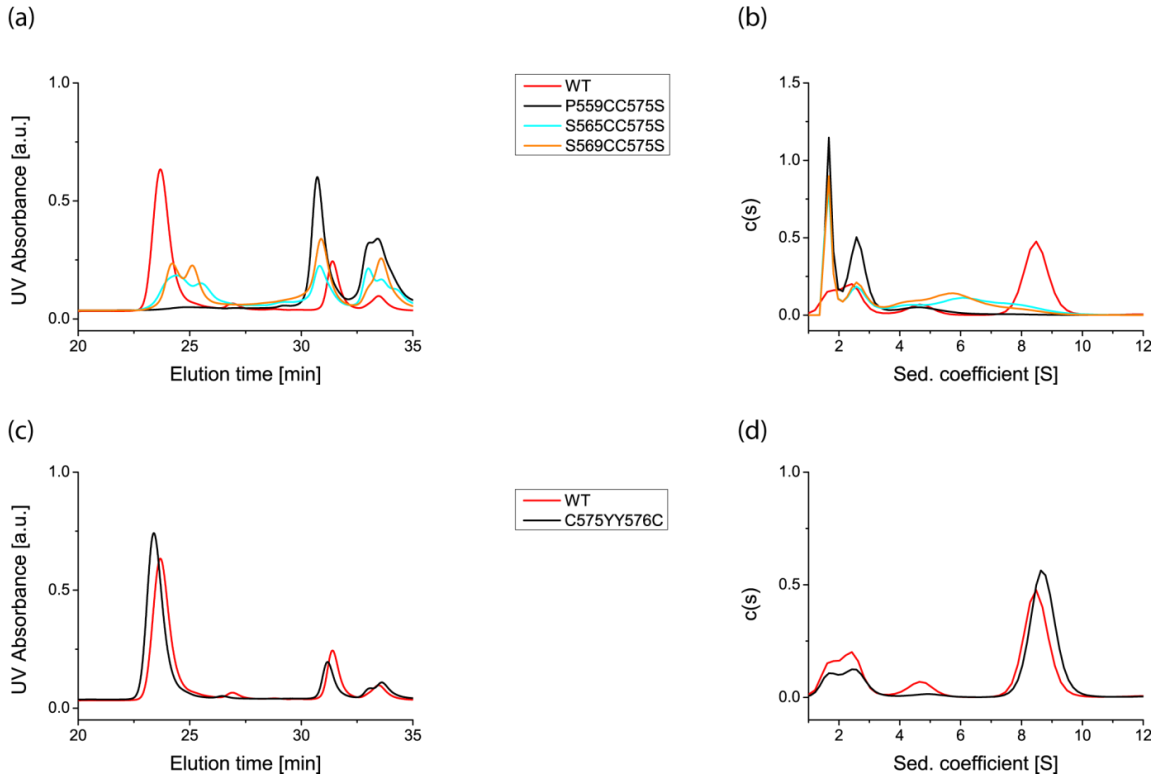

Figure 5.25 Oligomerization ability of the Cμ4-tp cysteine double mutants *in vitro*. (a) and (c) – SEC-MALS profiles at 1 mg/ml in PBS. (b) and (d) - aUC profiles at 0,5 mg/ml in PBS.

Finally, a mutant where the penultimate cysteine and the last tyrosine were exchanged was generated. Interestingly, this double mutation was beneficial to oligomerization since the C575YY576C mutant formed slightly more dodecamers than the wild type did, indicating that oligomerization is more flexible to cysteine shifting on the tp C-terminal part (Figure 5.25c and d).

5.3.2.5 Analysis of Cμ4-tp swap mutants

It has been already shown by IgM swap mutants expressed in cells that the tp alone does not possess all structural requirements for isotype-specific oligomerization (Sorensen *et al.*, 1996). To investigate whether this limit reflects only on entire IgM or it already appears at Cμ4-tp level, the oligomerization ability of two swap mutants was tested. Both mutants consisted of murine Cμ4 domain fused to the murine and human IgA tp (α tp). α tp confers the ability to IgA to be secreted as dimers as well as tetramers of dimers.

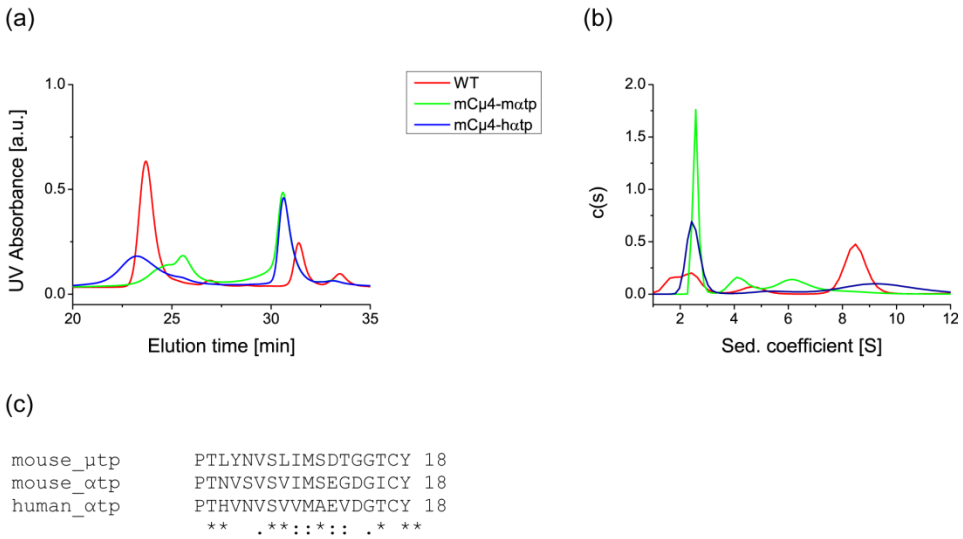

Figure 5.26 Oligomerization ability of the Cμ4-αtp swap mutants *in vitro*. (a) – SEC-MALS profiles at 1 mg/ml in PBS. (b) - aUC profiles at 0,5 mg/ml in PBS. (c) ClustalW2 alignment of the tp sequences.

Although IgM with the μ tp replaced by the α tp had been shown to form also hexamers of dimers when expressed in cells (Sorensen *et al*., 1996), this ability was not maintained when only the Cμ4 domain was fused to the α tp and analyzed *in vitro*. Both Cμ4-αtp swap mutants could form covalent dimers which could not associate into bigger defined oligomers (Figure 5.26), confirming that the isotype-specific form of antibody oligomerization is not given only by the C-terminal 18-amino acid extension but also by motifs of other Fc domains. IgM oligomer size differs among species. Human and murine IgM are decameric in the presence and dodecameric in the absence of the J chain; Xenopus IgM are predominantly dodecameric whereas those of bonyfish are octameric (Davis and Shulman, 1989). Additional three swap mutants were generated to investigate the ability of the tp to confer the species-specific oligomerization property. To this purpose, the murine Cμ4 domain was fused to human, Xenopus and Ladyfish tp.

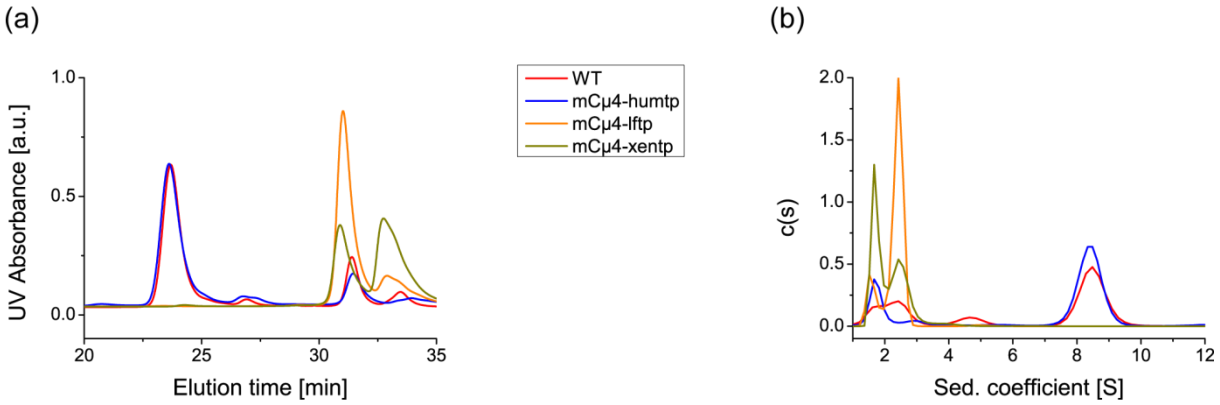

(c)

```
mouse_μtp          PTLYNVSLIMSDTGGTCY- 18
hum_μtp            PTLYNVSLVMSDTAGTCY- 18
Xenopus_μtp        PTNVNVSLVLSDT---C-- 14
Ladyfish_μtp       PTTVSLDLNVPQT---CKV 16
                    **  .:.* :.:*   *
```

Figure 5.27 Oligomerization ability of the Cμ4-tp μ tp swap mutants *in vitro*. (a) – SEC-MALS profiles at 1 mg/ml in PBS. (b) - aUC profiles at 0,5 mg/ml in PBS. (c) ClustalW2 alignment of the four tp sequences.

Among the μ tp swap mutants only the human tp fused to the murine Cμ4 domain preserved the ability to oligomerize into dodecamers (Figure 5.27). This was not surprising since the human μ tp differs from the mouse one in only two positions having similar amino acids. The Cμ4 domain fused to the Xenopus or Ladyfish μ tp could still form covalent dimers, which, however, could not associate and form bigger species at all. Both tps differ in length as well as in amino acid composition from the mouse μ tp. Thus, in order to oligomerize, the tp needs the proper neighboring environment localized on the Cμ4 domain.

5.3.3 Characterization of the μ tail piece

5.3.3.1 Analysis of the oligomerization ability of the tp

The μ tp confers the Cμ4 domain ability to form dodecamers. To gain a deeper insight into the oligomeric state and properties of the tp alone and into its secondary structure, the peptide consisting of 18 tp amino acids encompassing the μ chain residues 559-576 was synthesized and analyzed. The peptide lyophilisate was resuspended in Tris/EDTA buffer and the redox system (GSSG/GSH) was added in order to oxidize the Cys575. Finally, the peptide was reduced by addition of DTT in order to test how the reduction affects the investigated properties. After each step the sample was analyzed with SEC-HPLC, aUC and CD spectrometry.

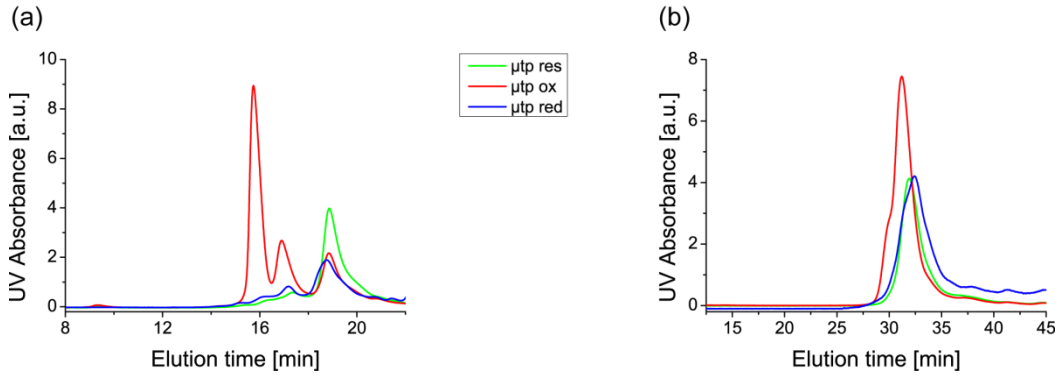

Figure 5.28 SEC profiles of the resuspended, oxidized and reduced µ tp peptide on the YMC diol-120 (a) and Superdex 75 10/300 GL (b) column. The peptide was resuspend in Tris/EDTA buffer pH 7,5 to a final concentration of 0,4 mg/ml (207 µM). To oxidize the peptide GSSG/GSH was added (1 mM/0,5 mM final) to the resuspended sample and incubated for 2 hours at RT under stirring. To reduce the sample DTT (5 mM final) was added to the oxidized sample and incubated for 20' at RT under stirring. For each run 20 µg of peptide were injected.

The wt µ tp was found to be prevalently a monomer (ca. 1,95 kDa) upon resuspension with the peak eluting at ca. 19 min. on the YMC diol-120 SEC column and at 32,5 min. on the Superdex 75 10/300 GL column (Figure 5.28). After addition of the redox system, two additional peaks corresponding to GSSG (0,6 kDa) and the tp dimer (ca. 3,9 kDa) appeared, the latter eluting at ca. 17 min. on the YMC diol-120 column and at 30 min. on the Superdex 75 column. On the latter column both the monomeric and dimeric form eluted after aprotinin (ca. 6 kDa) and very close to the lower limit of its separation range (3 kDa). Surprisingly, on the YMC diol-120 the two forms of the wt µ tp eluted after GSSG (elution time 16 min.) similar to the cytochrome c (12 kDa), probably due to repulsive interactions with the column which caused earlier elution. However, the peak resolution was better on the latter column. An additional evidence of the inability of the tp peptide to form oligomers was given by the aUC analysis. The smallest analyzed protein standard that sedimented after an ON run at a highest velocity of 47.000 rpm was aprotinin. When analyzed under the same conditions neither the monomeric nor dimeric tp form sedimented, indicating that both forms were smaller than 6 kDa, which corresponds to the monomer and dimer. Upon addition of DTT, the GSSG and the dimer peak disappeared and the monomer was again the prevalent species.

To assess whether the wt µ tp can oligomerize over time, the samples containing the resuspended peptide (sample 1) and the oxidized peptide (sample 2) were analyzed on SEC-HPLC three days after resuspension. Surprisingly, no other peak than that of the monomer in

the sample 1 and that of the monomer and of the dimer in the sample 2 were observed (Figure 5.29). These data indicated that the μ tp alone can form covalent dimers which are, however, not able to associate into oligomers in the absence of the Cμ4 domain.

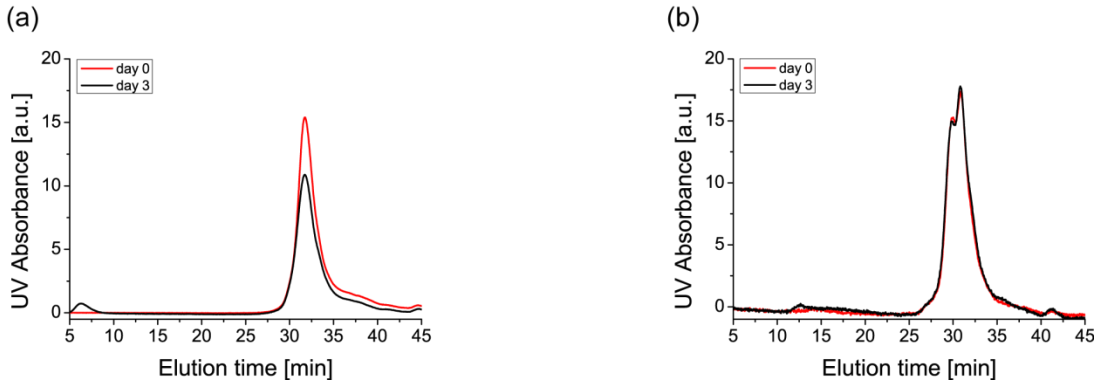

Figure 5.29 SEC profiles of the resuspended (a) and resuspended and oxidized (b) μ tp peptide on Superdex 75 10/300 GL column on day 0 and day 3 after resuspension/oxidation. (a) The peptide was resuspended to a final concentration of 0,4 mg/ml (207 μM) and stored at RT. (b) The redox system was added (GSSG/GSH = 1 mM/0,5 mM final) and the sample was incubated for 2 hours at RT under stirring. Glutathione was then removed by centrifugation and subsequent dilution with Tris/EDTA buffer. Samples were stored at RT.

To investigate a possible interaction between the μ tp and the Cμ4 domain, the resuspended as well as the oxidized μ tp was added to the Cμ4 domain and the mixture was stored at RT for three days. Any interaction of the Cμ4 domain with neither monomeric nor dimeric tp form was observed, indicating that the two segments do not have a natural tendency to interact with each other (data not shown).

5.3.3.2 Analysis of the tp secondary structure

To assess the secondary structure of the μ tp peptide, CD spectra were recorded. The μ tp peptide showed a very similar secondary structure to that of the Cμ4-tp fragment and to possess therefore, a β strand motif (Figure 5.30). After oxidation the wt μ tp became more structured, since the far-UV CD spectrum indicated a more pronounced ellipticity minimum. Reduction of the disulfide bond however, did not seem to destabilize or alter the β-strand-like conformation.

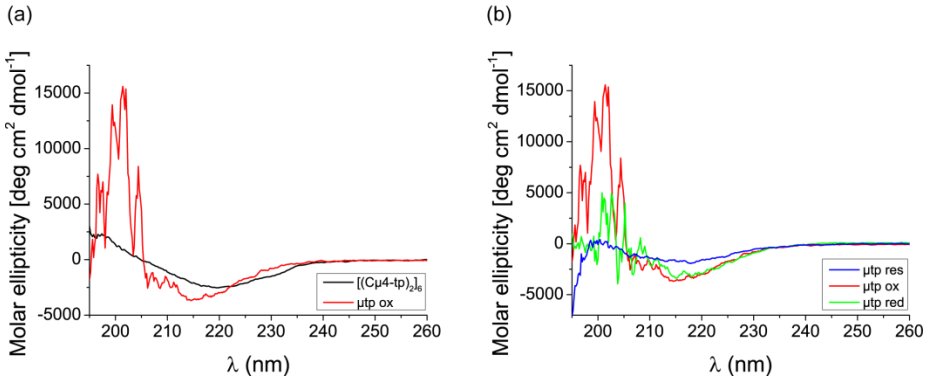

Figure 5.30 Secondary structure characterization of the wt μ tp within the far-UV range. (a) - Comparison of the Cμ4-tp dodecamer and the oxidized μ tp far-UV CD spectra. (b) - Overlay of the far-UV CD spectra of the resuspended (res), oxidized (ox) and reduced (red) wt μ tp wt. The spectra were acquired at 20°C in PBS at a concentration of 20 μM for Cμ4-tp dodecamer and in Tris/EDTA buffer at a concentration of 207 μM for the tp peptide.

Interestingly, the PSIPRED (protein structure prediction server) prediction concerning the secondary structure was fully in agreement with these findings in that the β strand conformation was predicted for the wt μ tp (Figure 5.31). Moreover, according to the PSIPRED prediction the same amino acids involved in the β strand conformation spanning from T560 to S569 are those identified by TANGO and AGGRESCAN to confer aggregation propensity to the tail piece. It might be therefore, that the replacement of any of these amino acids with alanine significantly affects the oligomerization ability of the Cμ4-tp domain by altering the tp secondary structure.

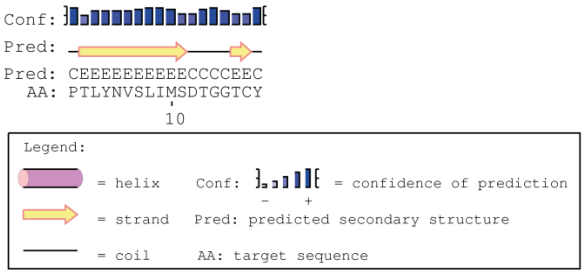

Figure 5.31 PSIPRED prediction of the tp secondary structure.

5.3.3.3 Analysis of the tp mutants: secondary structure and oligomerization ability

To assess whether the single-point tp mutations that fully impaired the oligomerization ability of the Cμ4-tp domain affect the tp secondary structure, seven tp peptide mutants including Y562A, V564A, L566A, I567A, two cysteine mutants C575A and C575S and finally,

the deletion mutant ΔY576 were synthesized and their secondary structure as well as their oligomeric state were evaluated.

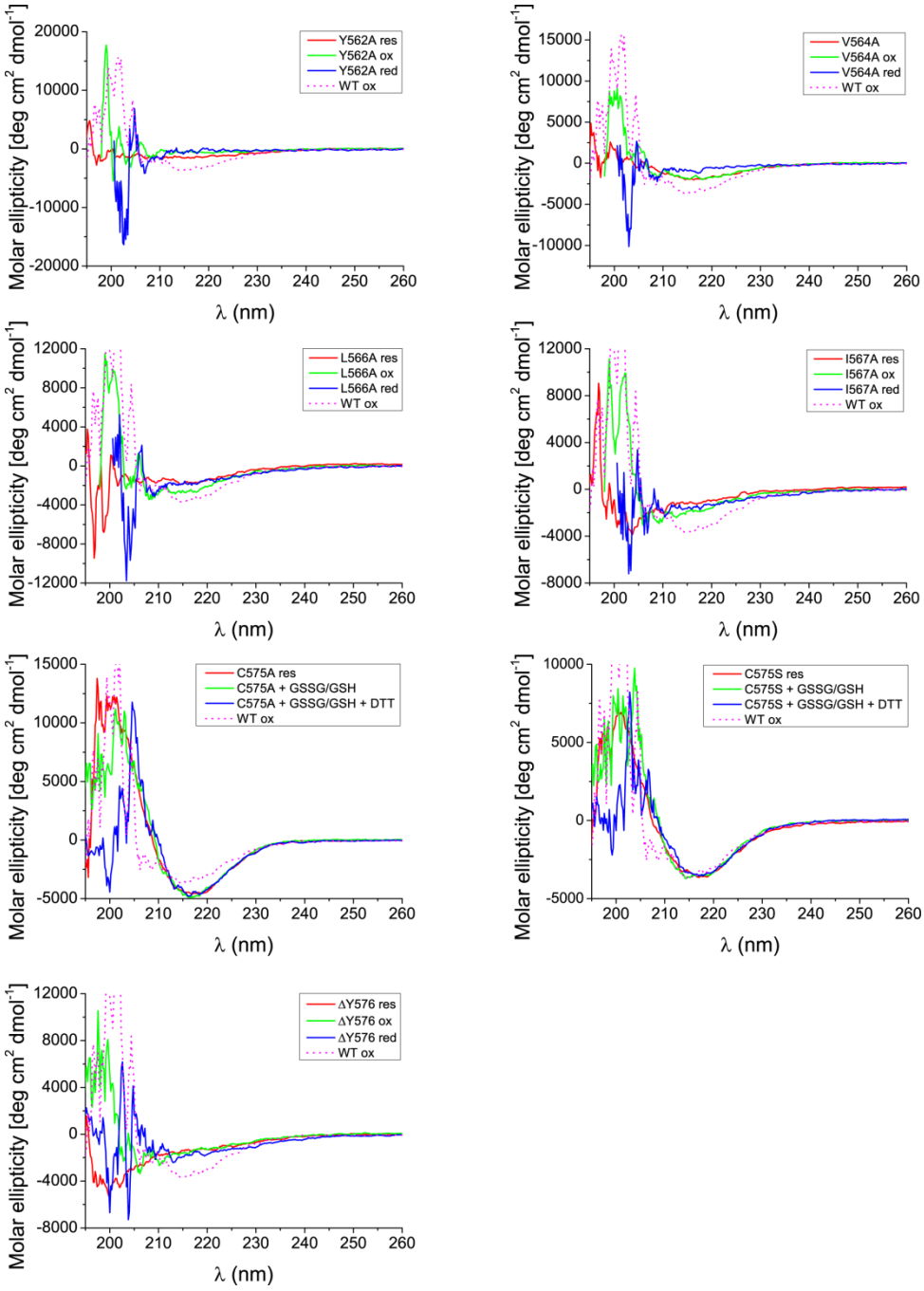

Figure 5.32 Characterization of the secondary structure of the μ tp mutants whitin the far-UV range. An overlay of the spectra of the resuspended (res), oxidized (ox) and reduced (red) form is shown for each μ tp mutant. Resuspension, oxidation and reduction was performed as described above for the wt μ tp.

In accordance with the expectations, all except two cysteine mutants showed a complete loss of the β strand conformation in both oxidized and reduced state, although the V564A mutant seemed to have some β strand features only in the oxidized form (Figure 5.32).

These findings indicate that every tp hydrophobic amino acid is important for the correct tp secondary structure, and that most likely the loss of its correct conformation might be the reason for the impaired oligomerization ability of the whole Cμ4-tp domain.

Interestingly, the same five mutations had no effect on the secondary structure of the analogous Cμ4-tp mutants. They, as well as all remaining 38 Cμ4-tp mutants, showed a β sheet conformation similar to that of the Cμ4-tp wt (data not shown), probably due to a major contribution of the β-folded Cμ4 domain to the secondary structure of the whole Cμ4-tp fragment.

In agreement with their Cμ4-tp counterparts, the five tp mutants were able to form covalent dimers upon addition of GSSG/GSH but were not able to form bigger oligomers since SEC-HPLC profiles very similar to that of the wt μ tp were obtained upon resuspension as well as after three days of incubation with the redox system (data not shown). Furthermore, no oligomerization of monomers in the case of non-oxidized samples could be observed after three days of sample storage at RT. Moreover, like the ΔY576 Cμ4-tp mutant, the respective tp mutant showed a less efficient oxidation. As expected, in the case of the two cysteine tp mutants no dimer peak was observed upon addition of the redox system (data not shown) nor any oligomer peak appeared after three-day storage at RT of the resuspended sample as well as of the one treated with GSSG/GSH.

5.4 Structural requirements for IgM oligomerization in a mammalian cell model

5.4.1 Analysis of the oligomerization ability of IgM-tp alanine mutants

To better define the role of the μ tp and its 18 amino acids in the IgM assembly and oligomerization, 18 single-point IgM tp mutants were generated by serially replacing every tp amino acid with alanine and expressed in a mammalian cell model. The λ-HEK293 cell line stably expressing the λ chain was established. This cell line was transiently transfected with each μ heavy chain mutant. Two days after transfection the cell medium was replaced with a minimal essential medium in which the cells were incubated for 4 hours. Finally, the supernatant was collected, its proteins were precipitated and secreted IgM were evaluated by gel electrophoresis. As negative control, a mock transfection with the empty expression plasmid was performed. IgM oligomer intermediates were evaluated by analyzing cell lysates by gel electrophoresis. Additionally, western blots (WB) were performed with an anti-μ and an anti-λ antibody. The specificity of both antibodies was confirmed by the presence of one single band at ca. 80 kDa corresponding to the μ chain after incubation with anti-μ antibody and one single band at ca. 25 kDa corresponding to the λ chain after incubation with anti-λ antibody when cell lysates were analyzed under reducing conditions (data not shown). Since the biggest protein of the marker had a MW of 250 kDa, the band position of the IgM decamer (5 $\mu_2\lambda_2$) was identified by the Invitrogen IgM standard which is in decameric form and by the decameric IgM purified from the J571B cell supernatant (data not shown).

Surprisingly, 15 of the 18 IgM-tp alanine mutants oligomerized in a comparable way to the Cμ4-tp alanine mutants analyzed *in vitro* (Figure 5.33). Thus, in agreement with the *in vitro* results, the N563A and the D570A were secreted as covalent oligomers larger than dodecamers, most likely aggregates. Furthermore, Y562A, V564A, L566A and I567A secreted only covalent dimers reflecting the behavior of their Cμ4-tp counterparts *in vitro* as well. The absence of secreted non-covalent oligomers for these four mutants was confirmed by sucrose gradient density ultracentrifugation of precipitated supernatants, in that their covalent dimer was found only in the second and the third fraction, where the wt covalent dimer also sedimented. Heavier and thus denser non-covalent molecules such as decamers and dodecamers would have sedimented in fractions 6 and 7, which was not the case (Figure 5.34). All other IgM-tp mutants were able to oligomerize into dodecamers or hexamers of covalent dimers. However, they were able to form decameric units or pentamers of covalent

dimers even in the absence of the J chain, which was not observed *in vitro* with their Cμ4-tp analogous mutants. The only exception was P559A which was secreted only in the form of dodecamers. On the other hand G573A was secreted prevalently in decameric form. Moreover, among mutants able to oligomerize, the L561A mutant showed lower oligomerization ability and was secreted prevalently in the form of covalent dimers (or IgM monomeric antibody unit). Similar oligomerization behavior was observed with the respective Cμ4-tp mutant *in vitro*.

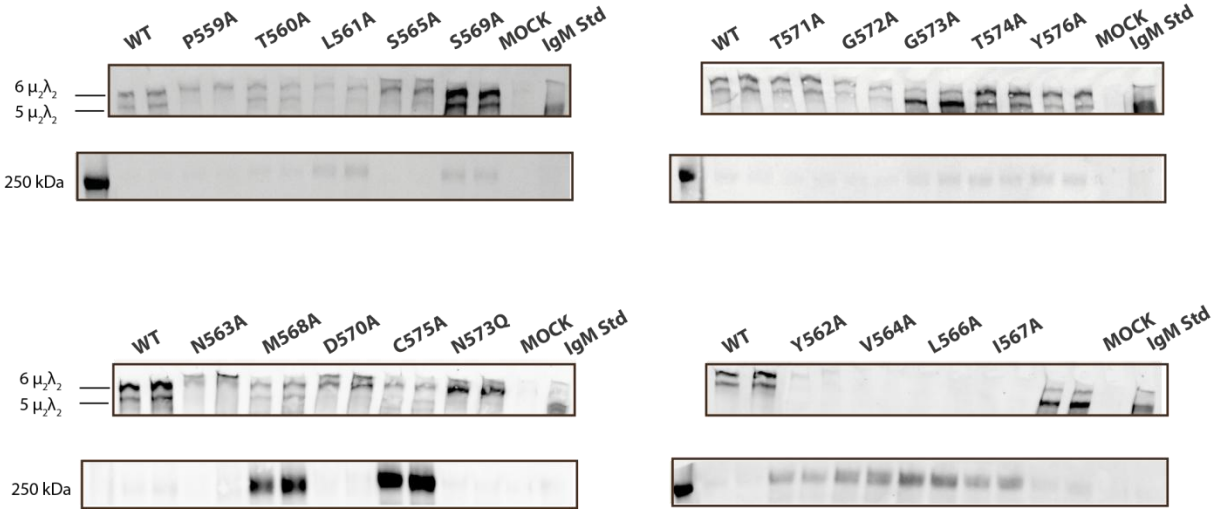

Figure 5.33 Oligomerization ability of IgM-tp alanine mutants. Cell supernatants were collected after 4 hours of incubation in minimal essential medium, normalized with respect to the cell number, precipitated and loaded on a 3-8% SDS-PAGE gel.

Three mutants showed oligomerization tendencies different from their Cμ4-tp counterparts. M568A was secreted prevalently in dimeric form (confirmed by sucrose gradient centrifugation, Figure 5.34) and S565A in the aggregate form rather than forming decamers and dodecamers, respectively, as observed *in vitro* for their respective Cμ4-tp mutants. Interestingly, the M568A tp mutant was predicted by AGGRESCAN to have a significantly lower aggregation propensity than that of the wt tp and similar to that of L561A, Y562A, V564A, L566A and I567A, whereas the S565A tp mutant was predicted by TANGO to have a higher aggregation propensity. Finally, the IgM C575A mutant was secreted prevalently in the form of covalent dimers, although a small portion was secreted in dodecameric form confirming the observations of Sitia *et al*. (1990) and of Davis *et al.* (1989) with the same mutant and with C575S, respectively. The respective Cμ4-tp mutant formed only monomers

in vitro. This mutant was lacking the C337 present on the Cμ2 domain which in the context of the whole IgM forms the intra-chain disulfide bridge with a second μ heavy chain giving rise to a covalent IgM dimer.

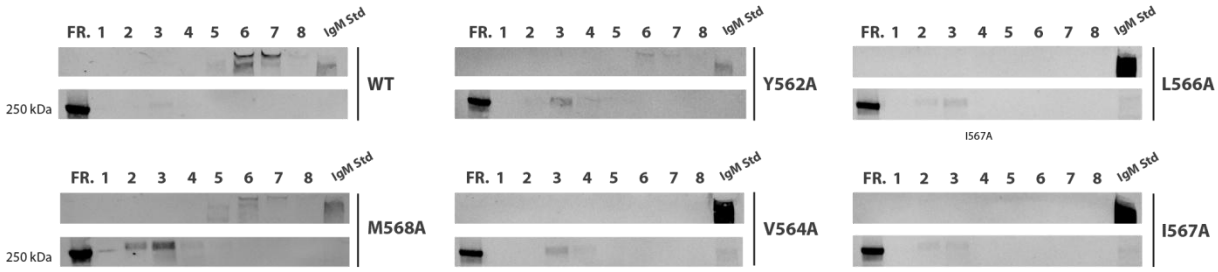

Figure 5.34 Sucrose gradient density ultracentrifugation characterization of IgM-tp alanine mutants secreted prevalently or exclusively as covalent dimers. Cell supernatants were processed as described above and fractionated on continuous (5-20%) sucrose gradient. 8 of the total 12 fractions were loaded on a 3-8% SDS-PAGE gel. On the right are fractions corresponding to the higher part of the gradient.

By investigating the cell lysates with the anti-μ-chain antibody, several IgM oligomer intermediates corresponding to the monomer (μλ) and the dimer ($\mu_2\lambda_2$) were observed (Figure 5.35). These findings were confirmed also with the anti-λ antibody (data not shown). Furthermore, four additional bands between those corresponding to the monomer and the dimer could be identified with the anti-μ antibody, whereas only one of them could be also identified by the anti-λ antibody (data not shown). These data indicated that three of those bands, having a lower MW, might correspond to the μ chain and the fourth band to the monomer μλ bound to some chaperones such as BiP or members of PDI family such as ERp44 assisting them during assembly (Cortini and Sitia, 2010; Anelli and van Anken, 2013). Moreover a smear was observed in the upper part of the gel corresponding to IgM oligomers of different size.

Two of three aggregating mutants, N563A and D570A showed a very low amount of intermediates in cells, which might be due either to a fast secretion of aggregates which somehow escape the quality control or to fast degradation of their intermediates.

All four non-oligomerizing mutants, Y562A, V564A, L566A and I567A exhibited also a band with a higher MW than that of the dimer, which was observed in the case of L561A, M568A and C575A, secreted prevalently in dimeric form as well. M568A and C575A showed a very high amount of covalent dimers in the cell lysate, which in turn reflected in high levels of dimers secreted.

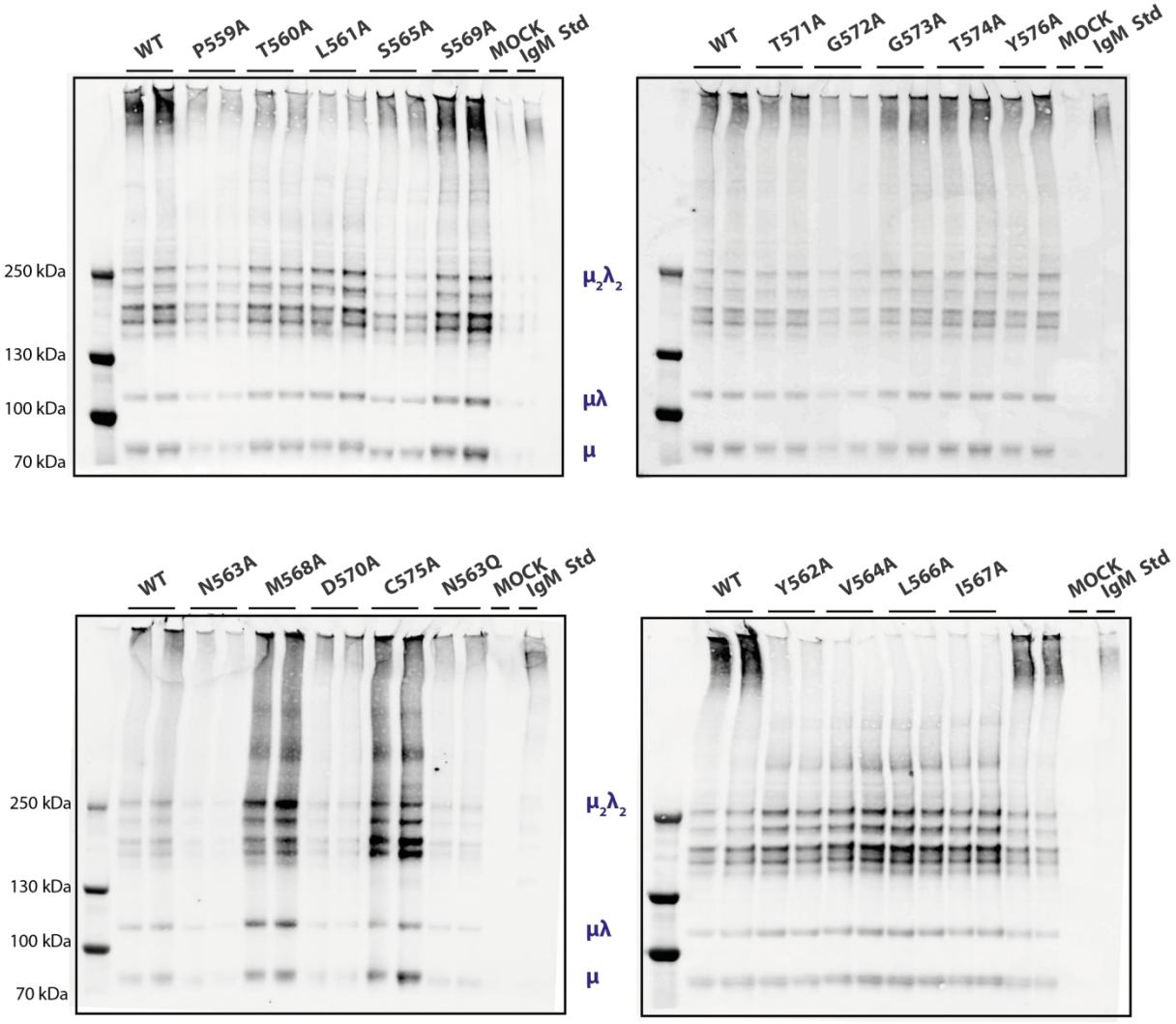

Figure 5.35 Characterization of the oligomer intermediates of the IgM-tp alanine mutants. Cells were collected after 4 hours of secretion, centrifuged and lysated. The lysates were normalized with respect to the cell number and loaded on a 3-8% SDS-PAGE gel.

To evaluate the impact of the mutation on protein secretion and retention, the amount of IgM-tp mutants was quantified in cell supernatants as well as cell lysates after 24 hours of secretion (Figure 5.36). All analyzed mutations had more or less a significant impact on mutant secretion with only one mutant, C575A, being able to increase the rate of its secretion, suggesting that this mutation may render the IgM less prone to the quality control before being secreted, which would enable in turn the mutant to be secreted faster.

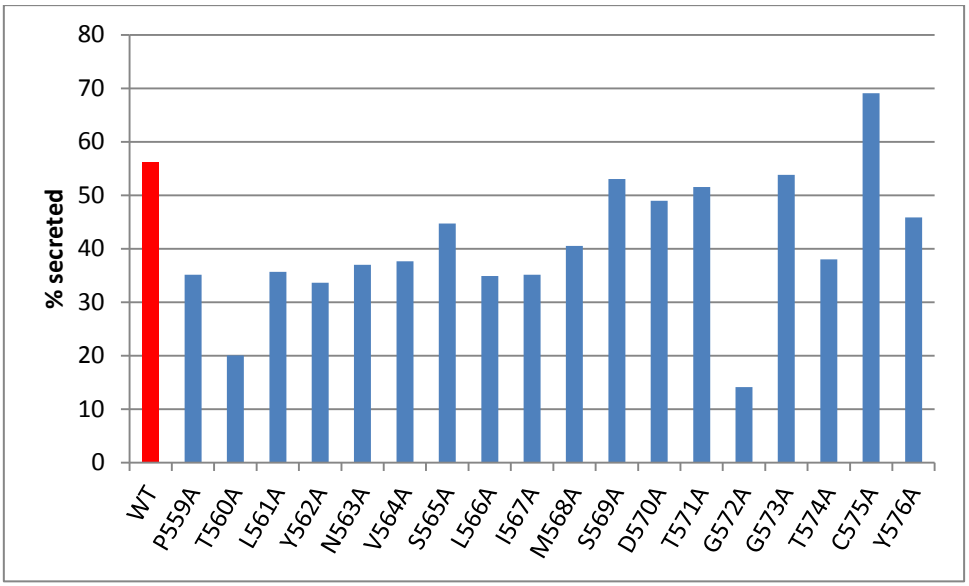

Figure 5.36 Mutation impact on secretion and retention of IgM-tp alanine mutants. Supernatants were processed as described above 24 hours after secretion in minimal essential medium. Cells were collected, centrifuged and lysated. Both lysates and supernatants were normalized with respect to the cell number and the amount of the mutants was quantified by an enzyme-linked immunosorbent assay (ELISA). The coating was performed with an anti-IgM antibody, and the IgM were revealed indirectly with an anti-λ antibody.

5.4.2 Analysis of the oligomerization ability of IgM Tyr576-tp mutants

To investigate the influence of the hydrophobicity and of charge in the very last C-terminal position on the oligomer formation, Y576 mutants analogous to the respective Cμ4-tp ones were expressed in λ-HEK293 cells. The deletion mutant ΔY576 was secreted significantly in dimeric form whereas the increase of hydrophobicity led to an increase of the secreted IgM decamers rather than dodecamers, whose levels seemed not to be altered by the analyzed mutations (Figure 5.37a). The exchange of Tyr576 and Cys575 reduced the amount of IgM decamers, whereas the insertion of the negative charge in the last position led to an increase of dimer secretion (Figure 5.37b). These behaviors correlated well with that of the analogous Cμ4-tp mutants *in vitro*, indicating the necessity of the last position to be occupied by a strongly hydrophobic amino acid for IgM decamer rather than dodecamer formation.

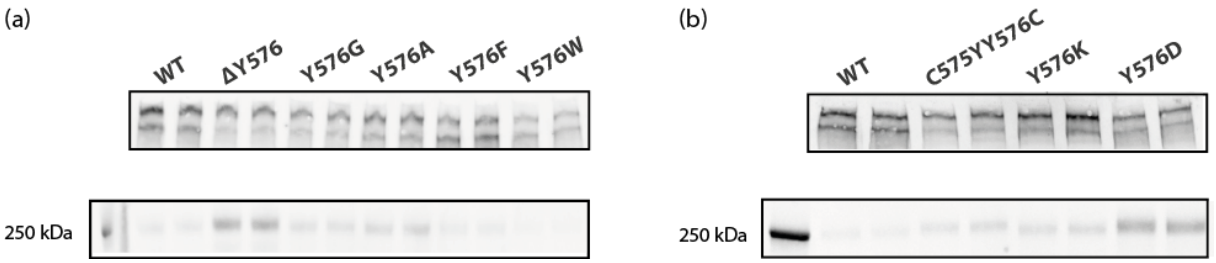

Figure 5.37 Characterization of secreted oligomers of IgM-tp alanine mutants. Cell supernatants were collected after 4 hours of incubation in minimal essential medium, normalized with respect to the cell number, precipitated and loaded on a 3-8% SDS-PAGE gel.

5.4.3 Analysis of the effect of tp glycosylation on oligomerization

Glycosylation on N563 was reported to be of relevance for the formation of IgM oligomers of correct size, in that the lack of glycans on the tail piece prevented the formation of IgM decamers and led to secretion of dodecamers and higher-MW oligomers (de Lalla *et al*., 1998). The fact that the Cμ4-tp domain forms exclusively dodecamers *in vitro* and that the glycosylated IgM is secreted from cells in dodecameric as well as decameric form indicates that either the tp glycosylation or the rest of the constant μ chain (Cμ1-Cμ3) might be relevant for the formation of decameric IgM. To better investigate the influence of the tp glycosylation on oligomer formation, a mutant carrying the glutamine in position 563 (N563Q) was generated, which resembles the wild type asparagine but differs in that it is not glycosylated. This mutant was secreted exclusively in dodecameric form, confirming that the tp glycosylation allows formation of decamers (Figure 5.33). Two other mutants, N563A and S565A, were also lacking glycans in the tp and both of them were not able to oligomerize into decamers but in dodecamers and higher-MW aggregates, supporting the importance of the tp glycosylation for the decamer formation (Figure 5.33). The lack of the tp glycosylation on these three mutants could be observed by a slight shift in electrophoretic mobility after processing their supernatants with SDS-PAGE under reducing conditions (Figure 5.38a).

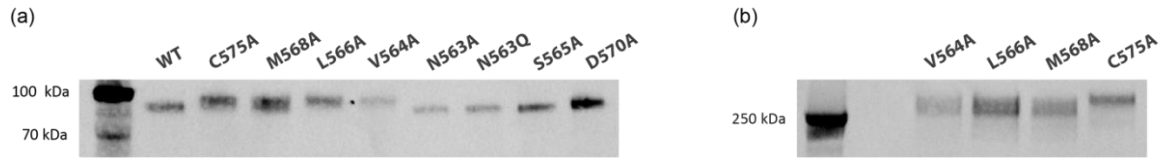

Figure 5.38 (a) SDS-PAGE characterization under reducing conditions of the glycosylation of secreted aggregating IgM-tp mutants and of those being secreted prevalently as well as exclusively as covalent dimers. (b) Characterization of the conformation of IgM-tp mutants secreted prevalently and exclusively as covalent dimers. Two representatives of the latter, V564A and L566A, were analyzed in (b). Supernatants were prepared as described above and loaded on 10% SDS-PAGE under reducing conditions (a) and on 3-8% SDS-PAGE gel under non-reducing conditions (b).

Secreted IgM contain five N-linked glycosylation sites, three of which carry complex glycans (Asn171, Asn332 and Asn395) and two of which (Asn402 and Asn563) contain oligomannose glycans (Arnold *et al*., 2005). Complex glycan derive from oligomannose precursors due to activity of glycosidases and glycosyl-transferases distributed in the pre Golgi compartment (Kornfeld and Kornfeld, 1985; Nilsson *et al*., 1993).

The oligomer size and conformation can determine the accessibility of the N563 for glycosyl-transferases (Davis and Shulman, 1989; Cals *et al*., 1995). Therefore, when oligomers are formed, their tp glycans are inaccessible to the enzyme remaining in the high-mannose state. On the other hand, tp glycans of dimeric C575A mutant do not present steric hindrances and thus can be processed by the enzyme into complex glycans (Sitia *et al*., 1990). The glycan processing slightly increases the molecular mass of the dimer and can be observed by a slight shift in electrophoretic mobility under reducing conditions (Figure 5.38a). Accordingly, electrophoretic mobility similar to that of C575A could be observed in the case of the IgM V564A, L566A and M568A mutants, which are dimeric as well, indicating that their glycans have been processed into a more complex form. To get a deeper insight into the conformation of the mutants which were prevalently (M568A and C575A) as well as exclusively (Y562A, V564A, L566A and I567A) secreted as covalent dimers, their electrophoretic mobility under non-reducing conditions was evaluated (Figure 5.38b). C575A showed a slight shift of the band compared to that of V564A, L566A and M568A. Thus, although all these mutants share dimeric form, the conformation of the former mutant differs slightly from that of the latter mutants.

5.5 Characterization of mouse and human J chain

5.5.1 Analysis of oligomeric state, structure and S-S bond arrangement

The protocol used to refold the Cμ4-tp domain was applied to refold the human and the mouse wt J chain. Under the same conditions most of the protein aggregated during the concentration step which precedes the gel filtration. By reducing the concentration during the refolding step to 0,2 mg/ml and the maximal concentration during the concentration step to 3 mg/ml, it was possible to isolate both proteins in monomeric form with a very low percentage of dimers (Figure 5.39a, b and c). J chain aggregates were of covalent nature (SDS-PAGE data not shown). To investigate whether the aggregation propensity could be decreased by reducing the number of cysteines, two of the eight cysteines (Cys16 and Cys70) in the murine J chain which bridge Cys575 in IgM decamers were replaced with serine (CSCS mutant) but no lower tendency for aggregation could be observed. The monomer of the human and mouse wt J chain as well as of the mouse CSCS mutant showed a random coil secondary structure in the far-UV CD spectrum (Figure 5.39d and e).

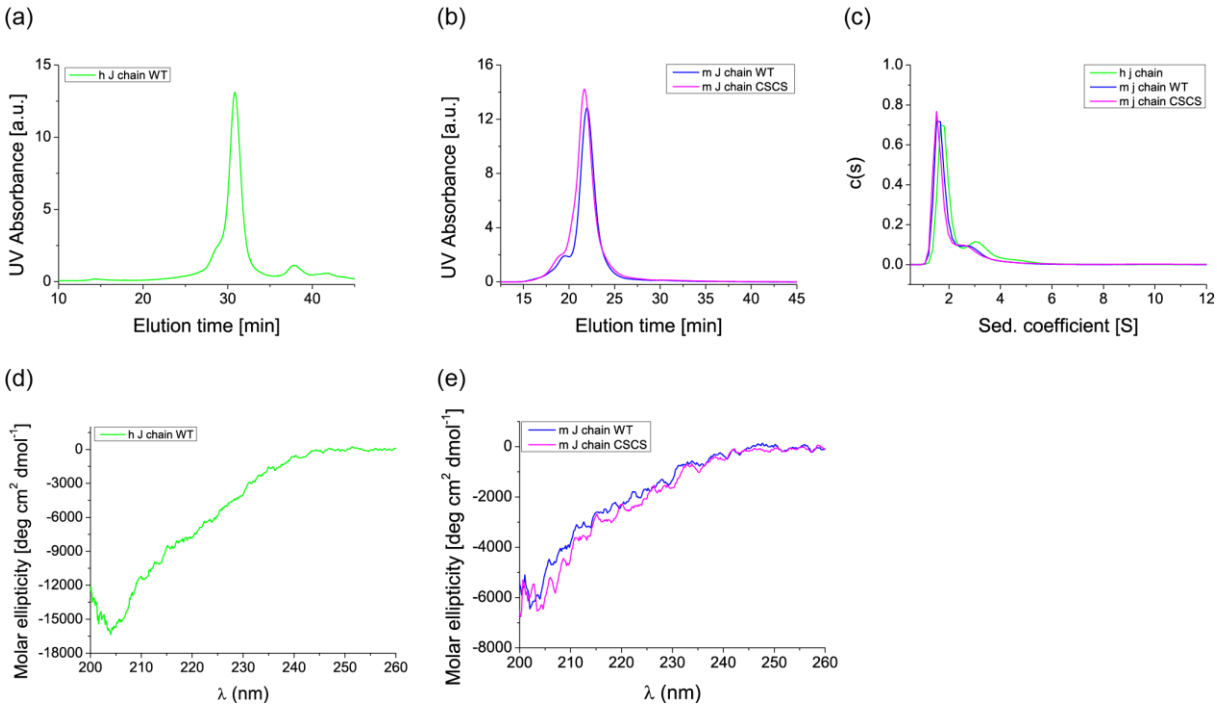

Figure 5.39 Characterization of the monomeric human and murine wt and mouse CSCS mutant J chain: (a) SEC profile on Superdex 200 10/300 GL and (b) on Superdex 75 10/300; (c) aUC; (d) and (e) far-UV CD spectra. The J chain was refolded and its monomer isolated as outlined above. SEC-HPLC analysis was performed in PBS injecting 100 µg of protein at a concentration of 1 mg/ml. aUC runs were performed in PBS at a protein concentration of 1 mg/ml. CD spectra were recorded in PBS at 20°C at a protein concentration of 20 µM.

Furthermore, the SDS-PAGE analysis showed a slight shift in electrophoretic mobility between the reduced and the oxidized form, since the latter migrated faster due most likely to disulfide bonds which make the protein structure more compact (Figure 5.40). Moreover, unlike the mouse J chain, the human J chain showed two main bands in the oxidized state, indicating the presence of two different conformations and therefore, most likely of two different disulfide bond arrangements. Ellman's assay of the monomers indicated no free cysteine present, indicating that all eight were involved in intra-molecular S-S bonds.

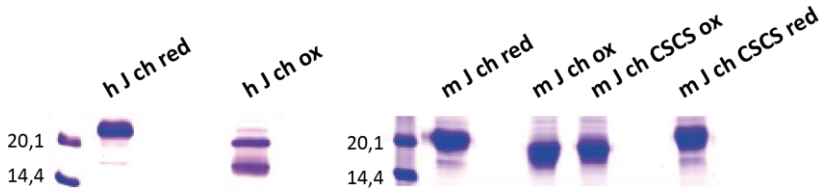

Figure 5.40 Characterization of the oxidized and reduced forms of human and mouse wt and mouse CSCS mutant J chain.

By blocking the free cysteines with AMS at time points during the oxidative refolding and subsequent SDS-PAGE analysis of the samples, it was possible to assess that the disulfide bond formation occurred very fast and was completed within the first 30 minutes of dialysis against the refolding buffer (data not shown). Trypsin digestion of the monomer bands, subsequent peptide analysis by MALDI-TOF mass spectrometry and comparison of the obtained MW between the oxidized and reduced peptides indicated no unique disulfide bond arrangement, but rather more than one combination (Table 5.1).

Hum J chain wt - upper band	
Cys position	Cys being bridged
C12	C68, C71, C100, C108
C14	C68, C108
C68	C12, C14, C133
C71	C12
C91	n.a.
C100	C12
C108	C12, C14, C133
C133	C68, C108

Hum J chain wt - lower band	
Cys position	Cys being bridged
C12	C108
C14	C68, C108, C133
C68	C14, C108, C133
C71	n.a.
C91	n.a.
C100	n.a.
C108	C12, C14, C68, C133
C133	C14, C68, C108

Mouse J chain wt	
Cys position	Cys being bridged
C14	n.a.
C16	n.a.
C70	C111, C136
C73	n.a.
C93	n.a.
C103	n.a.
C111	C136, C70
C136	C111, C70

Table 5.1 Disulfide bond arrangement of human and mouse wt J chain.

5.5.2 Interaction between J chain, Cμ4-tp and chaperones *in vitro*

To investigate whether the J chain structure could be influenced by the presence or possible interaction with the Cμ4-tp domain, the mouse wt J chain was mixed with the unfolded mouse Cμ4-tp domain at ratios of 1:1, 1:2 and 1:5 and the resulting mixture was subjected to refolding under standard conditions. After an ON refolding step, SEC-HPLC analysis of the mixture was performed. No interaction with Cμ4-tp and no change of J chain secondary structure could be observed (data not shown). To assess whether the refolded Cμ4-tp domain or chaperones such as Hsp90 or BiP could have some influence on the J chain secondary structure, the monomeric mouse wt J chain was incubated with the refolded mouse Cμ4-tp domain and with mouse BiP for 22 hours and for 30 minutes, respectively (Figure 5.41a and b). In addition, the monomeric human J chain was incubated with the human βHsp90 for 30 minutes (Figure 5.41c). Again neither any interaction nor any influence on the J chain structure could be observed, indicating that the J chain monomer had no affinity towards the analyzed proteins and that its structure could not be changed by their presence.

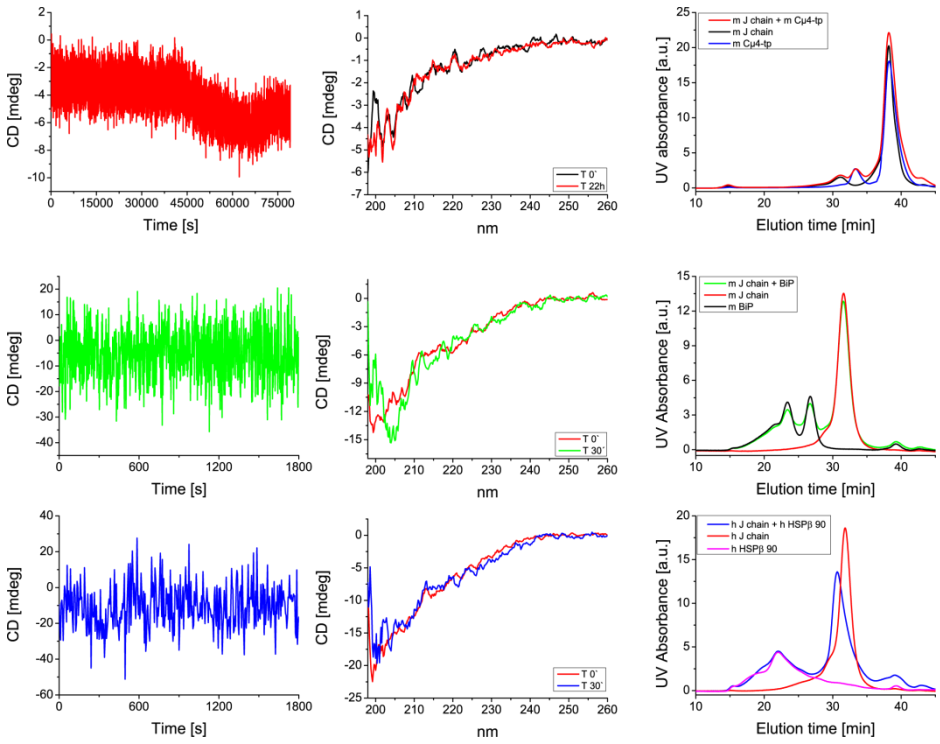

Figure 5.41 Analysis of interaction between the wt mouse (a) and (b) and human (c) J chain and the refolded mouse Cμ4-tp (a), mouse BiP (b) and human βHsp90 (c) by CD spectroscopy and SEC-HPLC analysis in PBS at 20°C. Cμ4-tp and J chain were obtained both in monomeric form as outlined above. The concentration of the single proteins alone and in the mixture was 0,2 mg/ml. CD kinetics were recorded at 205 nm.

6 Discussion

6.1 Structural requirements for Cμ4-tp and IgM oligomerization

IgM are secreted exclusively as oligomers, namely as pentamers and hexamers of dimeric subunits in order to compensate their low antigen affinity. On the other hand, high-affinity IgG are secreted as dimers. Upon antigen binding however, they form dodecameric clusters on cell surface (Diebolder *et al*., 2014). While IgG dodecamers are mainly non-covalent, IgM oligomers form exclusively through covalent inter-subunit interactions (Davis *et al.*, 1989; Wiersma and Shulman, 1995). The μ tail piece has been shown to be essential for IgM polymer formation (Davis *et al*., 1989; Davis and Shulman, 1989) and sufficient for formation of Cμ4-tp dodecamers *in vitro* (Müller *et al*., 2013). One of the main aims of this thesis was to better elucidate how this 18-amino acid extension at the C-terminus of the μ chain regulates the polymerization of IgM and to which extent each of its 18 amino acids is relevant for the assembly. To address this point, every single tp amino acid was serially replaced with alanine giving 18 Cμ4-tp mutants and 18 IgM mutants. The oligomerization ability of the former was investigated *in vitro*, whereas that of the latter was determined in HEK293 cells. Although these cells form and secrete IgM polymers to some extent less efficiently than plasmacytoid cells, they have been shown to be an adequate model for investigating interactions relevant in IgM assembly (Cortini and Sitia, 2010).

The two groups of mutants showed an unexpected agreement in oligomerization properties between the Cμ4-tp domain *in vitro* and the IgM antibody in cells (Figure 5.18), indicating that the μ tp fully dictates the oligomerization not only of the Cμ4 domain but also of the whole IgM antibody. Of the 18 mutants only 3 behaved differently *in vitro* and *in vivo* which corresponds to almost 83% identity of results.

Non-oligomerizing mutants, Y562A, V564A, L566A, I567A and M568A, were only those where a hydrophobic residue was replaced, indicating clearly how crucial the intra-subunit hydrophobic interactions between two Cμ4-tp domains are in IgM polymer assembly (Figure 5.33). However, while the first four mutants led to exclusive secretion of dimers, the M568A allowed secretion of a small amount of dodecamers and decamers as well. *In vitro* the M568A formed only decamers (Figure 5.19) and thus represents one of the three exception

mutants that behaved differently *in vitro* and in cells. This suggests that the effect of methionine replacement is more relevant when the µ chain carries additional domains on its N-terminus as it is in the context of the whole IgM. The M568 occupies exactly the middle position of the tp and might therefore reppresent a hinge able to determine the spatial orientation of the proximal C-terminal tp half which carries the C575 involved in covalent bonding of adjacent IgM subunits (Figure 6.2). By altering its orientation, the M568A mutation might therefore influence the spatial position of the neighbouring IgM subunits through the C575 S-S bond. This could reflect on the distance between and thus on the number of IgM subunits that can be incorporated into the oligomer. It might be that due to an increased inter-subunit distance, the formation of only M568A Cµ4-tp decamers was feasible *in vitro*. Additional domains present on IgM could however reppresent sterical hindrances for effective incorporation of additional entire IgM subunits, leading to a prevalent secretion of dimers in cells.

Figure 6.1 Cµ4 domain with the tp amino acid sequence. In colors are highlighted tp segments influencing IgM oligomerization. Orange: amino acids forming the hydrophobic core and whose replacement leads to prevalent or exclusive secretion of covalent dimers. Green: amino acids whose replacement leads to aggregation. Grey: Cys575, whose replacement leads to prevalent secretion of covalent dimers. Red: tp glycosylation site. Purple dotted line: region predicted by PSIPRED to form the β strand. Brown dotted line: region predicted by TANGO and AGGRESCAN to influence the aggregation propensity of the tp.

The replacement of the first hydrophobic tp residue, L561, led to reduced oligomerization both *in vitro* and *in vivo* (Figure 5.19 and Figure 5.33). Thus L561 can be considered the N-terminal and M568 the C-terminal borderline residue delimiting the hydropbobic core which plays a decisive role in assembly of IgM polymers (Figure 6.1). The tp hydrophobic core is a very important entity as the replacement of only one of its central 4 hydrophobic residues completely blocks the assembly at the stage of covalent dimers, most likely by rendering the C575 not accessible to adjacent IgM subunits. The effect of their replacement is even more drastic than that of the C575A, which leads to a prevalent secretion of covalent dimers but allows however assembly and secretion of a little amount of dodecamers (Figure 5.33). The analogous Cµ4-tp C575A mutant formed, on the other hand, only monomers *in vitro* (Figure

5.25), representing thus the second exception mutant. This mutant lacks the C337 present on the IgM Cμ2 domain which forms the intra-subunit disulfide bridge with a second μ heavy chain, giving rise to an IgM covalent dimer or one IgM subunit. This explains why the C575A Cμ4-tp mutant could not behave *in vitro* as its analogous IgM mutant.

The aggregating mutants were N563A, S565A and D570A. Among them, the S565A is the third exception mutant, in that it formed dodecamers as well as aggregates in cells (Figure 5.33) but only dodecamers *in vitro* (Figure 5.19). N563A and S565A both lack glycans which are normally present on Asp563 (Cals *et al*., 1995; Arnold *et al*., 2005). De Lalla *et al*. (1998) showed that the absence of the glycosylation on N563 due to the S565A mutation led to the formation of dodecamers and higher-order spiecies in cells suggesting a significant role of tp glycans in the formation of decamers. The fact that the Cμ4-tp domain obtained from in *E. coli* as well as the N563Q mutant, both lacking glycans at position 563, form exclusively dodecamers and do not aggregate (Figure 5.14 and Figure 5.33), confirmed the relevance of the tp glycans for assembly of IgM into decamers. Furthermore, the N563A, S565A and N563Q mutants indicated that it is the presence of the amide group in position 563 as well as of the serine hydroxylic group that plays a relevant role in preventing aggregation. An additional functional group that prevents aggregation is the negatively charged carboxylic group of D570. Asp570 is the only charged tp amino acid and it is placed directly on the C-terminal edge of the tp β strand and hydrophobic region. One of the mechanisms used by β sheet proteins to prevent aggregation is placing an inward pointing charged residue on the hydrophobic side of a β strand (Richardson and Richardson, 2002). Aggregation is then prevented due to either an electrostatic repulsion (Otzen *et al*., 2000) or to exposition of the charged residue to the solvent (Thirumalai *et al*., 2003). Thus, the last residue of the Cμ4 domain, K558, which is charged as well and the middle positioned tp D570 might act as charged gatekeepers that prevent aggregation of the tp, of the Cμ4-tp domain and of the whole IgM as well. The placement of the former at the N-terminal edge of the tp and of the latter in the middle region of the tp might help on the one hand, the hydrophobic core to assume the conformation of a pocket and on the other hand, to give the C-terminal tp half carrying C575 the necessary bending outwards due to repulsion between D570 of two neighboring intra-subunit tps. This in turn would favor the establishment of an inter-subunit S-S bond and thus, formation of IgM polymers. Similarly to hydrophobic residues, the absence of only one of these three functional groups leads to aggregation (Figure 6.2).

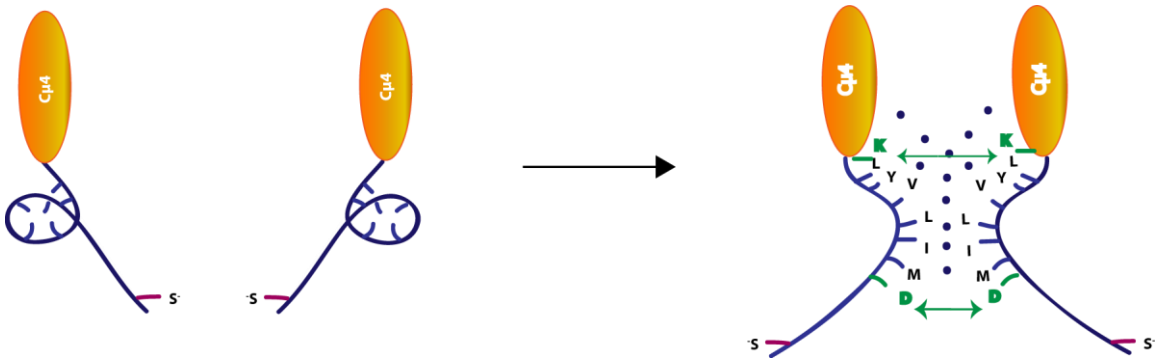

Figure 6.2 Hypothetical non-covalent hydrophobic (blue dots) and repulsive (green arrows) interactions occurring between two Cμ4-tp domains.

All together, the eighteen alanine-mutants helped identifying one region located in the N-terminal half of the tp encompassing residues 559-568 which is sensitive to alanine mutation with regard to oligomerization. Replacement of any residue within this region led to either imparied oligomerization (P569A), drastic decrease of oligomer formation (T560A, L561A and M568A), aggregation (N563A and S565A) or, finally, to a complete abolishment of oligomerization (Y562A, V564A, L566A and I567A) (Figure 5.19 and Figure 5.33). Interestingly, the same region on the tp was predicted by the PSIPRED algorithm to form the only secondary structure motif of the tp, the β strand (Figure 5.31 and Figure 6.1). This finding is not in line with results of Wormald *et al*. (1991) who used ^{1}H-NMR spectroscopy to investigate the conformation of the isolated tp from human serum IgM and of the synthesized peptide. Their 1D-NMR spectra of both peptides showed a random coil conformation. Of note, the synthesized as well the isolated peptide used in experiments of Wormald *et al*. (1991) consisted of 22 amino acids and the NMR measurements were performed after dissolving the sample in 90% H_20/10% $^{2}H_20$ at pH 4,4. The synthesized tp peptide analyzed here consists of 18 amino acids and the buffer used for all analysis was a Tris/EDTA buffer with a pH of 7,5. The CD far-UV spectra of the synthesized tp peptide obtained in this work resemble those of β sheet secondary structures (Figure 5.30). Thus, althouth not in line with the 1D-NMR spectra obtained by Wormald *et al*. (1991), they agree with PSIPRED predictions and could therefore explain the drastic behavior of the four Cμ4-tp and IgM non-oligomerizing mutants (Y562A, V564A, L566A, I567A). In fact, the analogous tp mutants together with the Y576A mutant all showed a loss of the β strand motif and a secondary structure which resembles a random coil, indicating that each of the tp

hydrophobic amino acid is essential for the correct tp secondary structure and thus its three-dimensional conformation, which in turn reflects the overall oligomerization properties of the µ chain. In accordance with these findings, the replacement of the remaining amino acids within this tp region led to other drastic effects such as aggregation or singificantly reduced oligomerization, probably due to a compromised conformation of the tp. One further interesting point is that the same tp region was predicted by the TANGO and AGGRESCAN algorithm to determine its aggregation propensity (Figure 5.22 and Figure 6.1). The same three amino acid substitutions which were predicted to substantially increase its aggregation propensity (N563A, S565A and D570A) led to aggregation of Cµ4-tp as well as of IgM, and the same six amino acid substitutions predicted to significantly decrease its aggregation tendency (L561, Y562A, V564A, L566A, I567A and M568A) abolished or drastically reduced the oligomerization ability of both Cµ4-tp and IgM.

The T576-mutants showed the influence of either a hydrophobic, aromatic or positively charged residue in the very last position of the tp on oligomerization, namely for formation of Cµ4-tp dodecamers *in vitro* and in cells of IgM decamers rather then dodecamers, most likely by influencing the reactivity of the nearby C575 (Figure 5.24).

Cysteine double point mutants carrying the alanine in position 575 and the cysteine in another position on the tp suggest that relocation of tp disulfide bonds towards its N-terminus interferes with ordered oligomerization, whereas its positioning on the very last tp position, with the Tyr in the penultimate position, results in almost unaltered oligomerization of Cµ4-tp and IgM (Figure 5.25).

The swap-mutants carring the murine Cµ4 and the human, Ladyfish or Xenopus tp indicate that the tp alone does not determine species-specific oligomerization of the Cµ4 domain (Figure 5.27). Additional swap mutants with the human and murine αtp confirmed findings of Sorensen *et al*., (1996) who showed that the tp cannot by itself drive the isotype-specific oligomerization (Figure 5.26).

6.1.1 Model for Cµ4-tp oligomerization *in vitro*

Previous work had shown that Cµ4 alone does not possess oligomerization properties and that Cµ4-tp is able to form dodecamers *in vitro* (Müller *et al*., 2013). This work demonstrated that Cµ4 acquires the ability to spontaneously undergo polymerization *in vitro* when fused to the tp (Figure 5.4), indicating that the information for oligomerization is contained in the tp

sequence and supported by the Cμ4 domain. Furthermore, the Cμ4-tp polymerization rate *in vitro* is temperature- and concentration-dependent (Figure 5.5 and Figure 5.6). Their increase accelerates the formation of oligomers. Nevertheless, the oligomerization process *in vitro* is still too slow compared to the polymerization rate of IgM in cells, where thousands of antibodies per second have to be correctly folded, assembled and finally secreted (Cortini and Sitia, 2010), suggesting that either other μ domains or cellular factors such as chaperones, oxidoreductases such as PDI members, which help proteins to fold and to form correct disulfide bonds, might contribute to accelerate the oligomerization of IgM.

The Cμ4-tp dodecamer formation requires covalent and non-covalent interactions to be established between associating units (Müller *et al*., 2013). The Cμ4-tp oligomerization seems to be triggered by formation of the Cys575 disulfide bond, since it was immediately arrested when remaining free cysteines were irreversibly blocked by addition of AMS during the kinetic experiment (Figure 5.11). Moreover, no bigger species and therefore no non-covalent interaction between Cμ4-tp monomers could be observed when Cys575 was replaced with serine and only a little amount of dodecamers could form when it was replaced with alanine (Figure 5.12a). However, this was observed only at a high concentration and in a high-salt buffer which favors hydrophobic interactions. Furthermore, when the Cys575 of the Cμ4-tp monomer was irreversibly blocked and the sample concentrated, no other species except the monomer could be observed (Figure 5.12b). Finally, when the Cys575 disulfide bond of Cμ4-tp dodecamers was disrupted by treatment with a reducing agent, the only species remaining was the Cμ4-tp monomer (Figure 5.15). Together these data indicate that non-covalent interactions can be established only once covalent Cμ4-tp dimers form. Moreover, four Cμ4-tp alanine mutants, Y562A, V564A, L566A and I567A, demonstrated that non-covalent interactions occurring between covalent dimers are mainly hydrophobic interactions (Figure 5.19). These mutants were the only ones among the 18 alanine single-point Cμ4-tp mutants whose covalent dimers did not oligomerize at all. The fact that 1) the replacement of just one hydrophobic amino acid allows formation of covalent dimers but precludes further non-covalent assembly and that 2) the replacement of Cys575 precludes both events indicates that S-S bond formation must precede the establishment of hydrophobic interactions. Therefore, the overall Cμ4-tp dodecamer formation process can be divided into two sequential steps. The first is the formation of

covalent Cμ4-tp dimers which then associate via hydrophobic interactions into final hexamers of dimers (Figure 6.3).

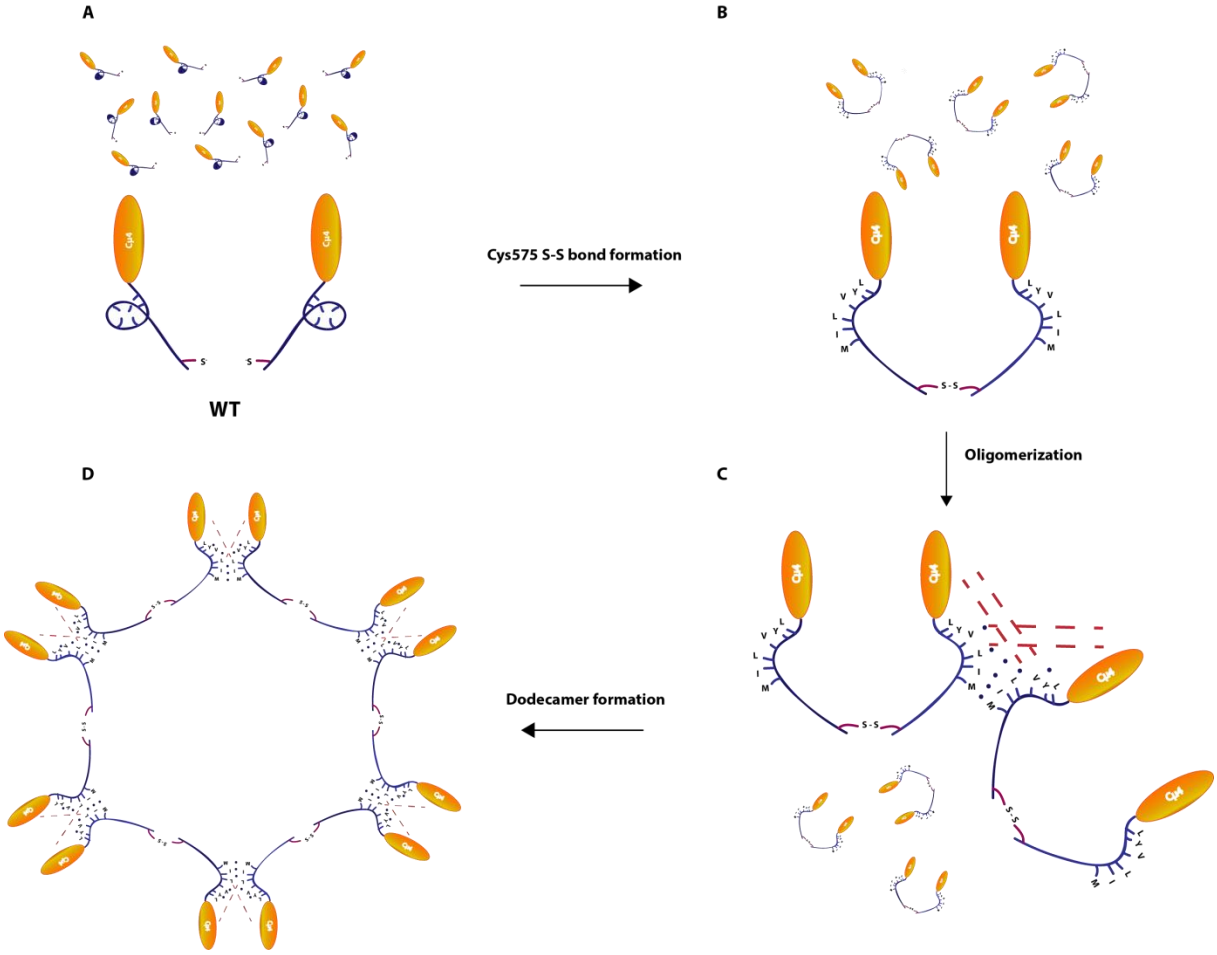

Figure 6.3 Two-step model for Cμ4-tp oligomerization *in vitro.* (A-B) tp conformational change induced by the S-S bond formation between C575. (C-D) The hydrophobic pocket opens exposing its hydrophobic amino acids allowing thus the non-covalent assembly of covalent dimers. Non-covalent interactions might occur either between two adjacent tps (blue dots) or between the tp and the Cμ4 domain belonging to two adjacent Cμ4-tp domains (red dotted lines).

Furthermore, these covalent and non-covalent interactions must take place at opposing interfaces of Cμ4-tp monomers in order to build the final dodecameric structure (Figure 6.3). Since non-covalent interactions cannot take place before the S-S bond is formed, it is likely that all amino acids involved in these interactions are buried in a hydrophobic pocket which prevents them from interacting. The formation of C575 disulfide bond must induce some conformational rearrangement within the tp which results in the removal of steric hindrances and the exposure of the hydrophobic core enabling the establishment of interactions between them. The four mutations that fully abolished the oligomerization

altered the tp structure so that that probably an appropriate exposure of the hydrophobic core could not be achieved (Figure 6.4).

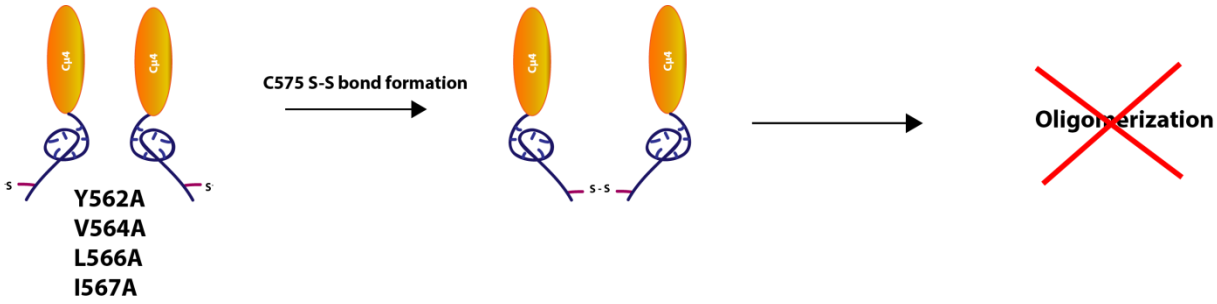

Figure 6.4 Mutations which alter the tp structure hindering the exposure of the hydrophobic core and thus, Cμ4-tp oligomerization.

However, the conformational change of the tp triggered by the formation of Cys575 S-S bonds seems to be feasible only in the Cμ4-tp and IgM context, namely when the Cμ4 domain or the rest of the μ chain is fused to its N-terminus, since the tp alone was not able to form any bigger oligomers than covalent dimers (Figure 5.28 and Figure 5.29). It might be thus, that the tp needs an anchoring point or support, given by the Cμ4 domain or the μ chain, in order to fulfill the structural rearrangement and expose its hydrophobic amino acids (Figure 6.5).

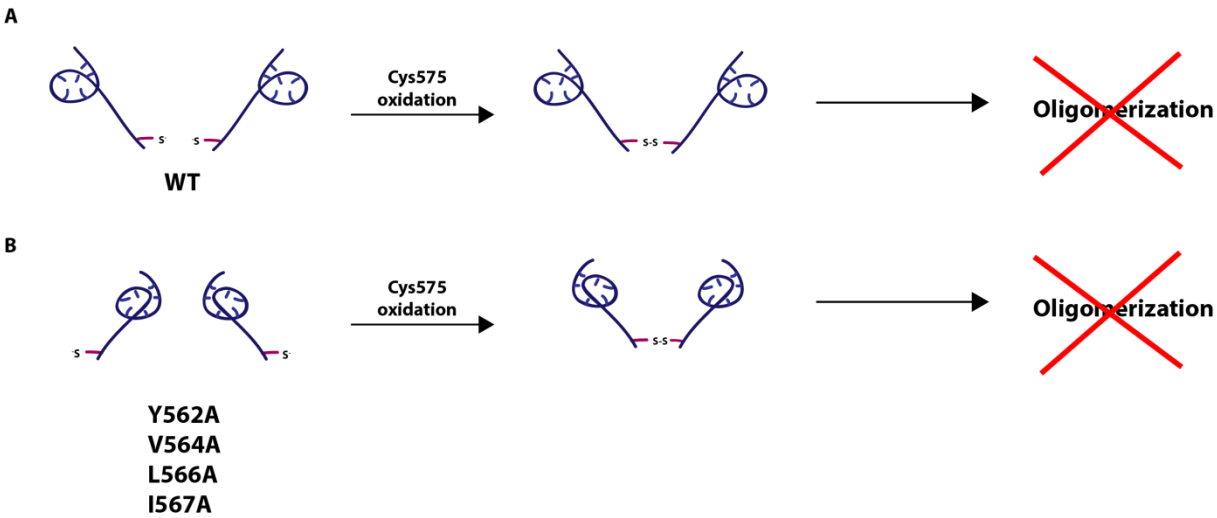

Figure 6.5 Proposed model for formation of tp covalent dimers *in vitro.* A) tp conformational change cannot occur after S-S bond formation without an anchoring point hanging on its N-terminus which would support the change of the tp conformation leading to subsequent oligomerization. B) Mutations altering the wild type tp secondary structure which do not support oligomerization of covalent dimers.

The monomeric as well as dimeric tp did not show any tendency to interact with the Cμ4 domain. This however, cannot exclude the occurrence of interactions between the tp of one chain and the Cμ4 domain of the adjacent chain once the change in conformation has occurred, since changes in tp structure can reflect on the contacts with the adjacent Cμ4 domain and thus on the three-dimensional structure of the whole Cμ4-tp domain.

6.1.2 Model for IgM oligomerization

C575 is involved in inter-IgM covalent bonding whereas the non-covalent hydrophobic interactions are supposed to occur on the intra-subunit Cμ4-tp interfaces. The absence of C575 S-S bonds has already been shown to severely impair the oligomerization, in that it leads to a prevalent secretion of covalent dimers (Davis *et al*., 1989; Sitia *et al*., 1990). This work showed however, that the single replacement of four hydrophobic tp amino acids (Y562, V564, L566 and I567), supposed to be involved in non-covalent intra-subunit interactions, had a more drastict effect, since these mutants formed solely covalent dimers (Figure 5.33). Moreover, the same mutations led to a complete loss of the tp β strand motiv turning it into a random coil (Figure 5.32). Together these data suggest that hydrophobic amino acids of the tp might influence the formation of IgM polymers by affecting the secondary structure of the tp, which in turn might reflect on the three-dimensional conformation not only of the tp but also of the rest of the μ chain. In order to establish connections with neighboring IgM subunits, either C575 or C414 must be accessible to them, i.e. they have to be exposed pointing outwards. The evidence that exclusively dimers formed, indicates that neither the C575 nor C414, normally involved in inter-subunit connections, were accessible, supporting further the hypothesis that changes in the conformation of the tp might affect the conformation of the Cμ4 and Cμ3 domain. The change in conformation might reflect on electrophoretic mobility of the dimers. Indeed, dimeric V564A, L566A and M568 showed a slight shift in electrophoretic mobility under non-reducing conditions compared to that of dimeric C575A (Figure 5.38b), which, together with C575S, did not seem to alter the tp secondary structure (Figure 5.32). Thus, the outward pointing of C575 and C414 is possible only in the presence of the intact hydrophobic core. Very likely in the Y562A, V564A, L566A, I567A and M568A mutants both of these cysteines were projected inwards due to tp conformational change hindering thus the formation of oligomers (Figure 6.6).

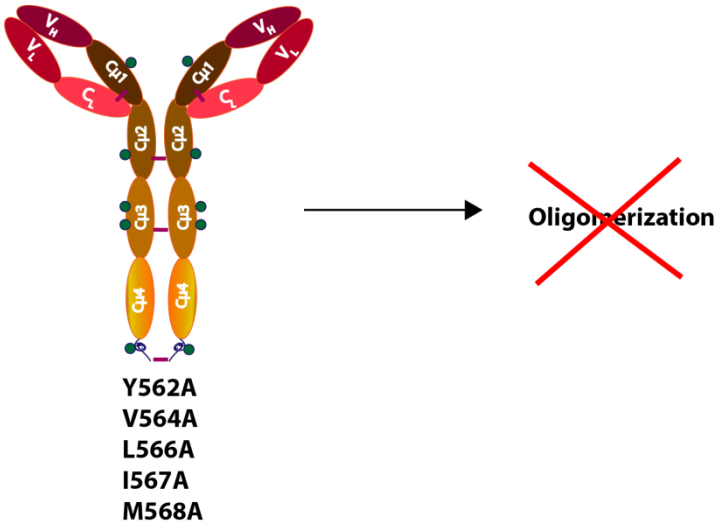

Figure 6.6 Hypothetical effect of the replacement of Y562, V564, L566, I567 and M568 with alanine on the overall conformation of the IgM subunit. The C575 points inwards establishing an intra-subunit rather than inter-subunit S-S bond hindering IgM oligomerization.

The correct structure of the tp could ensure the correct orientation of the cysteines, and therefore the predisposition for polymer formation, but is however not sufficient for the formation of non-covalent intra-subunit interactions between C-terminal domains of the µ chain. According to the Cµ4-tp two-step oligomerization model *in vitro* (Figure 6.3), they could take place once the C575 S-S bond and thus covalent inter-subunit interactions have been formed. In effect, in the case of the entire IgM antibody, the two µ chains of one IgM subunit are held together only by non-covalent and covalent interactions in correspondence of the Cµ2 domain (Wiersma and Shulman, 1995). Thus, intra-subunit interactions between the C-terminal µ domains might be necessary only then when the same domains have already established a covalent contact to another IgM subunit and therefore the need of additional interactions that reinforce and hold the two µ chains of the same IgM subunit, apart from the covalent C337 bond, arises (Figure 6.7).

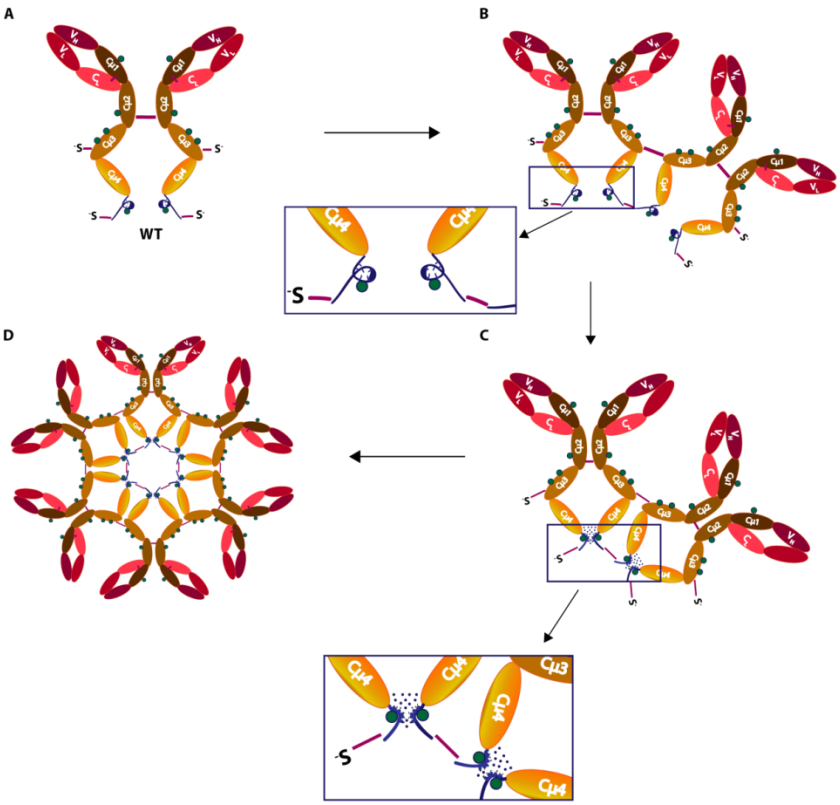

Figure 6.7 Model for formation of IgM polymers in cells. (A-B) Once the $\mu_2\lambda_2$ is assembled, the remaining two free cysteines in the wt IgM subunit, C575 and C414, are projected outwards allowing formation of inter-subunit disulfide bonds. (C-D) The establishment of C575 S-S disulfide bond results in conformational modification in correspondence of the Cμ4-tp domain, allowing the establishment of intra-subunit non-covalent interactions (represented in dots) either between two adjacent tps or between the tp of one μ chain and the Cμ4 domain on the adjacent μ chain.

The fact that oligomers of different high MW were present in the cells but only decamers and dodecamers were secreted in the case of the wild type IgM as well as all oligomerizing mutants (Figure 5.35) indicated how stringent the quality control is for the secretion of oligomers, which ensures on the one hand, that only correctly assembled oligomers such as dodecamers and decamers are secreted, and on the other hand that all other intermediates including dimers are prevented from secretion (Sitia *et al*., 1990 and references therein; Anelli *et al*., 2003; Anelli and van Anken, 2013). The thiol-mediated retention is one of the QC mechanisms adopted by immunoglobulins (Alberini *et al*., 1990). ERp44 (Anelli *et al*., 2003 and 2007) and the C575 (Sitia *et al*., 1990; Fra *et al*., 1993) play a crucial role in it. The six mutants secreted exclusively or prevalently as dimers must escape such a control most likely by the failed binding to ERp44. This would prevent them from being retained within the cell, leading to an uncontrolled secretion of their covalent dimers.

6.2 J chain characterization

The last attempts to obtain monomeric human J chain by recombinant expression in *E. coli* have failed since the protein showed a high tendency to aggregate (Symersky *et al*., 2000; Redwan el *et al*., 2006). Optimizing the protocol by reducing the protein concentration during the refolding step as well as during the sample concentration preceding the gel filtration, it was possible to isolate, although at a very low yield of ca. 4%, the J chain in its monomeric form (Figure 5.39a-c). In contrast with results reported by Redwan *et al*. (2006) with the human J chain CSCS mutant, the same mouse mutant did not show any increase in stability with respect to aggregation or gain of secondary structure compared to the wt protein. Both wild type proteins and the mouse CSCS mutant showed a random coil conformation (Figure 5.39d and e). The latter observation is in line with that of Zikan *et al*. (1985) for the human J chain. The authors however interpreted their CD data of the oxidized protein as a combination of 34% of β structure and of 66% of random coil conformation, after the random coil component has been subtracted from their experimental CD spectrum. The spectral decomposition was performed because their obtained spectrum differed in two aspects from that corresponding to the pure random coil conformation, namely in the less intense minimun at 195 nm and in a negative ellipticity between 210 nm and 240 nm, region where random coil structures have a slightly positive spectrum. The β sheet contribution of 34% was in a good agreement with 37% predicted from their amino acid sequence profiles. Based on these findings they proposed a single-domain β sheet bilayer model for J chain structure which differs from the two-domain model of Cann *et al.* (1982) (Figure 3.7).

Ellman's assay indicated that none of the eight thiol groups was free in both human and mouse J chain as well as in the mouse CSCS mutant. Trypsin digestion and consecutive MALDI-TOF analysis of peptides revealed the occurrence of more disulfide bond combinations (Figure 5.1) rather than the unique one reported for the human J chain by Frutiger *et al.* (1992) in IgM and by Bastian *et al*. (1992) in IgA, suggesting that the J chain might acquire the reported S-S bond arrangement only when bound to IgM or alternatively, that only the J chain with the reported S-S bond combination can be incorporated into decameric IgM. Furthermore, under the investigated conditions, the mouse J chain did not interact either with the Cμ4-tp domain or with the mouse BiP chaperone and the human J chain did not interact with the human βHsp90 (Figure 5.41). It might be that the J chain in

general does not interact with these chaperones. However, it is surprising that it did not show any tendency to establish a disulfide bond with the Cμ4-tp C575. De Lalla *et al*. (1998) hypothesized that glycans on Asp563 of the Cμ4-tp might be important for incorporation of the J chain into IgM decamers, since IgM dodecamers and aggregates formed when these glycans were absent. Although this work suggests that the tp glycans are essential for formation of decameric IgM, since the N563Q mutant formed solely dodecamers in the absence of the J chain (Figure 5.33), it can however not be excluded that the J chain does require the tp glycosylation in order to interact with the μ chain or that the J chain only glycosylation on Asn48 in mouse or Asn49 in human is required for that purpose. Thus, it would be interesting to investigate the role of both glycans in the interaction between the J and the μ chain.

7 Conclusions and perspectives

Up to date it has been shown that the absence of inter-subunit covalent interactions (Davis *et al.,* 1989; Sitia *et al*., 1990; Wiersma and Shulman, 1995) as well as of some charged residues located on the Cμ3 domain (Arya *et al*., 1994) severely impairs the formation of IgM polymers. This work demonstrates that all hydrophobic amino acids located on the tail piece negatively affect the IgM oligomerization and that four of them are essential for this process. Moreover, the single replacements of these four amino acids lead to a complete loss of the secondary structure of the tp, allowing the hypothesis that it is through changes in its conformation that the tp regulates the oligomerization ability of the IgM, most likely by influencing the orientation of the Cys575. Additionally, the results obtained in this work suggest that the formation of inter-subunit C575 S-S bonds might induce conformational rearrangement leading to the establishment of non-covalent intra-subunit interactions between C-terminal domains. Thus, future attempts might be directed to acquire more information first about the three-dimensional conformation of the tp alone and of the Cμ4-tp domain and second, about how their structure is affected by formation of the C575 S-S bond as well as by replacement of hydrophobic amino acids.

By investigating the role of single tp amino acids in the oligomerization process, a region located on its N-terminus, spanning from T560-M568 and probably affecting the tp secondary structure, was identified to dictate the oligomerization of the entire IgM. Amino acids within this region determine whether oligomerization, aggregation or abolishment of oligomerization occurs. Thus, these results provide structural basis on which it is possible to act in order to enhance the oligomerization properties of the tp, and thus engineer antibodies or antibody conjugates with improved biological activity. In effect, when the μ tp is fused to the C-terminus of IgG1, IgG2, IgG3 and IgG4, they acquire the ability to form dodecamers. Upon oligomerization they become dramatically more effective in activating the complement, even the IgG4, which is normally devoid of complement activating activity (Smith and Morrison, 1994; Smith *et al*., 1995).

J chain has been shown to possess one unique disulfide bond arrangement when incorporated into decameric IgM (Frutiger *et al.,* 1992). Data from this work indicated that free monomeric recombinant J chain has multiple combinations of intra-chain disulfide

bonds, suggesting that the reported disulfide bond arrangement might be influenced or chosed by IgM. It would be interesting performing chromatographic attempts in order to isolate from the mixture the J chains with single S-S bond combination and subsequently investigate the structure of their monomeric form. Moreover, since J chain is incorporated in decameric but not in dodecameric IgM, it would be worth investigating how the 18 tp mutations and glycosylation on the tp or on J chain itself also affect its incorporation into IgM oligomers.

8 Materials and methods

8.1 Materials

8.1.1 Chemicals

Name	Supplier
Acetic acid	Roth
Acetone	Sigma-Aldrich
Acetonitrile	J.T. Baker
Acrylamide/Bis solution (40% w/v)	Serva
Agarose, ultra pure	Roth
Albumin from bovine serum	Sigma-Aldrich
Albumin, Monomer bovine	Sigma-Aldrich
Ammonium bicarbonate	Merck
Ammonium sulfate	Merck
Ammonium peroxodisulfate (APS)	Roche
L-Arginine	Sigma-Aldrich
Bacto Agar Difco (Detroit, USA)	Difco
Bromephenol blue S	Serva
Calcium chloride	Merck
L- Cysteine	Sigma-Aldrich
Coomassie Brilliant Blue R-250	Serva
Dimethyl sulfoxide (DMSO)	Sigma-Aldrich
Disodium hydrogen phosphate	Merck
5,5'-dithiobis-(2-nitrobenzoic acid)	Sigma
1,4-Dithiothreithol (DTT)	Roth
Ethanol, p.a.	Roth
Ethylendiamintetraacidic acid (EDTA)	Merck
N-Ethylmaleimide (NEM)	Sigma-Aldrich
L-Glutatione reduced	Sigma-Aldrich
L-Glutathione oxidized	Sigma-Aldrich
Glycerol, 99%	ICN
Guanidine hydrochloride, p.a.	ICN
N-(2-Hydroxyethyl)-piperazine-N'-2-Ethanesulfonic acid (HEPES)	ICN
2-Iodoacetamide	Merck
Isopropanol	Roth
Isopropyl-β-D-thiogalaktopyranosid (IPTG)	Roth
Kanamycin	Roth
Magnesium chloride	Merck
Manganese chloride	Merck
β-Mercaptoethanol, pure	Merck
Methanol	Sigma-Aldrich

Polyethylenimine (PEI)	Polysciences Inc
Potassium dihydrogen phosphate	Merck
Potassium chloride	Roth
Sodium acetate	Roth
Sodium chloride	Merck
Sodium dodecyl sulfate (SDS)	Roth
Tergitol® solution, Type NP-40	Sigma-Aldrich
N,N,N',N'-Tetramethylethylendiamin (TEMED)	Roth
Trichloroacetic acid (TCA)	Sigma-Aldrich
Tris-(hydroxymethyl)-aminomethan (Tris)	ICN
Urea, p.a.	Roth
Tryton® x-100	Calbiochem
Polyoxyethylen-sorbitan-monolaurat (Tween-20)	Merck
Xylene cyanol	Merck

8.1.2 Reagents for cell culturing

Name	Supplier
LB medium, powder	Serva
Gibco® DMEM	Life Technologies
Gibco® FCS	Life Technologies
Gibco® L-Glutamine (200 mM)	Life Technologies
Gibco® Penicillin-Streptomycin (10.000 U/ml)	Life Technologies
Gibco® Sodium pyruvate (100 mM)	Life Technologies
Gibco® Trypsin-EDTA	Life Technologies
G418	Sigma
PBS	Euroclone
PBS with Ca^{2+}	Euroclone
PBS 10X	Euroclone
Sterile water	SALF Lab Farmacologico
Opti-MEM®	Life Technologies

8.1.3 Consumables, kits and markers

Name	Supplier
Consumables	
Acrodisc ® 0,1 µm syringe filter units	Pall
Amicon® Ultra – 15, 4 and 0,5 ml centrifugal filters	Millipore
Dialysis membrane Spectra/Por (6-8 kDa)	Spectrum
Membrane filter 0,22 µm	Millipore
Millex ®- GS 0,22 µm syringe filter units	Millipore
Nitrocellulose blotting membrane	Ge Healthcare
NuPAGE Tris-Acetate Protein Gels (3-8%)	Lifetechnologies
NuPAGE Bis-Tris Protein Gels (10%)	Lifetechnologies
Ultrafree ® - MC-GV centrifugal filters	Millipore
Vac-Man ® Laboratory Vacuum Manifold	Promega

Buffers

DpnI NEB 4 buffer 10x	New England Biolabs
NuPAGE® MES SDS Running Buffer (20X)	Life Technologies
NuPAGE® Tris-Acetate SDS Running Buffer (20X)	Life Technologies
Pfu buffer 10x	Promega

Reagents

Protease Inhibitor Cocktail Tablets	Roche
Desoxynucleotidetriphosphates (dNTPs)	Roche
Dimethyl Sulfoxide (DMSO)	Sigma-Aldrich
Ponceau S	Sigma-Aldrich
Protease Inhibitor Mix HP	Serva
o-Phenylenediamine dihydrochloride SIGMA*FAST*® OPD	Sigma-Aldrich
Water for TOC analysis	Fluka

Kits

Bicinchoninic Acid Kit for Protein Determination	Sigma-Aldrich
ECL+ plus Western Blotting Detection System	GE Healthcare
Wizard® Plus SV Mini-Preps DNA purification kit	Promega
Wizard® Plus Midipreps DNA purification kit	Promega

Markers

Gel filtration standard	Biorad
1 kb DNA ladder orange G	Peqlab
Low MW gel filtration Markers kit	Sigma-Aldrich
Low-Range-molecular weight marker (LMW for SDS-PAGE)	BioRad
PageRuler Plus Prestained Protein Ladder	Thermo Scientific

8.1.4 Fluorescence labels

Name	Supplier
4-Acetamido-4'-Maleimidylstilbene-2,2'-Disulfonic Acid (AMS)	Life Technologies
Hoechst 33342 nucleic acid stain	Life Technologies
DNA Stain Clear G	Serva

8.1.5 Antibodies and enzymes

Name	Supplier
Antibodies – ELISA	
mouse IgM, purified	Life Technologies
Rabbit anti-mouse IgM (RAM-M)	Zymed
Goat anti-mouse lambda-UNLB	Southern Biotech
Rabbit anti-goat IgG (H+L) HRP	Life Technologies
Antibodies – fluorescence microscopy	
Goat Anti-mouse lambda TRITC	Southern Biotech

Antibodies - WB

Alexa Fluor® 647 Goat anti-mouse IgM (μ chain)	Life Technologies
Goat anti-mouse lambda-HRP	Southern Biotech
Rabbit anti-mouse J chain	Kindly provided by Prof. Roberto Sitia (San Raffaele Scientific Institute, Milan, Italy)
Alexa Fluor® 546 Goat anti-Rabbit IgG (H+L)	Life Technologies

Enzymes

DNase I	AppliChem Panreac
DpnI	New England Biolabs
Trypsin Gold, MS grade	Promega
Pfu-Turbo® DNA polymerase	Agilent Technologies

8.1.6 Chromatographic columns

Name and type	Supplier
Preparative	
HiTrap Q FF 5 ml	GE Healthcare
HiTrap SP FF 5 ml	GE Healthcare
HiLoad 26/600 Superdex® 75	GE Healthcare
HiLoad 26/600 Superdex® 200	GE Healthcare
Analytical	
Superdex® 75 10/300 GL	GE Healthcare
Superdex® 200 10/300 GL	GE Healthcare
TSKgel® G3000SW	Tosoh Bioscience
YMC-Pack Diol-SEC	YMC

8.1.7 Buffers and media

8.1.7.1 Buffers

Buffers for electrophoresis

TAE (50x)	Tris/acetate pH 8,0	2 M
	EDTA	50 mM
1% Agarose solution	Agarose	1% (w/v) in TAE (1x)
	DNA Stain Clear G	0,001% (v/v)
DNA loading buffer	Glycerol	39% (v/v)
	SDS	0,5%
	EDTA	10 mM EDTA
	Bromphenol blue	0,05% (w/v)
	Xylene Cyanol	0,05% (w/v)
SDS running buffer (10x)	Tris/HCl, pH 6,8	250 mM
	SDS	1% (w/v)

	Glycerol	50% (v/v)
Separation gel buffer (4x)	Tris/HCl, pH 8,8	1,5 M
	SDS	0,8% (w/v)
Stacking gel buffer (2x)	Tris/HCl, pH 6,8	0,25 M
	SDS	0,4% (w/v)
Laemmli sample buffer (5x)	Tris/HCl, pH 6,8	312,5 mM
	SDS	10% (w/v)
	Glycerol	50% (v/v)
	Bromphenol blue	0,05% (w/v)
if reducing	β-Mercaptoethanol	5% (v/v)
Loading buffer (5x)	Tris/HCl, pH 6,8	5,5 mM
	SDS	9% (w/v)
	Glycerol	40% (v/v)
	Bromphenol blue	0,05% (w/v)
if reducing	DTT	200 mM
Fairbanks A	Coomassie Brilliant Blue R-250	0,05% (w/v)
	Ethanol	25% (v/v)
	Acetic acid	10% (v/v)
Fairbanks D	Acetic acid	10% (v/v)
Tris-Glycine buffer (10x)	Tris/HCl, pH 8,3	0,25 M
	Glycine	1,92 M
Western blotting	Tris-Glycine (10x)	10% (v/v)
	Methanol	20% (v/v)
Buffers for preapration of cell lysates and supernatants		
RIPA buffer	SDS	0,02% (w/v)
	NP-40	1% (v/v)
	NaCl	150 mM
	Tris/HCl, pH 7,4	50 mM
NEM (100x)	NEM	1 M in EtOH
Protease inhibitor cocktail solution (50x)	tablet	1
	ddH_2O	1 ml
Buffers for chromatography and refolding		
IB buffer (5x)	Tris/HCl, pH 7,5	250 mM
	EDTA	50 mM
	NaCl	50 mM
IB solubilization buffer	Tris/HCl, pH 7,5	50 mM
	EDTA	10 mM
	Urea	8 M
	β-Mercaptoethanol	14 mM

Q A buffer (low salt)	Tris/HCl, pH 7,5	50 mM
	EDTA	10 mM
	Urea	5 M
Q B buffer (high salt)	Tris/HCl, pH 7,5	50 mM
	EDTA	10 mM
	Urea	5 M
	NaCl	1 M
Refolding buffer	Tris/HCl, pH 8,0	250 mM
	EDTA	10 mM
	L-Arginine	100 mM
	GSSG	1 mM
	GSH	0,5 mM
PBS (10x)	NaCl	1,37 M
	KCl	27 mM
	Na_2HPO_4	100 mM
	KH_2PO_4	10,76 mM

Buffers for peptide dissolution

Peptide dissolution buffer	Tris/HCl pH 7,5	50 mM
	EDTA	10 mM

Solutions for *E. coli* competent cells

Solution A	3 M NaoAC (pH 5,5)	13 ml
	1 M $CaCl_2$	100 ml
	2,8 M $MnCl_2$	25 ml
	ddH_2O	862 ml
Solution B	Glycerol (87%)	69 ml
	Solution A	331 ml

For the preparation of buffers double distillate water from Millipore Direct-Q5 system was used.

8.1.7.2 Media

Medium for *E. coli* growth	Luria Bertani (LB_0)	20 g/l
	Bacto Agar (for plates)	20 g/l
	Kanamycin	35 µg/ml
Medium for HEK293FT cells	DMEM	
	FCS	5%
	L-Glutamine	2 mM
	Penicillin	100 U/ml
	Streptomycin	100 µg/ml
	Sodium pyruvate	1 mM

8.1.8 Equipment and programs

8.1.8.1 Equipment

Name and type	Supplier
Cell disruption machine Basic Z and Water bath Haake F6-K	Constant Systems and Haake
Eppendorf-Thermomixer	Eppendorf
Flask shaker Certomat® S	B Braun Biotech International
Flask shaker	GFL
Galaxy 170S cell incubator	New Brunswick Scientific
Ice machine	Ziegra
Magnetic stirrer Heidolph MR2000	Heidolph
Metal thermo block TB 1	Biometra
MJ Mini Thermal Cycler	BioRad
Mixer Homogenizer SilentCrusher M	Heidolph
pH-Meter WTW	WTW
Precision cells Quartz SUPRASIL	Hellma
Roller drum TC-7	New Brunswick
Bio-image analzyer	
Typhoon FLA 9000	Fujifilm
Chemidoc Imaging System	UVP
Analytical balance	
BP 121 S Sartorius	Sartorius
BL 310 Sartorius	Sartorius
Cell counter	
TC20® automated cell counter and counting slides	BioRad
Centrifuges and rotors	
Eppendorf-Centrifuge 5415 C	Eppendorf
Eppendorf-Centrifuge 5810-R	Eppendorf
Heraeus Primo R refrigerated centrifuge	Thermo Scientific
Rotina 46R	Hettich
Rotina 420R	Hettich
Savant DNA 120	Thermo Scientific
Universal 320R	Hettich
Avanti J-25 and J-26 XP	Beckman Colulter
JA-10 and JA-25.50 Rotor	Beckman Colulter
Chromatography devices	
ÄKTApurifier	GE Healthcare
ÄKTAexplorer	GE Healthcare
Density Gradient Fractionators	
Gradient maker Labconco	Labconco
Gel electrophoresis and blotting devices	

Hoefer Mighty Small II	GE Healthcare
Hoefer TE22 Mighty Small Transfer Tank	GE Healthcare
XCell SureLock® Mini-Cell Electrophoresis System	Life Technologies
HPLC devices	
Shimadzu HPLC system equipped with autosampler	Shimadzu
Jasco HPLC system	Jasco
Microscopes	
Leica Inverted Fluorescent microscope	Leica
Fluovert FU optical microscope - Leitz	Leitz
Multi-Angle light scattering detector	
Dawn® Heleos® II	Wyatt
Plate reader	
Multiskan Ascent	Thermo Labsystems
Power amplifier	
LKB-GPS 200/400	Amersham
EPS 3500, 301 and EPS 1001	GE Healthcare
Absorption Spectrophotometer	
Helios γ UV-VIS spectrophotometer	Thermo
Nanodrop	Peqlab
Circular dichroism spectropolarimeter	
Jasco J-715 and J-720 with PTC 343 Peltier temperature device	Jasco
Analytical ultracentrifuges	
ProteomLab XL-I equipped with absorbance and interference detection systems	Beckman Coulter
Ultracentrifuge	
Optima L-90K	Beckman Coulter

8.1.8.2 Computer programs and Web tools

Computer programs

Adobe CS4	Adobe Systems
DCDT	Sedanal
EndNote X7.1	Thomson Reuters
ImageJ	NIH
Microsoft Office 2010	Microsoft
Mmass V2.4.0	Open source
OriginPro 8.6	OriginLab
SedFit	Peter Schuck
SerialCloner 2.6	Frack Perez

Databases

NCBI/PubMed	http://www.ncbi.nlm.nih.gov/pubmed
PDB	http://www.rcsb.org/pdb/home/home.do
UniProt	http://www.uniprot.org/

Web tools

Aggrescan	http://bioinf.uab.es/aggrescan/
Expasy translate tool	http://web.expasy.org/translate/
Multiple Sequence alignment	http://www.ebi.ac.uk/Tools/msa/clustalw2/
NCBI/BLAST	http://blast.ncbi.nlm.nih.gov/Blast.cgi?PROGRAM=blastn&PAGE_TYPE=BlastSearch&LINK_LOC=blasthome
NEBcutter V2.0	http://nc2.neb.com/NEBcutter2/
ProtParam tool	http://web.expasy.org/protparam/
QuickChange primer design	http://www.genomics.agilent.com/primerDesignProgram.jsp
Tango	http://tango.crg.es/
UniProt Align	http://www.uniprot.org/align/

8.1.9 Cell strains

***E. coli* strain**	Genotype	Supplier
E. coli BL21 (DE3) Codon Plus	F^- *ompT* *hsd*S_B (rB^-mB^-) gal *end*A The [argU ileY leuW Cam^R]	Stratagene (La Jolla, USA)
Mammalian cell line		
HEK293FT	Mouse λ chain	Kindly generated and provided by Dr. Tiziana Anelli (Prof. Sitia's group, San Raffaele Scientific Institute, Milan, Italy)

8.1.10 Plasmids

8.1.10.1 Plasmids for expression in *E. coli*

Name	Vector	Cloning site	Origin
m_Cμ4-tp wt	pET28b	NcoI / HindIII	GeneArt, Roger Müller
m_Cμ4-tp P559A	pET28b	NcoI / HindIII	This work
m_Cμ4-tp T560A	pET28b	NcoI / HindIII	This work
m_Cμ4-tp L561A	pET28b	NcoI / HindIII	This work
m_Cμ4-tp Y562A	pET28b	NcoI / HindIII	This work
m_Cμ4-tp N563A	pET28b	NcoI / HindIII	This work
m_Cμ4-tp V564A	pET28b	NcoI / HindIII	This work
m_Cμ4-tp S565A	pET28b	NcoI / HindIII	This work
m_Cμ4-tp L566A	pET28b	NcoI / HindIII	This work

m_Cμ4-tp I567A	pET28b	NcoI / HindIII	This work
m_Cμ4-tp M568A	pET28b	NcoI / HindIII	This work
m_Cμ4-tp S569A	pET28b	NcoI / HindIII	This work
m_Cμ4-tp D570A	pET28b	NcoI / HindIII	This work
m_Cμ4-tp T571A	pET28b	NcoI / HindIII	This work
m_Cμ4-tp G572A	pET28b	NcoI / HindIII	This work
m_Cμ4-tp G573A	pET28b	NcoI / HindIII	This work
m_Cμ4-tp T574A	pET28b	NcoI / HindIII	This work
m_Cμ4-tp C575A	pET28b	NcoI / HindIII	This work
m_Cμ4-tp Y576A	pET28b	NcoI / HindIII	This work
m_Cμ4-tp C575S	pET28b	NcoI / HindIII	This work
m_Cμ4-tp P559CC575S	pET28b	NcoI / HindIII	This work
m_Cμ4-tp S565CC575S	pET28b	NcoI / HindIII	This work
m_Cμ4-tp S569CC575S	pET28b	NcoI / HindIII	This work
m_Cμ4-tp Y576G	pET28b	NcoI / HindIII	This work
m_Cμ4-tp Y576F	pET28b	NcoI / HindIII	This work
m_Cμ4-tp Y576W	pET28b	NcoI / HindIII	This work
m_Cμ4-tp Y576H	pET28b	NcoI / HindIII	This work
m_Cμ4-tp Y576K	pET28b	NcoI / HindIII	This work
m_Cμ4-tp Y576D	pET28b	NcoI / HindIII	This work
m_Cμ4-tp C575YY576C	pET28b	NcoI / HindIII	This work
m_Cμ4-tp ΔG572	pET28b	NcoI / HindIII	This work
m_Cμ4-tp ΔG572/G573	pET28b	NcoI / HindIII	This work
m_Cμ4-tp G573G^{ins}	pET28b	NcoI / HindIII	This work
m_Cμ4-tp G573G^{ins}G^{ins}	pET28b	NcoI / HindIII	This work
m_Cμ4-tp ΔY576	pET28b	NcoI / HindIII	GeneArt
m_Cμ4-tp ΔP559	pET28b	NcoI / HindIII	GeneArt
m_Cμ4-tp ΔP559/T560	pET28b	NcoI / HindIII	GeneArt
m_Cμ4-tp 559-561delPTL	pET28b	NcoI / HindIII	GeneArt
m_Cμ4-tp 559-562delPTLY	pET28b	NcoI / HindIII	GeneArt
m_Cμ4-mαtp	pET28b	NcoI / HindIII	GeneArt
m_Cμ4-hαtp	pET28b	NcoI / HindIII	GeneArt
m_Cμ4-humtp	pET28b	NcoI / HindIII	GeneArt
m_Cμ4-lftp	pET28b	NcoI / HindIII	GeneArt
m_Cμ4-xentp	pET28b	NcoI / HindIII	GeneArt

Mouse BiP and human βHsp90, used for interaction studies with J chain, were kindly provided by Mathias Rosam and Edgar Boczek, respectively.

8.1.10.2 Plasmids for expression in HEK293FT cells

Name	Vector	Cloning site	Origin
Mouse IgM wt	pcDNA 3.1(+)	EcoRI / XbaI	Kindly provided by Prof. Roberto Sitia, San Raffaele Scientific Institute, Milan, Italy)
IgM P559A	pcDNA 3.1(+)	EcoRI / XbaI	This work
IgM T560A	pcDNA 3.1(+)	EcoRI / XbaI	This work

IgM L561A	pcDNA 3.1(+)	EcoRI / XbaI	This work
IgM Y562A	pcDNA 3.1(+)	EcoRI / XbaI	This work
IgM N563A	pcDNA 3.1(+)	EcoRI / XbaI	This work
IgM V564A	pcDNA 3.1(+)	EcoRI / XbaI	This work
IgM S565A	pcDNA 3.1(+)	EcoRI / XbaI	This work
IgM L566A	pcDNA 3.1(+)	EcoRI / XbaI	This work
IgM I567A	pcDNA 3.1(+)	EcoRI / XbaI	This work
IgM M568A	pcDNA 3.1(+)	EcoRI / XbaI	This work
IgM S569A	pcDNA 3.1(+)	EcoRI / XbaI	This work
IgM D570A	pcDNA 3.1(+)	EcoRI / XbaI	This work
IgM T571A	pcDNA 3.1(+)	EcoRI / XbaI	This work
IgM G572A	pcDNA 3.1(+)	EcoRI / XbaI	This work
IgM G573A	pcDNA 3.1(+)	EcoRI / XbaI	This work
IgM T574A	pcDNA 3.1(+)	EcoRI / XbaI	This work
IgM C575A	pcDNA 3.1(+)	EcoRI / XbaI	This work
IgM Y576A	pcDNA 3.1(+)	EcoRI / XbaI	This work
IgM ΔY576	pcDNA 3.1(+)	EcoRI / XbaI	This work
IgM Y576G	pcDNA 3.1(+)	EcoRI / XbaI	This work
IgM Y576F	pcDNA 3.1(+)	EcoRI / XbaI	This work
IgM Y576W	pcDNA 3.1(+)	EcoRI / XbaI	This work
IgM Y576K	pcDNA 3.1(+)	EcoRI / XbaI	This work
IgM Y576D	pcDNA 3.1(+)	EcoRI / XbaI	This work
IgM C575YY576C	pcDNA 3.1(+)	EcoRI / XbaI	This work
IgM N563Q	pcDNA 3.1(+)	EcoRI / XbaI	This work

8.1.11 Peptides

Name	Sequence	N-terminus	C-terminus
µ tp wt	PTLYNVSLIMSDTGGTCY	Unmodified (charged)	Unmodified (charged)
µ tp Y562A	PTLANVSLIMSDTGGTCY	Unmodified (charged)	Unmodified (charged)
µ tp V564A	PTLYNASLIMSDTGGTCY	Unmodified (charged)	Unmodified (charged)
µ tp L566A	PTLYNVSLIMSDTGGTCY	Unmodified (charged)	Unmodified (charged)
µ tp I567A	PTLYNVSLIMSDTGGTCY	Unmodified (charged)	Unmodified (charged)
µ tp C575A	PTLYNVSLIMSDTGGTAY	Unmodified (charged)	Unmodified (charged)
µ tp C575S	PTLYNVSLIMSDTGGTSY	Unmodified (charged)	Unmodified (charged)
µ tp ΔY576	PTLYNVSLIMSDTGGTC	Unmodified (charged)	Unmodified (charged)

All peptides were kindly provided by Prof. Christian Becker, Institut für Biologische Chemie, Universität Wien, Austria.

8.2 Molecular methods

8.2.1 Site-directed mutagenesis

Cμ4-tp as well as IgM mutants were generated using Cμ4-tp wt in pET28b or IgM wt in pcDNA3.1 as templates. The reaction was performed according to the instructions of the Quick Change Site-Directed Mutagenesis Kit from Agilent Technologies. To introduce specific mutation, forward (fw) and reverse (rev) primers containing the corresponding modified codon were used to amplify the entire plasmid.

Standard reaction protocol:

Sterile ddH_20	38 µl
Pfu buffer 10x	5 µl
Pfu-Turbo polymerase (2,5 U/µL)	1 µl
dNTPs (10 mM)	2 µl
Fw primer (10 pmol/µL)	1 µl
Rev primer (10 pmol/µL)	1 µl
Template DNA (50 - 100 ng/µl)	2 µl
Total reaction volume	50 µl

Cycling parameters

Segment	Cycles	Temperature	Time
1	1	95°C	30 seconds
2	18	95°C	30 seconds
		55°C	1 minute
		68°C	12 minutes (for pET28b constructs)
			18 minutes (for pcDNA3.1 constructs)

The presence of the right PCR product was checked by loading 9 µl of sample on a 1% agarose gel**.** Positive samples were treated with DpnI (1 µl) + 5 µl of DpnI buffer (10x) at 37°C for 4 hours in order to digest the methylated non-mutated parental DNA template. 2-5 µl of the final mixture were used to transform *E. coli* cells in order to amplify the plasmid and check the presence of mutation.

8.2.2 Agarose gel electrophoresis

Agarose gel electrophoresis was used to check the presence of the amplified mutated plasmid after PCR site-directed mutagenesis. The samples were run on 1% agarose gel supplemented with 0,001% of DNA Stain Clear G in TAE buffer (1x) at 120 mV for 25 min. Plasmid size was determined with the 1 kb DNA ladder orange G.

8.2.3 Preparation of chemical competent *E. coli* cells

The preparation of competent *E. coli* cells was performed according to the protocol provided by Sambrook *et al*. (1989). An aliquot of frozen *E. coli* cells was thawed, inoculated in 100 ml of LB medium (w/o antibiotics) and incubated at 37°C under agitation. When OD_{600} value ranged between 0,5 - 1, 2 ml of 1 M $MgCl_2$ were added and the cells were first incubated at 37°C for 10 min. under agitation and then on ice for 1 hour. The cells were next pelleted by centrifugation at 5000 rpm for 5 min. and resuspended in Solution A. After incubation on ice for 1 hour, the cells were harvested by centrifugation and finally resuspended in 2 ml of Solution B. 200 µl-aliquots were made and stored at -80°C.

8.2.4 Transformation of *E. coli* cells

Aliquots of chemical competent *E. coli* cells (200 µl) were thawed and kept on ice for 10 minutes. 1 µl (50 - 100 ng) of plasmid DNA was added to each aliquot and the mixtures were incubated on ice for 10 minutes. The plasmid DNA was introduced in the cells by a heat-shock step at 42°C for 60 seconds. The cells were next incubated on ice for 20 min. After addition of 800 µl of LB medium (w/o antibiotics), the cells were incubated at 37°C for 1 hour under agitation. Subsequently, the cells were pelleted by centrifugation at 7000 rpm for 3 min., resuspended in 100 µl of the remaining supernatant and plated on the selection plates (kanamycin 35 µg/ml final). Colonies formed after an ON growth in incubator at 37°C.

8.2.5 Amplification, purification and storage of plasmid DNA

Competent *E. coli* cells were transformed and colonies obtained as outlined above. Depending on the quantity required for transformation or transfection, either 4 ml or 100 ml of LB medium supplemented with kanamycin (35 µg/ml final) were inoculated with one colony and the cultures grown ON at 37°C under agitation in incubator. Amplified plasmid DNA was purified with the Wizard Plus SV Mini- or Midipreps DNA purification kit. After plasmid purification a sample was sent for sequencing. DNA was stored at -20 °C in sterile ddH_2O.

8.2.6 Sequencing of DNA

To confirm their correct sequence purified plasmid DNA was sent to MWG-Biotech (Ebersberg, Germany) for sequencing.

8.3 Protein expression in *E. coli* and purification

8.3.1 Cultivation and storage of *E. coli*

Transformed *E. coli* cells were grown at 37°C on LB plates or in LB liquid medium supplemented with kanamycin (35 µg/ml final). Upon transformation cells were plated and incubated ON. Liquid cultures (4 ml, 50 ml or 100 ml) were inoculated by transferring single colony from a plate in freshly prepared medium. Cell growth was monitored photometrically. For long-term storage, when the cells reached the exponential phase of growth, to 1 ml of bacterial culture 500 µl of glycerol were added. The cells were shock-frozen in liquid nitrogen and stored at -80 °C.

8.3.2 Protein expression

Cµ4-tp wt and all mutants were expressed in *E. coli* cells in 2,5 l cultures. Transformation and inoculation in 100 ml cultures were performed as outlined above. After 24 hour-growth the overnight cultures were expanded in 2,5 l of fresh LB medium with kanamycin (35 µg/ml final). When the cells reached the exponential phase of growth, corresponding to an OD_{600} of 0,8-1, protein expression was induced by addition of IPTG (1mM final). After ca. 20 hours of expression, cells were harvested and inclusion bodies (IBs) were prepared.

8.3.3 Preparation of inclusion bodies

Cells were pelleted by centrifugation of overnight cultures at 7.000 rpm for 10’ in JA-10 rotor and Avanti J-25/J-26 XP Beckman Coulter centrifuge. The pellet deriving from each 2,5 L culture was resuspended in 100 ml of IB buffer (1x) supplemented with Protease inhibitor Mix HP (1 vial in 1 l of buffer). To this suspension ca. 1 mg of DNase I was added. The cells were mechanically disrupted in cell disruption machine (Basic Z) with an operating pressure of 2,2 kBar. Membrane and hydrophobic proteins were solubilized by addition of Triton x-100 (2% v/v final) and stirring at 4°C for 2 hours. Soluble components were removed by centrifugation at 20.000 rpm for 20’ in JA-25.50 rotor and Avanti J-25/J-26 XP Beckman Coulter centrifuge. The pellet, i.e. IBs, was washed with IB buffer by repeating centrifugation two more times at the same conditions. IBs were stored at at -80 °C.

8.3.4 Refolding of inclusion bodies

IBs deriving from each 2,5 L culture were solubilized in 50 ml of IB solubilization buffer by stirring at RT for 1 hour. Insoluble components were removed by centrifugation at 20.000 rpm for 20' in JA-25.50 rotor and Avanti J-25/J-26 XP Beckman Coulter centrifuge. Solubilized IBs were filtered 0,22 µm and loaded on HiTrap Q FF column at a flow rate of 2 ml/min, previously equilibrated with Q A buffer. The flow through was collected and diluted with Q A buffer until protein concentration was ca. 1 mg/ml for Cµ4-tp domain wt and its mutants and 0,2 mg/ml for J chain. Diluted Q FF flow through was dialyzed in Spectra/Por membrane (MW Cut-off (MWCO) 6-8 kDa) against refolding buffer ON at 4°C (sample volume/refolding buffer = 1/10).

To investigate the kinetics of the S-S bond formation during refolding, 1 ml of sample was removed from dialysis at indicated time points to which 10 µl of AMS (10 mM final) were added in order to block the free cysteines. The samples were stored at 4°C for the SDS-PAGE.

8.3.5 Purification and isolation of refolded proteins

Refolded Cµ4-tp domains (ca. 200 ml) were concentrated by centrifugation in Amicon® Ultra-15 centrifugal units (MWCO 10.000) at 5000 rpm in Universal 320R centrifuge 20°C in order to reach a sample volume ≤ 12 ml (ca. 15 mg/ml), required for the next purification step, the gel filtration. J chain after refolding step was concentrated to 3 mg/ml. Concentrated sample was filtered 0,22 µm and loaded on the HiLoad 26/600 Superdex 200 column, equilibrated with PBS, at a flow rate of 2 ml/min. Fractions containing the monomer (corresponding to an elution volume of 240 – 260 ml for MW of ca. 15 kDa) were pooled. To obtain dodecamers of Cµ4-tp wt and its mutants the monomer sample was concentrated to 15 mg/ml at the same conditions indicated above and loaded on the HiLoad 26/600 Superdex 200 column at a flow rate of 2 ml/ml. Fractions containing dodecamers (elution volume ca. 170 - 190 ml) were pooled and the concentration was adjusted, if not otherwise stated, to 1 mg/ml. For long-term storage protein aliquots were made, shock-frozen in liquid nitrogen and stored at -80 °C.

8.4 Protein expression in HEK293FT cells

8.4.1 Cell culturing

The HEK293FT cell line, stably expressing the λ chain, was kindly generated by Dr. Tiziana Anelli (San Raffaele Scientific Institute, Milan, Italy). Cells were grown in Dulbecco's Modified Eagle Medium (DMEM) supplemented with 5% FCS, L- glutamine (2 mM), penicillin/streptomycin (100 U/ml/100 µg/ml), sodium pyruvate (1 mM) and G418 (1 mg/ml) in humidified atmosphere of 5% CO_2 at 37°C in cell culture dishes until confluency. The passage was performed twice a week by treatment with trypsin/EDTA. For long-term storage cells were pelleted by centrifugation at 5000 rpm for 5', counted, resuspended in 10% DMSO/FCS with a concentration of $2x10^6$ cell/ml and stored at -80°C.

8.4.2 Transfection of HEK293 cells

HEK293FT cells were transiently transfected with µ chain point mutants. As positive control µ chain wt was used. For the negative control, mock transfection with empty pcDNA3.1 vector was performed. One day before performing transfection, cells were plated at $4x10^5$ cells/well in 6-well culture plates or at $3x10^6$ cells per 10 cm plate and grown in the above-mentioned culture medium w/o G418. Cells were transfected in duplicates for each mutant. For transfection the following mixture was prepared:

	For 6-well plate	For 10 cm plate
Pei (1 mg/ml)	20 µl/well	120 µl
PBS (10x)	4 µl/well	25 µl
plasmid DNA	2 µg/well	12 µg
sterile H_20	adjust to 40 µl/well	adjust to 250 µl
Culture medium w/o G418	1 ml/well	6 ml

The mixture was incubated for 20' at RT to allow PEI bind the DNA and then mixed with the corresponding volume of culture medium w/o G418. Old medium was removed and the cells were incubated for 4 hours with the fresh medium containing the transfection mix. This was then removed and replaced with fresh culture medium w/o G418.

8.4.3 Preparation of cell supernatants and lysates

48 hours after transfection, the medium was removed and the cells were first washed 2x with PBS supplemented with Ca^{2+} and then incubated for 4 hours in Opti-MEM, a minimal

essential medium containing insulin and transferrin. Opti-MEM volume of 1 ml/well in 6-well plates or 5 ml/plate was used. Supernatants (SN) were then removed and centrifuged at 5000 rpm for 3 minutes in order to remove the cells. Subsequently, NEM (100x) and protease inhibitor cocktail (50x) were added in order to block the free cysteines present on SN proteins and their proteolysis. If not immediately processed with TCA, the SN samples were stored at -20°C. Cells were detached using trypsin/EDTA and counted.

8.4.3.1 Cell counting

Cells were quantified with the TC20® automated cell counter using appropriate counting slides from Biorad.

8.4.3.2 Preparation of cell lysates

Once the total cell number per mutant has been determined, cells were resuspended in PBS containing NEM (100x), which penetrates the membrane and binds the free thiol groups of intracellular proteins. The cells were next centrifuged again and resuspended in RIPA buffer, supplemented with NEM (100x) and protease inhibitor cocktail (50x), adding 100 µl of buffer per $1x10^6$ cells in order to normalize the cell lysates. This step was followed by incubation on ice for 20' and centrifugation at 14.000 rpm for 10' at 4°C. The pellets were discarded and cell lysates stored at -20°C, if not immediately processed on SDS-PAGE.

8.4.3.3 TCA precipitation of supernatants

For TCA precipitation 500 µl of the SN, deriving from the well or plate with the lowest number of cells, were processed. The supernatant volume to be processed with TCA deriving from other wells or plates, was normalized with respect to the cell number. For these SN samples, PBS was added to reach 500 µl. 50 µl of TCA were added to the samples which were then incubated ON at 4°C. The samples were then centrifuged at 14.000 rpm for 10' and supernatants were discarded. 500 µl of ice cold 80% acetone were added to each sample followed by centrifugation at 14.000 rpm for 5', after which supernatants were discarded again. This step was repeated once more. Pellets were dried under chemical hood for 30' and stored at -20°C, if not immediately analyzed on SDS-PAGE.

8.5 Biochemical methods

8.5.1 SDS polyacrylamid gel electrophoresis

8.5.1.1 Electrophoresis with home-made gels

Home-made gels were prepared according to the following protocol:

Separating gel 15%	Acrylamide/Bis (40% w/v)	3,75 ml
	Separation gel buffer (4x)	2,5 ml
	10% (w/v) APS	65 µl
	TEMED	3,3 µl
	ddH_2O	3,75 ml
	Total volume	10 ml
Stacking gel 5%	Acrylamide/Bis (40% w/v)	0,625 ml
	Stacking gel buffer (2x)	2,5 ml
	10% (w/v) APS	65 µl
	TEMED	3,3 µl
	ddH_2O	1,875 ml
	Total volume	5 ml

Samples containing ca. 5 µg of protein were mixed with Laemmli buffer (5x) and cooked at 95°C for 2 min. prior loading on the gel. Electrophoresis run was performed in SDS running buffer (1x) at a constant current of 35 mA per gel for 51 min. Gels were stained with Coomassie by 1-minute incubation in the heated Fairbanks A solution followed by incubation in the heated Fairbanks D solution for 20 minutes (Fairbanks *et al*., 1971). The MW of the proteins was determined with the LMW marker standard.

8.5.1.2 Electrophoresis with precast gels

Non-reduced IgM samples were analyzed with precast NuPAGE Tris-Acetate Protein Gels (3-8%) whereas reduced samples with NuPAGE Bis-Tris Protein Gels (10%).

Normalized TCA-precipitated supernatants were resuspended with 25 µl of Loading buffer (1x). 20 µl of normalized cell lysates (deriving from 200.000 cells) were mixed with Loading buffer (5x). The samples were cooked at 95°C for 2 min. prior loading on the gel. Electrophoresis was performed in XCell SureLock® Mini-Cell Electrophoresis System according to the protocol for NuPAGE gels from Life Technologies. The MW of the proteins was determined with the PageRuler Plus Prestained Protein Ladder.

8.5.2 Western blotting

Proteins separated on NuPAGE gels were subsequently electrophoretically transferred ON on a nitrocellulose membrane in the Hoefer TE22 Mighty Small Transfer Tank (GE Healthcare) at a constant current of 70 mA. The transfer was checked by staining with Ponceau S incubating the membrane for 1 minute. The dye was removed with PBS-T1 buffer (PBS with Tween 20 0,1% v/v) and the membrane was incubated in PBS-T1 buffer supplemented with 5% of milk powder at RT for 1 hour under agitation to block unspecific free binding sites. Subsequently, the membrane was incubated with the Alexa Fluor® 647 goat anti-mouse IgM (µ chain) antibody, diluted 1 : 1000 in PBS-T1 buffer, for 1 hour at RT and then washed 3x for 5 min. with PBS-T1 buffer. The µ chain was revealed with Typhoon FLA 9000 instrument (Fujifilm) using the appropriate channel for detection. The membrane was next incubated with the Goat anti-mouse lambda-HRP antibody, diluted 1 : 1000 in PBS-T1 buffer, for 1 hour at RT and washed 3x for 5 min. with PBS-T1 buffer. The detection of this antibody was performed with the ECL detection kit according to the protocol provided by supplier (GE Healthcare).

To reveal the J chain, the membrane was first incubated with the primary antibody, the rabbit anti-mouse J chain, diluted 1 : 200 in PBS-T1 buffer, for 2 hours. This step was followed by three washing steps with PBS-T1 buffer, 5 minutes each. The membrane was subsequently incubated with the Alexa Fluor® 546 goat anti-Rabbit IgG (H+L) antibody, diluted 1: 1000 in PBS-T1, and finally washed 3x for 5 minutes with PBS-T buffer. J chain was revealed with Typhoon FLA 9000 instrument using the appropriate channel for detection.

8.5.3 Determination of protein concentration with BCA

The total protein concentration in cell supernatants was determined with the Bicinchoninic Acid Kit (Sigma-Aldrich). Bicinchoninic acid (BCA) is a highly specific chromogenic reagent for Cu(I). The quantification is based on the principle that proteins reduce alkaline Cu(II) to Cu(I) in a concentration-dependent manner. When bound to Cu(I) bicinchoninic acid forms a purple complex with an absorbance maximum at 562 nm. The absorbance is directly proportional to protein concentration. For the reaction 49 ml of BCA were mixed with 1 ml of $CuSO_4$ solution. The mixture was pipetted in a 96-well plate (180µl/well). To each well 2 µl of sample and 18 µl of PBS were added. The plate was incubated at 37°C for 30'and the

absorption at 562 nm was measured. The calibration curve was obtained with BSA standard (1 mg/ml in PBS) with points ranging from 0-15 µg.

8.5.4 SEC-HPLC analysis

Size-exclusion chromatography (SEC)-HPLC runs were performed on Shimadzu HPLC system. Cμ4-tp as well as J chain were analyzed on Superdex 200 10/300 GL column in PBS buffer at a flow rate of 0,5 ml/min at 20 °C, by injecting 100 µg of sample if not otherwise stated. Peptides were analyzed on Superdex 75 10/300 GL as well as on YMC-Pack Diol column in peptide dissolution buffer at 20°C at a flow rate of 0,5 ml/min and 0,6 ml/min, respectively, by injecting 20 µg of sample. The absorbance at 280 nm was detected. HMW and LMW gel filtration markers were used as MW reference. For kinetic data analysis the area percentage for peaks at retention time of 22 min. (dodecamer), 31 min. (dimer) and 33 min. (monomer) corrected for baseline drifts was plotted against the time. Data only of the C575A and the C575S mutants, analyzed at 1 mg/ml and 15 mg/ml, were normalized.

8.5.5 SEC coupled with multi-angle light scattering (MALS)

A Tosoh TSKgel G3000SW SEC column on Shimadzu HPLC system was employed for the determination of the protein absolute mass. The instrument was coupled with the Wyatt Dawn Heleos II multi-angle light scattering detector, the Shimadzu refractive index- and UV-detector. The column was equilibrated with PBS filtered 0,1 µm for 24 hours to obtain stable baseline signals from the detectors before data collection. The inter-detector delay volumes and band broadening, the light-scattering detector normalization, and the instrumental calibration coefficient were calibrated using a standard 2 mg/ml BSA solution (Albumin, monomer, Sigma) run in the same buffer, on the same day, according to standard Wyatt protocols. The absolute refractive index of the buffer was measured using the refractive index detector. Samples having concentration of 1 mg/ml were analyzed by injecting 20 µL on the column. All experiments were performed at room temperature at a flow rate of 0.3 ml/min in PBS buffer. The molecular mass and mass distribution of the sample were determined using the ASTRA 5 software (Wyatt Technology).

8.5.6 Analytical ultracentrifugation (aUC)

Analytical ultracentrifugation was performed on ProteomLab XL-I equipped with absorbance optics. All experiments were performed using PBS at 20°C. For the determination of the masses of proteins and peptides sedimentation velocity experiments were performed at a rotor speed of 42.000 rpm and of 47.000 rpm, respectively. Sedimentation was detected at 280 nm. Data analysis was carried out by the C(s) method with TI (time invariant) and RI (radial invariant) noise fitting using SedFit software.

8.5.7 Sucrose gradient

λ-HEK293FT cells were seeded in 10 cm plates at a concentration of $3x10^6$ cell/plate. On the next day transfection was performed as described above. Two days after transfection the cell medium was replaced with 5 ml of Opti-MEM and after 5 hours additional 5 ml were added. After 10 hours of incubation of transfected cells in Opti-MEM, cell supernatants were collected, centrifuged in order to remove the cells and NEM (50x) was added. After incubation on ice for 20' cell supernatants were concentrated by centrifugation from 10 ml to 0,5 ml, resuspended in 11 ml of homogenization buffer (0,25 M Sucrose, PBS 1% BSA) and fractionated by centrifugation on continuous sucrose gradient (25% - 5%) for 7 hours at 4°C at 273.000×g in a SW 41 Ti Beckman rotor using Optima L-90k ultracentrifuge. 12 fractions of the gradient, 1 ml each, were collected with Labconco instrument. 1/2 of each fraction was precipitated with TCA (10% final) ON at 4°C. Precipitates were resuspended in Loading buffer (5x) and loaded on gradient precast NuPage Tris-Acetate 3-8% gels.

8.5.8 ELISA

Enzyme-linked immunosorbent assay was used in order to quantify IgM present in lysates and supernatants of transfected cells after 1, 2, 3, 4 and 24 hours of incubation in Opti-MEM. 96-well plate were coated with 100 µl/well of rabbit anti-mouse IgM (RAM-M), diluted 1 : 200 in PBS, and incubated ON at 4°C. On the next day, wells were washed 3x with 200 µl/well of PBS. Unspecific binding sites were blocked by 1-hour incubation at 37°C with 100 µl/well of PBS-T2 buffer (PBS with Tween 20 0,05% v/v) supplemented with 3% of milk powder. The wells were then washed 3x with 200 µl/well of PBS-T2 buffer. Samples, 200 µl (adjusted with PBS)/well, were added and incubated for 2 hours at 37°C. Wells were then washed 3x with 200 µl/well of PBS-T2 buffer and incubated with 200 µl/well of primary

antibody, the goat anti-mouse lambda-UNLB, diluted 1 : 1000 in PBS-T2 buffer, for 1 hour at 37°C. After 3 washing steps, the wells were incubated with 200 µl/well of peroxidase-conjugated secondary antibody, the rabbit anti-goat IgG (H+L), diluted 1 : 1000 in PBS-T2 buffer for 1 hour at 37°C and then washed again 3x. Detection was performed by addition of 200 µl/well of OPD solution (1 tablet in 10 ml of ddH_2O) and measuring the absorption at 450 nm. Calibration curve with points ranging from 0 – 100 ng was obtained with IgM standard (mouse IgM, purified, Life Technologies).

8.5.9 Ellman's assay

Ellman's assay was used in this work to quantify free sulfhydryl groups of J chain monomer. The assay was developed by Ellman (1959) and exploits the ability of 5,5'-dithiobis-(2-nitrobenzoic acid) or DTNB to react with free thiol group producing a mixed disulfide and 2-nitro-5-thiobenzoic acid (TNB), which is yellow colored and has an absorption maximum at 412 nm.

Reagents	
Ellman's reagent (DTNB)	4 mg/ml
Reaction buffer	0,1 M sodium phosphate, 1 mM EDTA, pH 8,0
Cysteine standard	0 -1,5 mM

To prepare cysteine standards for calibration curve, L-cysteine was dissolved in reaction buffer. DTNB was also dissolved in reaction buffer. Sample concentration was adjusted so that the concentration of sulfhydryls was in the range 0,1-1 mM prior to mixing with reagents. Following mixture was prepared and incubated at RT for 15 minutes:

Mixture	
DTNB	15 µl
Reaction buffer	2,5 ml
Sample	250 µl

The absorbance was measured at 412 nm.

8.5.10 Tryptic digestion

SDS-PAGE was performed as outlined above by loading 5 µg/well of protein. A spot (diameter ca. 2 mm) within the desired band was cut and incubated 2x for 10' at RT with 100 µl of 10 mM ammonium bicarbonate, and then with 100 µl of a mixture of acetonitrile/10 mM ammonium bicarbonate (1/1) for 10'. In the case the oxidized protein was intended for

trypsin digestion, the gel spot was incubated 3x for 10' with 100 µl of the same mixture, alternated with an incubation of 10' with 100 µl of acetonitrile.

If a reduced protein was intended for analysis, a reduction procedure consisting of three steps was performed before the last 5 washing steps mentioned above. The reduction step was performed by incubating the gel spot with 100 µl of DTT solution (80 mM DTT, 0,5 mM Gua/HCl, 0,8 mM EDTA, 0,1 mM Tris/HCl, pH 8,2) for 30' at 37°C under agitation. Subsequently, to this solution 10 µl of IAA solution (0,5 M IAA, 0,1 M Tris/HCl, pH 8,2) were added and, protected from light, gel spots were agitated for 15' at RT. Subsequently, the solution was removed and 5 µl of 1 mM β-mercaptoethanol and additional 100 µl of 10 mM ammonium bicarbonate were added and agitated for 5'. The solution was removed and 5 above-mentioned washing steps were performed. After the last incubation step with acetonitrile-ammonium bicarbonate mixture, the gel spots were dried in a vacuum centrifuge for 5'. Finally, 2 µl of trypsin were added and incubated ON at 37°C. The samples were then analyzed by MALDI-TOF after addition of 10 µl of acetonitrile and subsequent sonication. Molecular masses of peptides deriving from reduced protein were compared to those of peptides originating from non-reduced protein in order to assign the S-S bond arrangement.

8.5.11 MALDI-TOF MS analysis

Mass spectrometry analysis was performed in order to check the molecular mass, and thus identity, as well as the purity of all purified proteins. The samples were processed on ZipTip (Millipore) according to manufacturer's instructions in order to remove PBS. The HCCA (α-Cyano-4-hydroxycinnamic) matrix was solubilized in 0,1% TCA, 80% acetonitrile and 20% ddH_20 and the samples were spotted on the matrix solution. After evaporation of the solvent, the analysis was performed on Bruker Ultraflex-2 MALDI-TOF/TOF spectrometer.

8.6 Oligomerization kinetics

Upon isolation the Cµ4-tp monomer concentration was adjusted to 1 mg/ml, 1,5 ml-aliquots were made and kinetics was started, if not otherwise specified, at 4°C (Day 0). The number of the aliquots corresponded to the number of the time points to be investigated. For each time point 100 µl (100 µg) of a new aliquot were analyzed by SEC-HPLC on Superdex 200 10/300 GL column in PBS buffer at a flow rate of 0,5 ml/min at 20 °C. For subsequent SDS-

PAGE analysis of the same samples, 100 µl were removed from the corresponding aliquot and 1 µl of AMS (10 µM final) was added in order to block the free cysteines at indicated time points. The samples were stored at 4°C. To investigate the influence of the covalent bond formation on oligomerization, free cysteines were irreversibly blocked at different days of kinetics by addition of AMS. Thus, 1,5-ml aliquots of freshly isolated Cµ4-tp monomer were stored at RT and 15 µl of AMS (10 mM final) were added on the indicated day of kinetics to an aliquot, which was then analyzed by SEC-HPLC at determinate time points.
µ tp peptide was resuspended and filtered 0,22 µm to a final concentration of 0,4 mg/ml (207 µM). Oligomerization ability of the resuspended µ tp peptide as well as of the oxidated peptide was investigated. To oxidize the peptide the redox system was added (GSSG/GSH: 1 mM/0,5 mM final) and incubated for 2 hours at RT under stirring. Glutathione was then removed by centrifugation with Amicon® Ultra MWCO 3.000 and subsequent dilution with peptide dissolution buffer to a concentration of 0,4 mg/ml. Samples were aliquoted, stored at RT and analyzed at indicated time points.

8.7 Resuspension, oxidation and reduction of peptides

Peptide lyophilisate were resuspended in an adequate volume of the Peptide dissolution buffer in order to reach the final concentration of 0,4 mg/ml (207 µM). Upon resuspension the samples were filtered. To oxidize the peptides, 100x concentrated solution of GSSG/GSH = 1/0,5 in Peptide dissolution buffer was prepared and added in order to reach the final concentration of GSSG and GSH of 1 mM and 0,5 mM, respectively. The samples were then incubated for 2 hours at RT under stirring. To reduce the oxidized peptides, 100x solution of DTT in Peptide dissolution buffer was prepared and added to peptides to obtain the final concentration of DDT of 5 mM. The samples were incubated for 20’ at RT under stirring.

8.8 Fluorescence microscopy

The stable expression of the λ chain in the HEK293FT cells was checked with a fluorescent antibody after several passages of the cells. Cells ($5x10^4$/well) were seeded on slides, which were previously sterilized by immersion in 100% ethanol, dried and placed in wells of a 24-well plate. On the next day, the medium was removed from the wells, the slides carrying adherent cells were immerged shortly in ice cold 100% methanol and placed again in the

wells filled with PBS. PBS was then removed and cells were incubated with 250 µl/well of 0,1% Triton x-100/PBS at RT. This step was followed by 2 washing steps with PBS. To saturate unspecific biding sites cells were incubated with 250 µl/well of 1% FCS/PBS for 30' on RT. Subsequently, the cells were incubated with 250 µl/well with goat anti-mouse lambda TRITC (tetramethylrhodamine isothiocyanate) antibody, diluted 1 : 200 in 1% FCS/PBS, for 30' at RT, and then washed 3x with PBS. 250 µl/well of Hoechst, diluted 1 : 1000 in PBS, was added for 5' at RT and subsequently, cells were washed 3x with PBS. Finally, the slides were mounted in glycerol and subsequently sealed with 100 µl of nail polish around the edges of the coverslip. Slides were observed under fluorescence microscope with TRITC filter and stored at -20°C.

8.9 Spectroscopic methods

8.9.1 Absorption spectroscopy (UV-VIS)

Proteins absorb light in ultraviolet (UV)-visible (VIS) range of the spectrum due to their aromatic amino acids and peptide bonds. Aromatic amino acids such as tryptophan, tyrosine and phenylalanine absorb in the near UV range at 280, 274 and 257 nm, respectively. Peptide bonds have absorbance maximum at 250 nm. Thus, proteins have maximal absorbance at 280 nm, mainly due to a contribution of tryptophan indole groups, and in the range 190 – 220 nm, due to peptide bonds. This property allows determination of protein concentration at 280 nm according to the Lambert-Beer law (Equation 8.1)

$$A = \varepsilon \cdot c \cdot d \qquad [8.1]$$

where A is absorbance, ε is molar extinction coefficient (M^{-1}/cm^{-1}), c is protein molar concentration (M) and d is the path length (cm).

Theoretical molar extinction coefficients were calculated based on protein amino acid composition using the Expasy ProtParam tool. All UV single-wavelength or spectra measurements were acquired in UV quartz cuvette (d = 1 cm) at RT in a final volume of 500 µl with Helios γ or, alternatively, with a nanodrop spectrometer. All measurements were buffer corrected.

8.9.2 Circular dichroism spectroscopy

CD measurements were performed in this work to check the correct folding of proteins and to assess the effect of point mutations on their secondary structure.

Circular dichroism (CD) spectroscopy measures the difference in absorption of right- and left-hended circularly polarized light by chiral molecules. Due to their chiral α-carbon atom in amino acids (exception is glycine) and the polypeptide chain, proteins are asymmetric macromolecules and thus, optically active. CD spectra in the far-UV range (190 – 260 nm) allow determining the presence of the secondary structure motifs, such as α helices and β sheets, in proteins. Peptide bonds within this range absorb differentially when placed in asymmetric environment giving rise to distinct signals. Thus, α helix possess two characteristic minima at 222 and 208 nm and a positive band at 190 nm, whereas β sheet has one minimum around 218 nm and a positive band around 198 nm. Random coli has a positive band at 212 nm and one negative band at 195 nm. CD spectra in the near-UV range (260 – 330 nm) can provide information about the tertiary structure. Aromatic amino acids as well as disulfide bonds generate signals within this range, depending on the asymmetry of their environment. Thus, phenylalanines generate signals from 250-270 nm, tyrosines from 270-290 nm and tryptophans from 280-300 nm. S-S bonds give weak and broad signals throughout the near-UV spectrum.

All CD spectra were acquired with either Jasco J-715 or J-720 spectropolarimeter equipped with a Peltier temperature element. For far-UV spectra 0,5 mm-pathlength quartz cuvette and a protein concentration of 20 µM (ca. 0,3 mg/ml) for Cμ4-tp domain and J chain and 207 µM (ca. 0,4 mg/ml) for peptides was used, whereas for near-UV spectra proteins were concentrated to 6 – 10 mg/ml. All measurements were performed with three accumulations at 20°C. For interaction studies with J chain the CD kinetics was performed at a wavelength of 205 nm. The measured signal was ellipticity, θ (measured in millidegrees, mdeg) which was converted into mean residue ellipticity, θ_{MRW} (in deg.cm^2.dmol^{-1}) using the following equation (Equation 8.2)

$$\theta_{MRW} = \frac{\theta * 100}{d * c * N_{aa}} \qquad [8.2]$$

where θ is the ellipticity (mdeg), d is the cell length (cm), c concentration (mM) and N_{aa} is the number of amino acids. All recorded spectra were buffer-corrected.

9 Abbreviations

A – Ampere

a.a. - amino acid

AMS - 4-acetamido-4′-maleimidylstilbene-2,2′-disulfonic acid

APS - ammonium persulfate

aUC - analytical ultracentrifugation

BSA - bovine serum albumin

CD - circular dichroism

Da - dalton

E - energy

E_a - activation energy

E. coli - *Escherichia coli*

ELISA - enzyme-linked immunosorbent assay

EM - electron microscopy

ER - endoplasmatic reticulum

ERGIC - ER-Golgi intermediate compartment

Fw - forward

g - gram

GSSG - oxidized glutathione

GSH - reduced glutathione

h – hour

HC - heavy chain

HPLC - high-performance liquid chromatography

HRP - horseradish peroxidase

IBs - inclusion bodies

IgM - immunoglobulin M

J chain - joining chain

kDa - kilo Dalton

λ – wavelength

LC - light chain

MAb - monoclonal antibody

min - minute

ml - milliliter

mM - millimolar

µM - micromolar

MM - molecular mass

MW - molecular weigh

MWCO - MW Cut-off

NAb - natural antibody

nm – nanometer

NMR - nuclear magnetic resonance

OD - optical density

ON - overnight

PAB - polyclonal antibody

PAGE - polyacrylamide gel electrophoresis

PCR - polymerase chain reaction

pH - potentia hydrogenii

pIg - polymeric Ig

pIgR - polymeric immunoglobulin receptor

QC - quality control

Rev - reverse

RT - room temperature

rpm - rounds per minute

S – Svedberg

SAXS - small angle x-ray scattering

SC - secretory component

SDS - sodium dodecylsulfate

SEC - size exclusion chromatography

SN - supernatants

S-S bond - disulfide bond

TGN - trans-Golgi network

tp - tail piece

TRITC - tetramethylrhodamine isothiocyanate

UV - ultraviolet

v/v - volume per volume

WB - western blot

w/v - weight per volume

w/o - without

wt - wild type

10 References

Alberini, C. M., Bet, P., Milstein, C., & Sitia, R. (1990). Secretion of immunoglobulin M assembly intermediates in the presence of reducing agents. Nature, 347(6292), 485-487.

Alugupalli, K. R., Leong, J. M., Woodland, R. T., Muramatsu, M., Honjo, T., & Gerstein, R. M. (2004). B1b lymphocytes confer T cell-independent long-lasting immunity. Immunity, 21(3), 379-390.

Anelli, T., Alessio, M., Bachi, A., Bergamelli, L., Bertoli, G., Camerini, S., Mezghrani A., Ruffato E., Simmen T., & Sitia, R. (2003). Thiol-mediated protein retention in the endoplasmic reticulum: the role of ERp44. EMBO J., 22(19), 5015-5022.

Anelli, T., Ceppi, S., Bergamelli, L., Cortini, M., Masciarelli, S., Valetti, C., & Sitia, R. (2007). Sequential steps and checkpoints in the early exocytic compartment during secretory IgM biogenesis. EMBO J., 26(19), 4177-4188.

Anelli, T., & Sitia, R. (2008). Protein quality control in the early secretory pathway. EMBO J., 27(2), 315-327.

Appenzeller, C., Andersson, H., Kappeler, F., & Hauri, H. P. (1999). The lectin ERGIC-53 is a cargo transport receptor for glycoproteins. Nat. Cell Biol., 1(6), 330-334.

Arnold, J. N., Wormald, M. R., Sim, R. B., Rudd, P. M., & Dwek, R. A. (2007). The impact of glycosylation on the biological function and structure of human immunoglobulins. Annu. Rev. Immunol., 25, 21-50.

Arnold, J. N., Wormald, M. R., Suter, D. M., Radcliffe, C. M., Harvey, D. J., Dwek, R. A., Rudd P. M., & Sim, R. B. (2005). Human serum IgM glycosylation: identification of glycoforms that can bind to mannan-binding lectin. J. Biol. Chem., 280(32), 29080-29087.

Arya, S., Chen, F., Spycher, S., Isenman, D. E., Shulman, M. J., & Painter, R. H. (1994). Mapping of amino acid residues in the C mu 3 domain of mouse IgM important in macromolecular assembly and complement-dependent cytolysis. J. Immunol., 152(3), 1206-1212.

Atkin, J. D., Pleass, R. J., Owens, R. J., & Woof, J. M. (1996). Mutagenesis of the human IgA1 heavy chain tailpiece that prevents dimer assembly. J. Immunol., 157(1), 156-159.

Baba, Y., Pelayo, R., & Kincade, P. W. (2004). Relationships between hematopoietic stem cells and lymphocyte progenitors. Trends Immunol., 25(12), 645-649.

Balciunas, A., Fless, G. M., Scanu, A. M., & Copeland, R. A. (1993). Interactions of a fluorescently labeled peptide with kringle domains in proteins. J. Protein Chem., 12(1), 39-43.

Bastian, A., Kratzin, H., Eckart, K., & Hilschmann, N. (1992). Intra- and interchain disulfide bridges of the human J chain in secretory immunoglobulin A. Biol. Chem. Hoppe Seyler, 373(12), 1255-1263.

Baumgarth, N., Herman, O. C., Jager, G. C., Brown, L. E., Herzenberg, L. A., & Chen, J. (2000). B-1 and B-2 cell-derived immunoglobulin M antibodies are nonredundant components of the protective response to influenza virus infection. J. Exp. Med., 192(2), 271-280.

Beale, D., & Buttress, N. (1969). Studies on a human 19-S immunoglobulin M. The arrangement of inter-chain disulphide bridges and carbohydrate sites. Biochim. Biophys. Acta, 181(1), 250-267.

Bendtzen, K., Hansen, M. B., Ross, C., & Svenson, M. (1998). High-avidity autoantibodies to cytokines. Immunol. Today, 19(5), 209-211.

Bergmann-Leitner, E. S., Leitner, W. W., & Tsokos, G. C. (2006). Complement 3d: from molecular adjuvant to target of immune escape mechanisms. Clin. Immunol., 121(2), 177-185.

Bornemann, K. D., Brewer, J. W., Beck-Engeser, G. B., Corley, R. B., Haas, I. G., & Jack, H. M. (1995). Roles of heavy and light chains in IgM polymerization. Proc. Natl. Acad. Sci. U. S. A., 92(11), 4912-4916.

Borsos, T., & Rapp, H. J. (1965). Complement fixation on cell surfaces by 19S and 7S antibodies. Science, 150(3695), 505-506.

Braakman, I., & Bulleid, N. J. (2011). Protein folding and modification in the mammalian endoplasmic reticulum. Annu. Rev. Biochem., 80, 71-99.

Braathen, R., Sorensen, V., Brandtzaeg, P., Sandlie, I., & Johansen, F. E. (2002). The carboxyl-terminal domains of IgA and IgM direct isotype-specific polymerization and interaction with the polymeric immunoglobulin receptor. J. Biol. Chem., 277(45), 42755-42762.

Brewer, J. W., & Corley, R. B. (1997). Late events in assembly determine the polymeric structure and biological activity of secretory IgM. Mol. Immunol., 34(4), 323-331.

Brewer, J. W., Randall, T. D., Parkhouse, R. M., & Corley, R. B. (1994). IgM hexamers? Immunol. Today, 15(4), 165-168.

Brezski, R. J., & Monroe, J. G. (2008). B-cell receptor. Adv. Exp. Med. Biol., 640, 12-21.

Bruggemann, M., & Rajewsky, K. (1982). Regulation of the antibody response against hapten-coupled erythrocytes by monoclonal antihapten antibodies of various isotypes. Cell. Immunol., 71(2), 365-373.

Bubb, M. O., & Conradie, J. D. (1978). Studies on the structural and biological functions of the Cmu4 domains of IgM. Immunology, 34(3), 449-458.

Cals, M. M., Guenzi, S., Carelli, S., Simmen, T., Sparvoli, A., & Sitia, R. (1996). IgM polymerization inhibits the Golgi-mediated processing of the mu-chain carboxy-terminal glycans. Mol. Immunol., 33(1), 15-24.

Cann, G. M., Zaritsky, A., & Koshland, M. E. (1982). Primary structure of the immunoglobulin J chain from the mouse. Proc. Natl. Acad. Sci. U. S. A., 79(21), 6656-6660.

Carroll M. C. (2008). Complement and humoral immunity. Vaccine, 26(Suppl 8), 128-133.

Casali, P., & Schettino, E. W. (1996). Structure and function of natural antibodies. Curr. Top. Microbiol. Immunol., 210, 167-179.

Cattaneo, A., & Neuberger, M. S. (1987). Polymeric immunoglobulin M is secreted by transfectants of non-lymphoid cells in the absence of immunoglobulin J chain. EMBO J., 6(9), 2753-2758.

Chen, Z., Koralov, S. B., Gendelman, M., Carroll, M. C., & Kelsoe, G. (2000). Humoral immune responses in Cr2-/- mice: enhanced affinity maturation but impaired antibody persistence. J. Immunol., 164(9), 4522-4532.

Cooper, N. R., Nemerow, G. R., & Mayes, J. T. (1983). Methods to detect and quantitate complement activation. Springer Semin. Immunopathol., 6(2-3), 195-212.

Cortini, M., & Sitia, R. (2010). ERp44 and ERGIC-53 synergize in coupling efficiency and fidelity of IgM polymerization and secretion. Traffic, 11(5), 651-659.

Czajkowsky, D. M., & Shao, Z. (2009). The human IgM pentamer is a mushroom-shaped molecule with a flexural bias. Proc. Natl. Acad. Sci. U. S. A., 106(35), 14960-14965.

Davis, A. C., Collins, C., Yoshimura, M. I., D'Agostaro, G., & Shulman, M. J. (1989). Mutations of the mouse mu H chain which prevent polymer assembly. J. Immunol., 143(4), 1352-1357.

Davis, A. C., Roux, K. H., Pursey, J., & Shulman, M. J. (1989). Intermolecular disulfide bonding in IgM: effects of replacing cysteine residues in the mu heavy chain. EMBO J., 8(9), 2519-2526.

Davis, A. C., Roux, K. H., & Shulman, M. J. (1988). On the structure of polymeric IgM. Eur. J. Immunol., 18(7), 1001-1008.

Davis, A. C., & Shulman, M. J. (1989). IgM--molecular requirements for its assembly and function. Immunol. Today, 10(4), 118-122; 127-118.

de Lalla, C., Fagioli, C., Cessi, F. S., Smilovich, D., & Sitia, R. (1998). Biogenesis and function of IgM: the role of the conserved mu-chain tailpiece glycans. Mol. Immunol., 35(13), 837-845.

Diebolder, C. A., Beurskens, F. J., de Jong, R. N., Koning, R. I., Strumane, K., Lindorfer, M. A., Voorhorst M., Ugurlar D., Rosati S., Heck A. J., van de Winkel J. G., Wilson I. A., Koster A. J.,

Taylor R. P., Saphire E. O., Burton D. R., Schuurman J., Gros P., & Parren, P. W. (2014). Complement is activated by IgG hexamers assembled at the cell surface. Science, 343(6176), 1260-1263.

Edberg, S. C., Bronson, P. M., & Van Oss, C. J. (1972). The valency of IgM rabbit anti-dextran antibody as a function of the size of the dextran molecule. Immunochemistry, 9(3), 273-288.

Ellman G. L. (1959). Tissue sulfhydryl groups. Arch. Biochem. Biophys. 82(1), 70–7.

Erdei, A., Isaak, A., Torok, K., Sandor, N., Kremlitzka, M., Prechl, J., & Bajtay, Z. (2009). Expression and role of CR1 and CR2 on B and T lymphocytes under physiological and autoimmune conditions. Mol. Immunol., 46(14), 2767-2773.

Fairbanks, G., Steck, T. L., & Wallach, D. F. (1971). Electrophoretic analysis of the major polypeptides of the human erythrocyte membrane. Biochemistry, 10(13), 2606-2617.

Fazel, S., Wiersma, E. J., & Shulman, M. J. (1997). Interplay of J chain and disulfide bonding in assembly of polymeric IgM. Int. Immunol., 9(8), 1149-1158.

Fearon, D. T. (1993). The CD19-CR2-TAPA-1 complex, CD45 and signaling by the antigen receptor of B lymphocytes. Curr. Opin. Immunol., 5(3), 341-348.

Fearon, D. T., & Carroll, M. C. (2000). Regulation of B lymphocyte responses to foreign and self-antigens by the CD19/CD21 complex. Annu. Rev. Immunol., 18, 393-422.

Feeney, A. J. (1990). Lack of N regions in fetal and neonatal mouse immunoglobulin V-D-J junctional sequences. J. Exp. Med., 172(5), 1377-1390.

Feige, M. J., Groscurth, S., Marcinowski, M., Shimizu, Y., Kessler, H., Hendershot, L. M., & Buchner, J. (2009). An unfolded CH1 domain controls the assembly and secretion of IgG antibodies. Mol. Cell, 34(5), 569-579.

Feinstein, A., & Munn, E. A. (1969). Conformation of the free and antigen-bound IgM antibody molecules. Nature, 224(5226), 1307-1309.

Feinstein A., Richardson N., & Taussig M. J. (1986). Immunoglobulin flexibility in complement activation. Immunol Today, 7, 169–174.

Ferguson, A. R., Youd, M. E., & Corley, R. B. (2004). Marginal zone B cells transport and deposit IgM-containing immune complexes onto follicular dendritic cells. Int. Immunol., 16(10), 1411-1422.

Flach H., Rosenbaum M., Duchniewicz M., Kim S., Zhang S. L., Cahalan M. D., Mittler G., & Grosschedl R. (2010). Mzb1 protein regulates calciumhomeostasis, antibody secretion, and integrin activation in innate-like B cells. Immunity, 33(5), 723–735.

Flajnik, M. F., Miller, K., & Du Pasquier, L. (2003). Evolution of the Immune System. *Fundamental Immunology*. Edited by W. E. Paul. Philadelphia, Lippincott Williams & Wilkins, 519-570.

Fra, A. M., Fagioli, C., Finazzi, D., Sitia, R., & Alberini, C. M. (1993). Quality control of ER synthesized proteins: an exposed thiol group as a three-way switch mediating assembly, retention and degradation. EMBO J., 12(12), 4755-4761.

Frutiger, S., Hughes, G. J., Paquet, N., Luthy, R., & Jaton, J. C. (1992). Disulfide bond assignment in human J chain and its covalent pairing with immunoglobulin M. Biochemistry, 31(50), 12643-12647.

Getahun, A., & Heyman, B. (2006). How antibodies act as natural adjuvants. Immunol. Lett., 104(1-2), 38-45.

Haas, I. G., & Wabl, M. (1983). Immunoglobulin heavy chain binding protein. Nature, 306(5941), 387-389.

Haas, K. M., Poe, J. C., Steeber, D. A., & Tedder, T. F. (2005). B-1a and B-1b cells exhibit distinct developmental requirements and have unique functional roles in innate and adaptive immunity to S. pneumoniae. Immunity, 23(1), 7-18.

Hardy, R. R., & Hayakawa, K. (1994). CD5 B cells, a fetal B cell lineage. Adv. Immunol., 55, 297-339.

Hauri, H. P., Kappeler, F., Andersson, H., & Appenzeller, C. (2000). ERGIC-53 and traffic in the secretory pathway. J. Cell Sci., 113 (Pt 4), 587-596.

Hauri, H. P., Nufer, O., Breuza, L., Tekaya, H. B., & Liang, L. (2002). Lectins and protein traffic early in the secretory pathway. Biochem. Soc. Symp. (69), 73-82.

Hayakawa, K., & Hardy, R. R. (2000). Development and function of B-1 cells. Curr. Opin. Immunol., 12(3), 346-353.

Hendershot L., & Sitia R. (2005). Immunoglobulin assembly and secretion. In Molecular Biology of B Cells. Honjo T., Alt F. W., Neuberger M. S. (eds). Amsterdam NL: Elsevier Acad Press, 261–273.

Henry, C., & Jerne, N. K. (1968). Competition of 19S and 7S antigen receptors in the regulation of the primary immune response. J. Exp. Med., 128(1), 133-152.

Hester, R. B., Mole, J. E., & Schrohenloher, R. E. (1975). Evidence for the absence of noncovalent bonds in the Fcmu region of IgM. J. Immunol., 114(1 Pt 2), 486-491.

Hickman, S., & Kornfeld, S. (1978). Effect of tunicamycin on IgM, IgA, and IgG secretion by mouse plasmacytoma cells. J. Immunol., 121(3), 990-996.

Hochstenbach F., David V., Watkins S., & M. B. Brenner, (1992). Endoplasmic reticulum resident protein of 90 kilodaltons associates with the T- and B-cell antigen receptors and major histocompatibility complex antigens during their assembly. Proc. Natl. Acad. Sci. U. S. A., 89(10), 4734–4738.

Hohman, V. S., Stewart, S. E., Rumfelt, L. L., Greenberg, A. S., Avila, D. W., Flajnik, M. F., & Steiner, L. A. (2003). J chain in the nurse shark: implications for function in a lower vertebrate. J. Immunol., 170(12), 6016-6023.

Hughey, C. T., Brewer, J. W., Colosia, A. D., Rosse, W. F., & Corley, R. B. (1998). Production of IgM hexamers by normal and autoimmune B cells: implications for the physiologic role of hexameric IgM. J. Immunol., 161(8), 4091-4097.

Johansen, F. E., Braathen, R., & Brandtzaeg, P. (2000). Role of J chain in secretory immunoglobulin formation. Scand. J. Immunol., 52(3), 240-248.

Johansen, F. E., Braathen, R., & Brandtzaeg, P. (2001). The J chain is essential for polymeric Ig receptor-mediated epithelial transport of IgA. J. Immunol., 167(9), 5185-5192.

Kantor, A. B., & Herzenberg, L. A. (1993). Origin of murine B cell lineages. Annu. Rev. Immunol., 11, 501-538.

Kehry, M., Sibley, C., Fuhrman, J., Schilling, J., & Hood, L. E. (1979). Amino acid sequence of a mouse immunoglobulin mu chain. Proc. Natl. Acad. Sci. U. S. A., 76(6), 2932-2936.

Klimovich, V. B. (2011). IgM and its receptors: structural and functional aspects. Biochemistry (Mosc.), 76(5), 534-549.

Klimovich, V. B., Samoilovich, M. P., & Klimovich, B. V. (2008). Problem of J-chain of immunoglobulins. J. Evol. Biochem. Physiol., 44(2), 151-166.

Kohler, G., Potash, M. J., Lehrach, H., & Shulman, M. J. (1982). Deletions in immunoglobulin mu chains. EMBO J., 1(5), 555-563.

Kornfeld, R., & Kornfeld, S. (1985). Assembly of asparagine-linked oligosaccharides. Annu. Rev. Biochem., 54, 631-664.

Koshland, M. E. (1985). The coming of age of the immunoglobulin J chain. Annu. Rev. Immunol., 3, 425-453.

Kurosaki, T. (1999). Genetic analysis of B cell antigen receptor signaling. Annu. Rev. Immunol., 17, 555-592.

Lee, Y. K., Brewer, J. W., Hellman, R., & Hendershot, L. M. (1999). BiP and immunoglobulin light chain cooperate to control the folding of heavy chain and ensure the fidelity of immunoglobulin assembly. Mol. Biol. Cell, 10(7), 2209-2219.

Lindh, E., & Bjork, I. (1976). Binding of secretory component to human immunoglobulin M. Eur. J. Biochem., 62(2), 271-278.

Martin, F., & Kearney, J. F. (2001). B1 cells: similarities and differences with other B cell subsets. Curr. Opin. Immunol., 13(2), 195-201.

McHeyzer-Williams, L. J., & McHeyzer-Williams, M. G. (2005). Antigen-specific memory B cell development. Annu. Rev. Immunol., 23, 487-513.

Melchers, F. (1972). Difference in carbohydrate composition and a possible conformational difference between intracellular and extracellular immunoglobulin M. Biochemistry, 11(11), 2204-2208.

Melnick, J., Aviel, S., & Argon, Y. (1992). The endoplasmic reticulum stress protein GRP94, in addition to BiP, associates with unassembled immunoglobulin chains. J. Biol. Chem., 267(30), 21303-21306.

Meng, Y. G., Criss, A. B., & Georgiadis, K. E. (1990). J chain deficiency in human IgM monoclonal antibodies produced by Epstein-Barr virus-transformed B lymphocytes. Eur. J. Immunol., 20(11), 2505-2508.

Mestecky, J., & Schrohenloher, R. E. (1974). Site of attachment of J chain to human immunoglobulin M. Nature, 249(458), 650-652.

Mestecky, J., Schrohenloher, R. E., Kulhavy, R., Wright, G. P., & Tomana, M. (1974). Site of J chain attachment to human polymeric IgA. Proc. Natl. Acad. Sci. U. S. A., 71(2), 544-548.

Montecino-Rodriguez, E., Leathers, H., & Dorshkind, K. (2006). Identification of a B-1 B cell-specified progenitor. Nat. Immunol., 7(3), 293-301.

Morgan, B. P., Marchbank, K. J., Longhi, M. P., Harris, C. L., & Gallimore, A. M. (2005). Complement: central to innate immunity and bridging to adaptive responses. Immunol. Lett., 97(2), 171-179.

Muller, R., Grawert, M. A., Kern, T., Madl, T., Peschek, J., Sattler, M., Groll M., & Buchner, J. (2013). High-resolution structures of the IgM Fc domains reveal principles of its hexamer formation. Proc. Natl. Acad. Sci. U. S. A., 110(25), 10183-10188.

Nielsen, C. H., Fischer, E. M., & Leslie, R. G. (2000). The role of complement in the acquired immune response. Immunology, 100(1), 4-12.

Nilsson, I. M., & von Heijne, G. (1993). Determination of the distance between the oligosaccharyltransferase active site and the endoplasmic reticulum membrane. J. Biol. Chem., 268(8), 5798-5801.

Nilsson, T., Pypaert, M., Hoe, M. H., Slusarewicz, P., Berger, E. G., & Warren, G. (1993). Overlapping distribution of two glycosyltransferases in the Golgi apparatus of HeLa cells. J. Cell Biol., 120(1), 5-13.

Notkins, A. L. (2004). Polyreactivity of antibody molecules. Trends Immunol., 25(4), 174-179.

Otzen, D. E., Kristensen, O., & Oliveberg, M. (2000). Designed protein tetramer zipped together with a hydrophobic Alzheimer homology: a structural clue to amyloid assembly. Proc. Natl. Acad. Sci. U. S. A., 97(18), 9907-9912.

Perkins, S. J., Nealis, A. S., Sutton, B. J., & Feinstein, A. (1991). Solution structure of human and mouse immunoglobulin M by synchrotron X-ray scattering and molecular graphics modelling. A possible mechanism for complement activation. J. Mol. Biol., 221(4), 1345-1366.

Petrusic, V., Zivkovic, I., Stojanovic, M., Stojicevic, I., Marinkovic, E., Inic-Kanada, A., & Dimitijevic, L. (2011). Antigenic specificity and expression of a natural idiotope on human pentameric and hexameric IgM polymers. Immunol. Res., 51(1), 97-107.

Pillai, S., Cariappa, A., & Moran, S. T. (2005). Marginal zone B cells. Annu. Rev. Immunol., 23, 161-196.

Plaut, A. G., & Tomasi, T. B., Jr. (1970). Immunoglobulin M: pentameric Fcmu fragments released by trypsin at higher temperatures. Proc. Natl. Acad. Sci. U. S. A., 65(2), 318-322.

Poon, P. H., Morrison, S. L., & Schumaker, V. N. (1995). Structure and function of several anti-dansyl chimeric antibodies formed by domain interchanges between human IgM and mouse IgG2b. J. Biol. Chem., 270(15), 8571-8577.

Prinsloo, E., Oosthuizen, V., Van de Venter, M., & Naude, R. J. (2009). Biological inferences from IgM binding characteristics of recombinant human secretory component mutants. Immunol. Lett., 122(1), 94-98.

Pumphrey, R. S. H. (1986). Computer models of the human immunoglobulins. II. Binding sites and molecular interactions, Immunol. Today, 7, 206-211.

Qin, D., Wu, J., Carroll, M. C., Burton, G. F., Szakal, A. K., & Tew, J. G. (1998). Evidence for an important interaction between a complement-derived CD21 ligand on follicular dendritic cells and CD21 on B cells in the initiation of IgG responses. J. Immunol., 161(9), 4549-4554.

Randall, T. D., Brewer, J. W., & Corley, R. B. (1992). Direct evidence that J chain regulates the polymeric structure of IgM in antibody-secreting B cells. J. Biol. Chem., 267(25), 18002-18007.

Randall, T. D., King, L. B., & Corley, R. B. (1990). The biological effects of IgM hexamer formation. Eur. J. Immunol., 20(9), 1971-1979.

Reddy, P., Sparvoli, A., Fagioli, C., Fassina, G., & Sitia, R. (1996). Formation of reversible disulfide bonds with the protein matrix of the endoplasmic reticulum correlates with the retention of unassembled Ig light chains. EMBO J., 15(9), 2077-2085.

Redwan el, R. M., Matar, S. M., & Serour, I. A. (2006). Recombinant human J-chain: fix the protein aggregations and yield maximize. Hum. Antibodies, 15(3), 95-102.

Reth, M. (1992). Antigen receptors on B lymphocytes. Annu. Rev. Immunol., 10, 97-121.

Reth, M., & Wienands, J. (1997). Initiation and processing of signals from the B cell antigen receptor. Annu. Rev. Immunol., 15, 453-479.

Richardson, J. S., & Richardson, D. C. (2002). Natural beta-sheet proteins use negative design to avoid edge-to-edge aggregation. Proc. Natl. Acad. Sci. U. S. A., 99(5), 2754-2759.

Richardson, J. S., Richardson, D. C., Thomas, K. A., Silverton, E. W., & Davies, D. R. (1976). Similarity of three-dimensional structure between the immunoglobulin domain and the copper, zinc superoxide dismutase subunit. J. Mol. Biol., 102(2), 221-235.

Robinson, E. A., & Appella, E. (1980). Complete amino acid sequence of a mouse immunoglobulin alpha chain (MOPC 511). Proc. Natl. Acad. Sci. U. S. A., 77(8), 4909-4913.

Rogers, J., Early, P., Carter, C., Calame, K., Bond, M., Hood, L., & Wall, R. (1980). Two mRNAs with different 3' ends encode membrane-bound and secreted forms of immunoglobulin mu chain. Cell, 20(2), 303-312.

Sambrook L., Fritsch F., & Maniatis T. (1989). Molecular Cloning. Cold Spring Harbor Press, Cold Spring Harbor, New York.

Schroeder, H. W., Jr., & Cavacini, L. (2010). Structure and function of immunoglobulins. J. Allergy Clin. Immunol., 125(2 Suppl 2), S41-52.

Shimizu Y., Meunier L., & Hendershot L. M. (2009). pERp1 is significantly up-regulated during plasma cell differentiation and contributes to the oxidative folding of immunoglobulin. Proc. Natl. Acad. Sci. U. S. A., 106(40), 17013–17018.

Sitia, R., Neuberger, M., Alberini, C., Bet, P., Fra, A., Valetti, C., Williams G., & Milstein, C. (1990). Developmental regulation of IgM secretion: the role of the carboxy-terminal cysteine. Cell, 60(5), 781-790.

Smith, R. I., Coloma, M. J., & Morrison, S. L. (1995). Addition of a mu-tailpiece to IgG results in polymeric antibodies with enhanced effector functions including complement-mediated cytolysis by IgG4. J. Immunol., 154(5), 2226-2236.

Smith, R. I., & Morrison, S. L. (1994). Recombinant polymeric IgG: an approach to engineering more potent antibodies. Biotechnology. (N. Y.), 12(7), 683-688.

Sorensen, V., Rasmussen, I. B., Norderhaug, L., Natvig, I., Michaelsen, T. E., & Sandlie, I. (1996). Effect of the IgM and IgA secretory tailpieces on polymerization and secretion of IgM and IgG. J. Immunol., 156(8), 2858-2865.

Sorensen, V., Rasmussen, I. B., Sundvold, V., Michaelsen, T. E., & Sandlie, I. (2000). Structural requirements for incorporation of J chain into human IgM and IgA. Int. Immunol., 12(1), 19-27.

Sorensen, V., Sundvold, V., Michaelsen, T. E., & Sandlie, I. (1999). Polymerization of IgA and IgM: roles of Cys309/Cys414 and the secretory tailpiece. J. Immunol., 162(6), 3448-3455.

Symersky, J., Novak, J., McPherson, D. T., DeLucas, L., & Mestecky, J. (2000). Expression of the recombinant human immunoglobulin J chain in Escherichia coli. Mol. Immunol., 37(3-4), 133-140.

Tack B. F., Harrison R. A., Janatova J., Thomas M. L., & Prahl J. W. (1980). Evidence for presence of an internal thiolester bond in third component of human complement. Proc Natl Acad Sci U S A, 77(10), 5764–5768.

Takahashi, T., Iwase, T., Takenouchi, N., Saito, M., Kobayashi, K., Moldoveanu, Z., Mestecky J., & Moro, I. (1996). The joining (J) chain is present in invertebrates that do not express immunoglobulins. Proc. Natl. Acad. Sci. U. S. A., 93(5), 1886-1891.

Tartakoff, A., & Vassalli, P. (1979). Plasma cell immunoglobulin M molecules. Their biosynthesis, assembly, and intracellular transport. J. Cell Biol., 83(2 Pt 1), 284-299.

Thirumalai, D., Klimov, D. K., & Dima, R. I. (2003). Emerging ideas on the molecular basis of protein and peptide aggregation. Curr. Opin. Struct. Biol., 13(2), 146-159.

van Anken, E., Pena, F., Hafkemeijer, N., Christis, C., Romijn, E. P., Grauschopf, U., Oorschot V. M., Pertel T., Engels S., Ora A., Lástun V., Glockshuber R., Klumperman J., Heck A. J., Luban J., & Braakman, I. (2009). Efficient IgM assembly and secretion require the plasma cell induced endoplasmic reticulum protein pERp1. Proc. Natl. Acad. Sci. U. S. A., 106(40), 17019-17024.

Vassalli, P., Tartakoff, A., Pink, J. R., & Jaton, J. C. (1980). Biosynthesis of two forms of IgM heavy chains by normal mouse B lymphocytes. Membrane and secretory IgM. J. Biol. Chem., 255(24), 11822-11827.

Vestweber, D., & Schatz, G. (1988). Mitochondria can import artificial precursor proteins containing a branched polypeptide chain or a carboxy-terminal stilbene disulfonate. J. Cell Biol., 107(6 Pt 1), 2045-2049.

Wiersma, E. J., Chen, F., Bazin, R., Collins, C., Painter, R. H., Lemieux, R., & Shulman, M. J. (1997). Analysis of IgM structures involved in J chain incorporation. J. Immunol., 158(4), 1719-1726.

Wiersma, E. J., Collins, C., Fazel, S., & Shulman, M. J. (1998). Structural and functional analysis of J chain-deficient IgM. J. Immunol., 160(12), 5979-5989.

Wiersma, E. J., & Shulman, M. J. (1995). Assembly of IgM. Role of disulfide bonding and noncovalent interactions. J. Immunol., 154(10), 5265-5272.

Woof, J. M., & Mestecky, J. (2005). Mucosal immunoglobulins. Immunol. Rev., 206, 64-82.

Wormald, M. R., Wooten, E. W., Bazzo, R., Edge, C. J., Feinstein, A., Rademacher, T. W., & Dwek, R. A. (1991). The conformational effects of N-glycosylation on the tailpiece from serum IgM. Eur. J. Biochem., 198(1), 131-139.

Xia, X., Longo, L. M., & Blaber, M. (2014). Mutation Choice to Eliminate Buried Free Cysteines in Protein Therapeutics. J. Pharm. Sci., 104(2), 566-576.

Yoo, E. M., Coloma, M. J., Trinh, K. R., Nguyen, T. Q., Vuong, L. U., Morrison, S. L., & Chintalacharuvu, K. R. (1999). Structural requirements for polymeric immunoglobulin assembly and association with J chain. J. Biol. Chem., 274(47), 33771-33777.

Zikan, J., & Bennett, J. C. (1973). Isolation of F(c)5mu and Fabmu fragments of human IgM. Eur. J. Immunol., 3(7), 415-419.

Zikan, J., Novotny, J., Trapane, T. L., Koshland, M. E., Urry, D. W., Bennett, J. C., & Mestecky, J. (1985). Secondary structure of the immunoglobulin J chain. Proc. Natl. Acad. Sci. U. S. A., 82(17), 5905-5909.

11 Declaration

I, Džana Pašalić, hereby declare that this thesis was prepared by me independently and using only the references and resources stated here. The work has so far not been submitted to any audit commission. Parts of this work will be published in scientific journals.

Hiermit erkläre ich, Džana Pašalić, dass ich die vorliegende Arbeit selbständig verfasst und keine anderen als die angegebenen Quellen und Hilfsmittel verwendet habe. Die Arbeit wurde bisher keiner Prüfungskommission vorgelegt. Teile dieser Arbeit werden in wissenschaftlichen Journalen veröffentlicht.

_____

Džana Pašalić

12 Acknowledgements

This PhD thesis was prepared at the Technische Universität München, Department Chemie, Lehrstuhl Biotechnologie under supervision of Prof. Dr. Johannes Buchner from September 2011 to January 2015.

Thanks to the One who enriched my life with this experience and gave me the strength to complete the journey.

To my research advisor, Prof. Dr. Johannes Buchner, I would like to express my sincere gratitude for giving me the opportunity to work in his group and on such an exciting project, for his continuous presence, guidance and support during my research work and thesis preparation. I would like to thank Prof. Dr. Roberto Sitia for inviting me to join shortly his excellent group and perform part of significant experiments for this thesis at San Raffaele Scientific Institute in Milan and for his involvement in this project with constructive discussions and suggestions. I thank Prof. Dr. Christian Becker for his support and for providing us promptly with peptides which contributed to achieve exciting results. For their precious indications, suggestions and comments I express my appreciation to my TAC members, Prof. Dr. Michael Sattler and Dr. Tobias Madl. I would like to extend my appreciation to IMPRS and our PhD program coordinators for their organization, support and assistance.

I want to thank all members of both group of the Lehrstuhl Biotechnologie and Prof. Sitia's group. Here I had the opportunity to meet incredible people who taught me a lot. Thanks to Roger for his initial hints, to Christine for aUC measurements and to Helmut for MS analysis. My special thank goes to Asia, Tiziana and Maria who I had the pleasure to get to know and whose advices I treasure. Another special thank goes to our wonderful secretaries, Mrs. Susanne Hilber and Mrs. Margot Rubinstein, for being always kind and helpful. I am also thankful to all practical students for their contribution to this work and all the people I have met at the University.

Finally, I would like to express my deepest gratitude to all my family. To my parents and my sister for their encouragement, care and their, always present, comprehension. To my husband for his love, care, irrespective of mine, for his patience and understanding. Thank you, my family, for having given me support throughout the years and all my life. This achievement is dedicated to you.